NOTICE

AVIS

THE UNIVERSITY OF ALBERTA

Sedimentology and development of the Grande Prairie dune field, Alberta, Canada

by

Linda A. Halsey

A THESIS

SUBMITTED TO THE FACULTY OF GRADUATE STUDIES AND RESEARCH

IN PARTIAL FULFILMENT OF THE REQUIREMENTS FOR THE DEGREE

OF

MASTER of SCIENCE

DEPARTMENT OF GEOLOGY

EDMONTON, ALBERTA

Spring, 1989

ISBN 0-315-53027-8

Table 2: Descriptive and interpretative summary of aeolian sediments observed in the Grande Prairie dune field.

escription	Set/Bed thickness	Strata Thickness (cm)	Set/Bed Dip, Orientation	Strata Dip, Orientation	Contacts Lower	Contacts Upper	Interpretation	Range of Mean grain size (ø)	Average mean grain size (ø)	Range of Sorting (ø)	Mean of Sorting (ø)	Number of Samples
r fine sand beds	1.1 - 7.0 cm	—	0° - 10°, 000 - 360	—	grad. to, abrupt, erosional to noner.	grad. to abrupt	Wet and vegetatively induced grainfall	2.35-2.70	2.72	0.37-0.61	0.51	15
nedium sand beds	0.8 - 7.0 cm	—	0° - 18°, 000 - 245	—	smooth, abrupt. erosional to noner.	abrupt, irreg. undulat. to rippled	Movement of waterlogged sediment	1.52-2.17	1.86	0.50-0.81	0.64	11
gh angle concave-rds cross-strata	0.4-15 m	0.3 - 0.8	0° - 20°, 045 - 240	26° - 33°, 060-135	smooth, abrupt. erosional to noner.	smooth, abrupt	Avalanching generated mainly from brink accum.	2.02-2.72	2.47	0.35-0.70	0.50	8
gh angle concave-s cross-strata	1.0 - 1.7 m	0.1 - 3.0	near horizontal	22° - 33°, 040 115	smooth, abrupt. erosional to noner.		Avalanching generated mainly from slipface undercutting	2.05-2.70	2.43	0.33-0.72	0.55	7
igh angle planar r cross-strata	40 cm	0.1 - 0.6	5° - 10°, 045-060	33° - 36°, 055	smooth, abrupt. erosional to noner.	smooth, abrupt	Wet grainfall on a slipface without avalanching	—	2.73	—	0.38	1
sets of low angle ss-laminae	0.1 - 1.5 m	0.1 - 0.8	0° - 10°, 040-120	6° - 26°, 035-150	smooth, abrupt. erosional to noner.	smooth, abrupt	Dune migration without slipface development	1.78-2.73	2.31	0.36-0.78	0.51	31
ets of low angle ss-laminae	2.0 - 30.0 cm	0.1 - 0.5	0° - 28°, 045-150	0° - 12°, 340-250	smooth, abrupt. erosional to noner.	smooth, abrupt	Ripple migration on dune aprons from winds oblique to the dune surface	2.10-2.65	2.41	0.36-0.61	0.52	10
rmally graded near laminae which dip easterly	3 - 100 cm	0.1 - 1.2	0°-14°,035-150	0°-14°, 035-150	smooth-undulat. to rippled noneros.	smooth, and abrupt	Grainfall on the lee side of a dune surface	2.22-2.52	2.40	0.6-0.61	0.47	4
raded to inversely r horizontal laminae ch dip easterly	3 - 150 cm	<0.1 - 0.5	0°-5°, 0-200	0°-5°, 0-200	smooth, abrupt, erosional to noner.	smooth to rippled abrupt	Ripple migration on the lee side of a dune surface	1.98-2.38	2.36	0.39-0.77	0.55	24
f ungraded near laminae which dip vesterly	5 - 80 cm	<0.1 - 0.5	3°-15°,245-340	3°-15°,245-340	smooth, abrupt, erosional to noner.	smooth, and abrupt	Deposition on the stoss side of a dune surface	1.92-2.38	2.15	0.35-0.78	0.55	8
d rich laminae	< 1 cm	—	near horizontal	—	smooth, abrupt, erosional to noner.	abrupt, ridged	Unlimited growth of ridges	1.82-2.00	1.92	0.62-0.92	0.77	2
ex lenses of sand e associated with ous root tubules	10 - 60 cm	—	near horizontal	—		smooth, and abrupt	Grainfall in and to the lee of vegetation	2.32-2.57	2.45	0.45-0.61	0.53	4
x lenses of sand t associated with s root tubules	0.5 - 2.0 cm	—	near horizontal	—	smooth, abrupt, noner.	smooth, and abrupt	Wind sculpturing of a moist rippled or planar surface	—	2.90	—	0.40	1
gated laminae e sand	2 - 5 cm	< 0.1 - 0.3	near horizontal	near horizontal	grad. to abrupt, smooth	smooth, and abrupt	Adhesion laminae	2.40-2.80	2.55	0.40-0.80	0.63	7
avy laminae of e sand	10 - 30 cm	0.1 - 1.0	near horizontal	near horizontal	smooth, abrupt, noner.	smooth to wavy, grad. to abrupt	Adhesion ripples, or loading-dewatering, or niveo-aeolian deposition in spring/fall (local snow patches)	2.23-2.62	2.43	0.57-0.72	0.64	4

THE UNIVERSITY OF ALBERTA

RELEASE FORM

NAME OF AUTHOR: LINDA ANN HALSEY

TITLE OF THESIS: SEDIMENTOLOGY AND DEVELOPMENT OF THE GRANDE PRAIRIE DUNE FIELD, ALBERTA, CANADA

DEGREE: MASTER of SCIENCE

YEAR THIS DEGREE GRANTED: SPRING, 1989

L. Halsey

Department of Geology

University of Alberta

Edmonton, Alberta

Date: April 26/89

THE UNIVERSITY OF ALBERTA

FACULTY OF GRADUATE STUDIES AND RESEARCH

The undersigned certify that they have read, and recommend to the Faculty of Graduate Studies and Research for acceptance, a thesis entitled, "Sedimentology and development of the Grande Prairie dune field, Alberta, Canada", submitted by Linda Ann Halsey in partial fulfilment of the requirements of the degree of Master of Science in Geology.

....

Supervisor: Dr. N. W. Rutter

....

Dr. B. Jones

....

Dr. T. Moslow

....

External Examiner: Dr. I. Campbell

Date: April 26/89

ABSTRACT

The Grande Prairie dune field is in northwest-central Alberta and is composed of stabilised parabolic and dome dunes which developed under a westerly wind. Dune development began before 9,000 years BP., and continued throughout the Holocene, as terrace cutting and fires exposed sediment surfaces. Spatial variations in sediment supply and sediment budget resulted in the development of dome dunes and two types of parabolic dunes. Dome dunes developed with a low sediment supply and a high sediment budget. Type 1 parabolic dunes are low (6 m), have long arms, and short crest widths, and resulted from a low sediment supply and budget. Type 2 parabolic dunes are high (20 m), have short arms and wide crests, and resulted from a high sediment supply and budget.

Ten facies and eight subfacies were distinguished, with the frequency and locations of these facies in the different dune types being controlled by geomorphology, wind direction(s) and velocity(s), sediment supply, and sediment budget. Lee side deposits of parabolic dunes are typically composed of avalanche deposits generated by preferential brinkline accumulation. Low-angled cross-strata predominate in lee side deposits of dome dunes, suggesting sediment supply was lower.

Lee side deposits of all dune types are interbedded downwind with low-angle to horizontal ripple laminations of bottomset deposits. Lee side deposits are overlain by shallow dipping topset deposits. Topset deposits of

dome and type 2 parabolic dunes may be composed of up to 15% of sedimentary units which are indicative of moisture (eg. adhesion laminae and ripples). These dunes also have topset deposits which may be composed of up to 5% of sedimentary units which are indicative of vegetation having been present during deposition (eg. scour surfaces). Indicators of moisture and the presence of vegetation suggest that dome and type 2 parabolic dunes had a high sediment budget. Type 2 parabolic dunes also contain grainfall deposits which indicate a high sediment supply.

Compound parabolic dunes are present in the Grande Prairie dune field, resulting from downwind dune migration onto upwind dunes. These compound dunes contain complex structures which are dependent on the angle of climb during migration and the generation of secondary airflow at the intersection point.

ACKNOWLEDGEMENTS

There are many people who have contributed their time and knowledge in assisting me to complete this thesis and I take great pleasure in thanking them. Funding for this study was provided by the Boreal Institute for Northern Studies and from an NSERC grant awarded to Nathaniel W. Rutter.

I would like to thank my supervisor, Nat Rutter, who encouraged and supported me, and who asked many questions, some of which I have attempted to answer in this thesis. I would also like to thank Dr. Nat Rutter, Dr. Norm Catto, Dave Liverman, and Dr. Fred Bachhuber, as well as the members of the committee Dr. Brian Jones, Dr. Tom Moslow, and Dr. Ian Campbell who read and commented on earlier drafts of this thesis, greatly improving it. I am grateful to Dr. P. David who answered many questions and provided encouragement.

I am indebted to my father Fred Halsey, and my husband Mike Ashby for their assistance in the field. I would also like to thank Michelle Perras for her extensive assistance in conducting the grain size analysis.

Finally, I would like to thank all the members of the QRG who gave me their moral support, and made the lab and office an enjoyable place to be. Thank-you.

TABLE OF CONTENTS

LIST OF TABLES

LIST OF FIGURES

LIST OF PLATES

LIST OF SYMBOLS

U^* is the surface friction speed

pF is the density of the fluid

pp is the density of the particle

g is acceleration due to gravity

Dp is the diameter of the particle

Ø negative log to the base two of the diameter of a grain in millimetres

CHAPTER ONE: INTRODUCTION

The Grande Prairie dune field is one of the largest stabilised parabolic and dome dune fields in central Alberta. Parabolic and dome dune fields represent approximately four to five percent of surficial sediments in Alberta. Almost no detailed work has been done on the development and sedimentology of these dune fields, therefore there are major questions on the environment necessary for their formation and reactivation. This study will provide qualitative information to answer these questions.

Parabolic dunes are considered to be typical of aeolian sedimentation in temperate climates (Smith 1949, Brookfield 1984), yet most work on parabolic and dome dunes have concentrated on tropic coastal and desert environments. Though these studies have a general application to their temperate equivalents, they can not be directly applied to Alberta dunes as environmental conditions differ. This investigation will provide a detailed qualitative account of parabolic and dome dune development and sedimentology in one temperate dune field.

The major objectives of this investigation are to:

1) describe the sedimentary structures and sequences found in selected parabolic and dome dunes;

2) interpret the environments of deposition and the processes resulting

in the deposition of these sediments;

3) to establish facies models for parabolic and dome dunes in temperate climates to act as a comparative model to ancient aeolian dune sequences.

Location of study area

The study area is the Grande Prairie dune field which straddles the Wapiti and Smoky Rivers in the vicinity of Grande Prairie, Alberta (Figure 1). The dune field is composed of dome dunes and solitary and compound parabolic dunes which are surrounded by a thin, discontinuous aeolian sand sheet with localized areas of blowout development and deflation. The dune field is generally restricted to the river valleys, extending slightly outside the limits of Holocene river terraces.

Climate

The study area has a continental climate with cool summers and long cold winters (Figure 2). Mean daily temperature for the years 1977 - 1982 averaged 3.9 °C, with the coldest month being January and the warmest July (Figure 2a). Precipitation is moderate with the majority falling between May and August (Figure 2b). The Wapiti River generally has permanent ice by the first week of November with break-up usually beginning during the second week of April (Ojamaa 1978).

Figure 1: Location of study area. Shaded areas represent the Grande Prairie dune field.

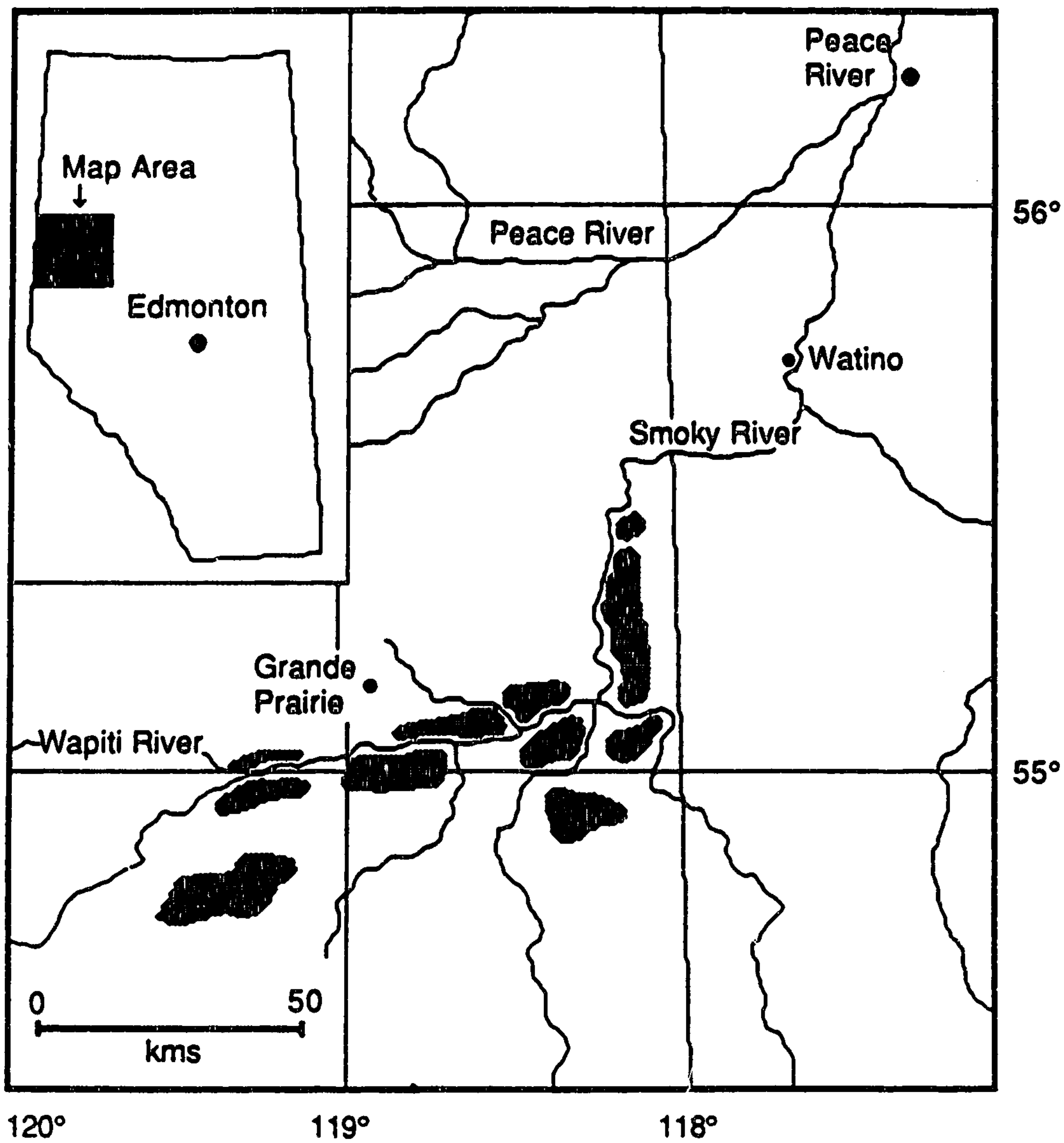

Figure 2: Average climatic data recorded at Grande Prairie for the years 1977 -1982. A) Mean monthly temperatures, and B) mean monthly rainfall and snowfall. Source for data: Environment Canada (1977-1982).

A)

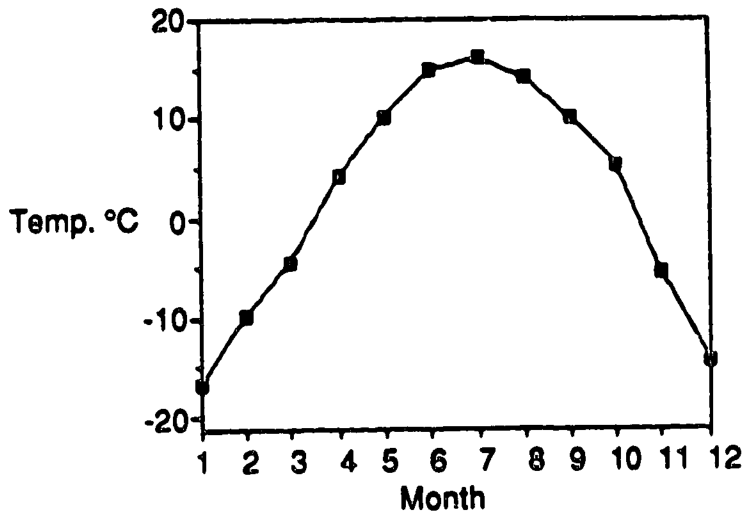

B)

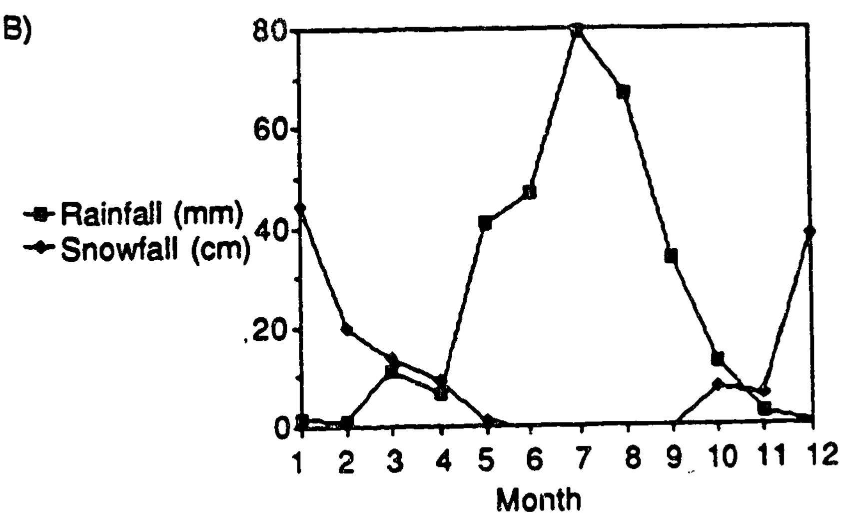

The prevailing wind direction in the Grande Prairie region is westerly, except during the winter months when it is west-southwesterly (Figure 3). The strongest winds are in the same direction as the prevailing winds (Figure 3). Wind speed is moderate, averaging 14 km/hour for the years 1977 - 1982 (Ojamaa 1978). The windiest months are from May to September, with winds being strongest and most frequent during the spring (Figure 3).

Vegetation and Soils

The Grande Prairie dune field is located within the Boreal Forest as defined by Rowe (1972). Variation of both soils and vegetation are controlled by slope position, aspect, elevation, and drainage (Twardy and Corns 1980). Well drained sites, found on large parabolic dunes, support *Pinus contorta* (lodgepole pine) with *Arctostaphylos uva-ursi* (bearberry) and various grasses composing the majority of the understory (Ojamma 1978). Soils are eluviated eutric brunisols of the Heart Soil Group (Odynsky*et al.*1956, 1961).

Well drained areas also occur on smaller dunes, sand sheets and northern slopes of larger dunes and are dominated by *Populus tremuloides* (aspen poplar) with local occurrences of *Betula papyrifera* (paper birch), *Picea glauca* (white spruce) and *Populus balsamifera* (balsam poplar) (Ojamma 1978). The understory is dominantly composed of *Alnus crispa* (alder), *Salix* (willow), *Rosa acicularis* (wild rose), *Shepherdia canadensis* (buffaloberry), grasses and feathermoss (Ojamma 1978). The soils are eluviated eutric brunisols of the Heart Soil Group (Odynsky *et. al.* 1956,

Figure 3: Average wind velocity and frequency of direction recorded at Grande Prairie for the years 1977-1982. A) Winter months of January, February, and March; B) spring months of April, May and June; C) summer months of July, August, and September and D) fall months of October, November, and December. Source of data Environment Canada 1977-1982.

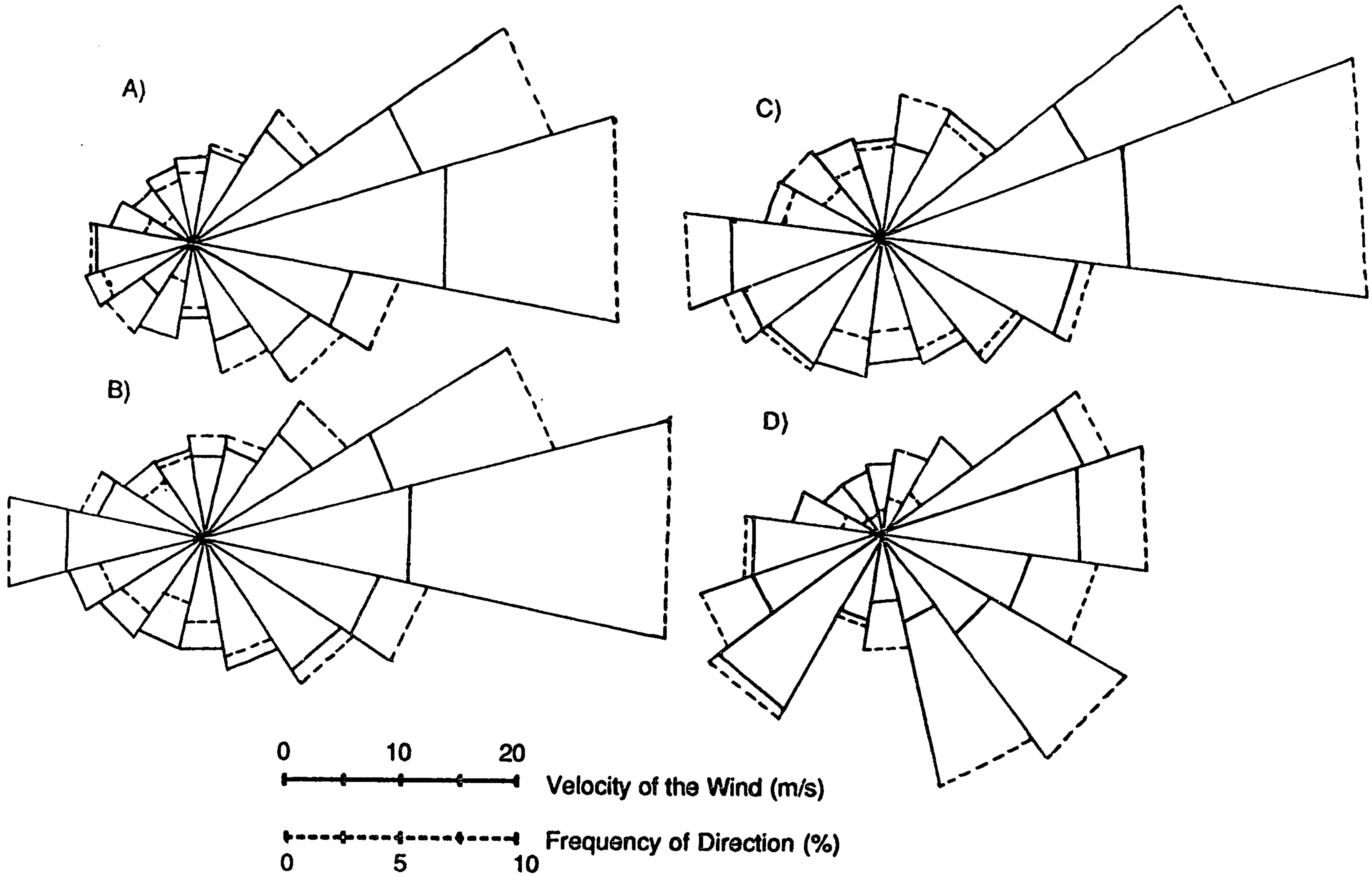

A)
B)
C)
D)
0
10
20
Velocity of the Wind (m/s)
0
5
10
Frequency of Direction (%)

1961).

Low lying, poorly drained interdune areas support a *Picea mariara* (black spruce)- *Larix laricina* (tamarack) community, with *Ledum groenlandicum* (Labrador tea), *Salix* (willow), and *Sphagnum* forming the understory (Ojamma 1978). Treeless areas of*Carex* (sedge) and *Calamagrastis* (reed grass) also occur (Ojamma 1978). Soils are gleysols or organic soils, depending on the drainage. The thickness of the organic layer rarely exceeds 1.5 m (Odynsky *et. al.* 1956).

Definition of dune types present in the study area

A sand dune is defined as a mound or hill of sand sized sediment which accumulates by the action of the wind (Stone 1967). Dune classification is based on the morphology of the dune in plan view and the location and number of slipfaces present (McKee 1979). In plan view parabolic dunes have a U- to V-shaped morphology (Figure 4a). Two arms which are parallel to the dominant wind direction merge downwind into a nose which is transverse to the dominant wind direction (Figure 4a). The nose tends to migrate in the direction of aeolian sediment transport, while the arms remain stationary. One or more slipfaces may be present on the lee side of the nose of a parabolic dune. The upwind end of a parabolic dune is composed of a lee side which is followed downwind by topset, slipface and bottomset deposits in the lee of the dune (Figure 4a).

Figure 4: Schematic diagram of basic dune types present in the Grande Prairie dune field. A) Parabolic dune, and B) dome dune.

A)

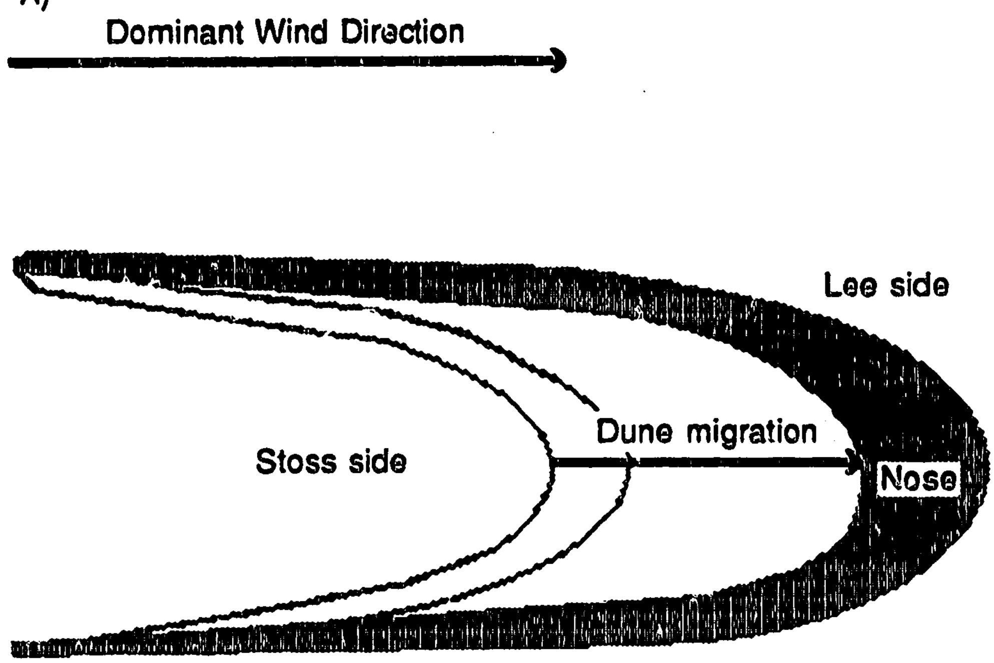

B)

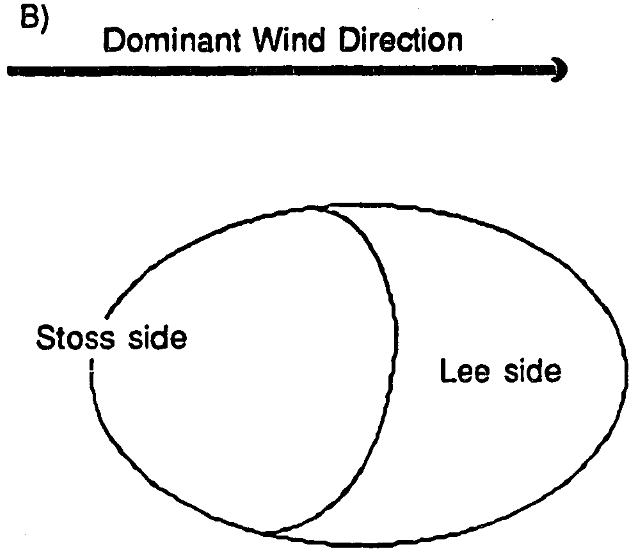

Dome dunes vary in plan view from circular to elliptical and are mound shaped in cross section (Figure 4b). Dome dunes do not have slipfaces (Figure 4b). The upwind end of a dome dune is composed of a lee side which is followed downwind by topset, lee side and bottomset deposits (Figure 4b).

Previous work

"Sand ridges" were first reported in the valley of the Wapiti River by Dawson (1881). These "sand ridges" were not identified as dunes until they were observed from aerial photographs (Lang *et al.* 1947). Subsequently, the dunes were identified as both barchans, suggesting an easterly palaeowind direction (Thornbury 1954), and as parabolic dunes suggesting a westerly palaeowind direction (American Geological Institute 1951, Gravenor 1956). Odynsky (1958) established that the dunes of the Grande Prairie area are parabolic. He noted that the effective sand moving palaeowind direction coincides with the direction of strongest and the most frequent winds today which are westerly.

Odynsky (1958) considered the source of the sand for the dunes to be high level terrace deposits from the early river system. Glaciolacustrine sediments were suggested by Henderson (1959) and Gravenor *et al.* (1960), whereas Jones (1961, 1966) suggested that glacial outwash sands and gravels supplied the source of sediment for the dunes.

The timing of dune development and stabilisation in the Grande Prairie area is unknown. Henderson (1959) speculated that the dunes were formed by periglacial winds immediately after glacial lake drainage and stabilised when sufficient vegetation invaded the area. Gravenor *et al.* (1960) noted the presence of dunes on some of the lower terraces of the Wapiti River and concluded dune formation followed the development of the lowermost terrace. As the dunes are presently stabilised the conditions under which they developed must have been different than today (David 1977).

Investigations of postglacial palaeoenvironments have been conducted approximately 50 km to the northwest of the study area, using pollen analysis and radiometric dating (White 1983, White *et al.* 1985, White and Mathewes 1986). On the basis of pollen analysis, White *et al.* (1985) and Mathewes (1986) concluded that a shrub-grass assemblage was present in the area c. 12,000 years B.P. A distinct pine and spruce rise followed and was subsequently replaced by a paper birch rise and a spruce decline c. 8,700 - 8,200 years B.P. (White 1983, White *et al.* 1985, White and Mathewes 1986). The paper birch rise is interpreted to result from enhanced seasonality due to a weakening of the anticyclone (high pressure cell) associated with the Laurentide ice sheet (White *et al.* 1985, White and Mathewes 1986). Salient features and a pine peak at 7,400 years B.P. are interpreted to result from a drier habitat, presumably the time transgressive Hypsithermal (White 1983, White *et al.* 1985, White and Mathewes 1986). After 7,400 years B.P., pine declined and alder and birch increased (White 1983). This marks an increase in available moisture with conditions similar to the present being reached by about 5,000 years B.P. (White 1983).

CHAPTER TWO: METHODOLOGY

Field research

Detailed observations of aeolian deposits in the Grande Prairie region were made during the summers of 1985, 1986, and 1987. Associated fluvial, glaciolacustrine, and interdune pond deposits were also examined. Twelve well exposed sections (Figure 5) were systematically described with emphasis placed on sedimentary structures and unit morphology. Eight of these sections were through parabolic dunes (Plates 1 and 2), two were through dome dunes (Plate 3), and two were located in sand sheets. Major section descriptions are presented in Appendix 1. In addition to these twelve major sections, numerous poorly exposed sites were also briefly examined.

One hundred and thirty samples were collected for textural and mineralogical analyses. Bulk samples were collected from finely laminated units. Samples taken from units with strata thicker than 0.5 cm were collected from individual laminae or beds using a small spoon.

Figure 5: Locations of major dome dune and sand sheet site investigations and coverage of aerial photographs showing parabolic dune and interdune section locations.

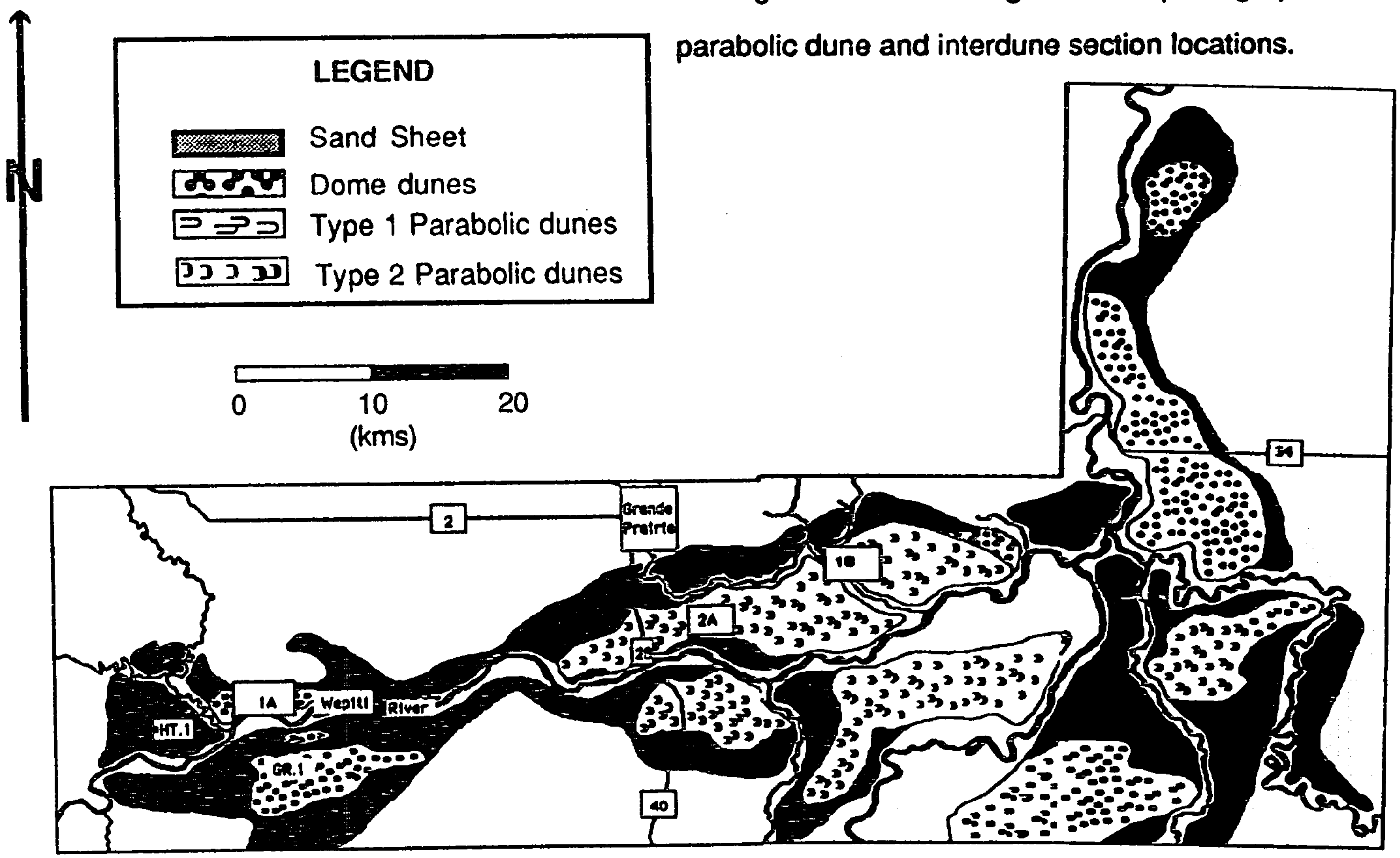

Plate 1: A) Aerial photograph showing sections P.1 - P.5. B) Aerial photograph showing section B.1. Sections P.1 and P.2 are both located in a compound parabolic dune where the nose of one dune has encroached downwind onto the arm of another dune. Sections P.3 and B.1 are present on the arms of parabolic dunes. Section P.4 is present in an interdune area. Section P.5 is present in the nose of a parabolic dune.

A)

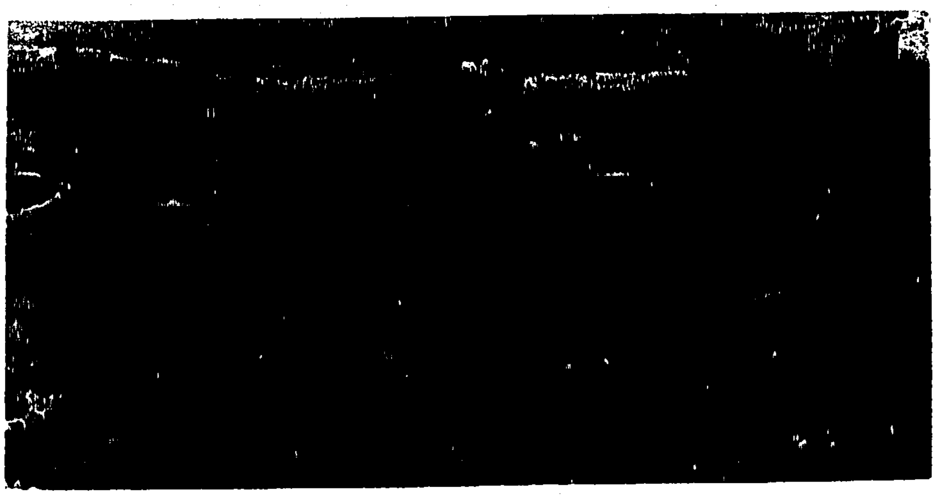

B)

Plate 2: A) Aerial photograph showing sections GP.2, GP. 4 , and GP.5.

B) Aerial photograph showing sections GP.1 and GP.3.

Sections GP.1 and GP. 4 both located in a compound parabolic dune where the nose of one dune has encroached downwind onto the arm of another dune. Section GP.3 is present on the arm of a parabolic dune. Section GP.3 is present in an interdune area. Section GP.5 is present in the nose of a parabolic dune.

A)

B)

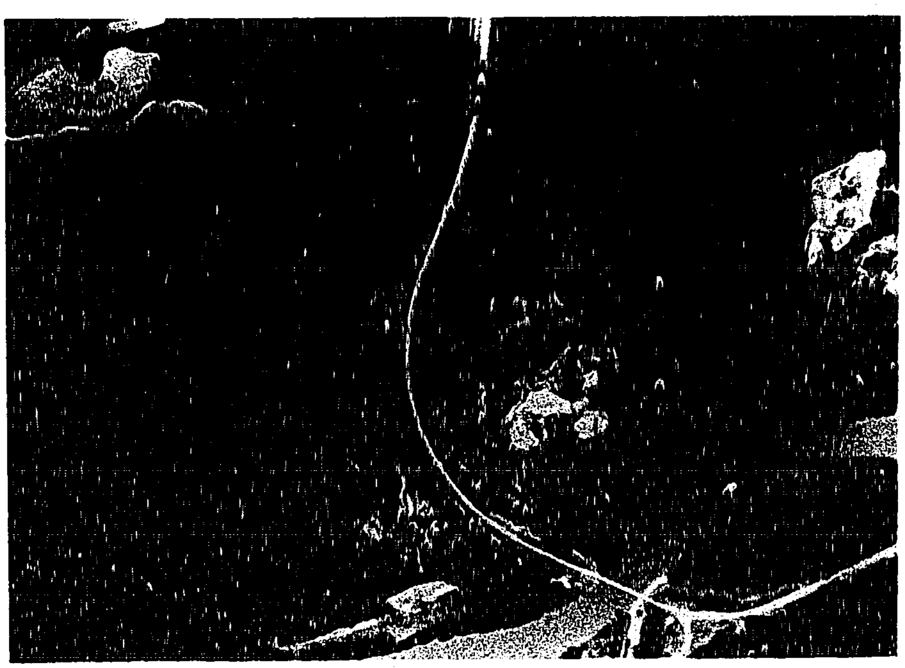

Plate 3: Photographs of sections in dome dunes. A) Section G.1 looking to the northeast. B) Section G.2 looking west. See figure 2.1 for locations of sections.

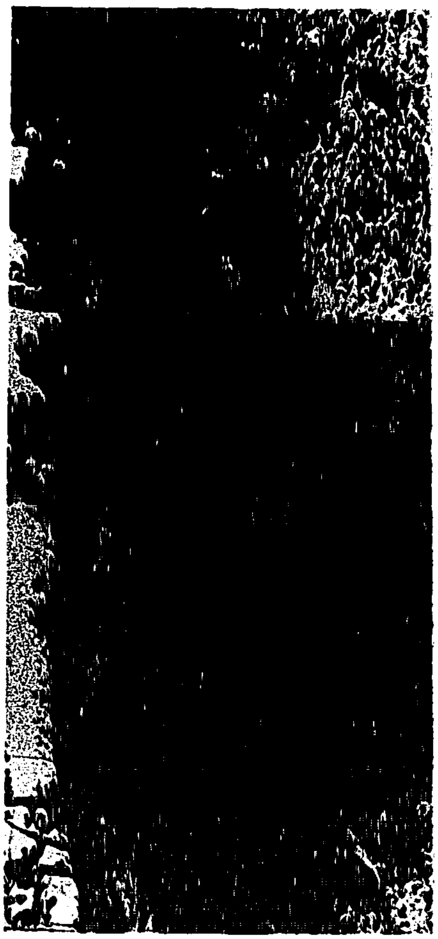

A)

B)

Laboratory Research

One hundred and eighty parabolic dunes were arbitrarily selected throughout the dune field to quantify dune morphology. Nose width, north and south arm lengths, and dune orientation were measured directly from aerial photographs. Dune orientation was estimated by calculating the vector which bisects the chord connecting the outer edge of the dune arms. These results are presented in Appendix 2.

Textural analyses of sediments were conducted to aid in the interpretation of the processes responsible for the deposition of sediment. Sieves were spaced at 1/4 Ø intervals following the procedures of the American Society for Testing Materials (D423 1964). Hydrometer analyses were also performed (ASTM D422 1964) for samples with a silt and clay content greater than 5%. Textural data is recorded here as ø units (negative log to the base two of the diameter in millimetres). Samples collected near the surface had abundant calcareous root tubules. Samples containing disaggregated tubules were treated with 10 % HCl before textural analyses were conducted.

Grain size parameters were calculated using the graphical method of Folk and Ward (1957). A summary of results is given in Appendix 3. Duplicate sample runs were done to test for the replicability of the method. These showed that mean and sorting were repeatable and statistically significant, whereas skewness and kurtosis were not (Figure 6).

Figure 6: Comparison of grainsize statistics for duplicate samples showing that mean and sorting are repeatable and statistically significant, whereas skewness and kurtosis are not repeatable and are not statistically significant. A) Mean, B) Sorting, C) Skewness, and D) Kurtosis.

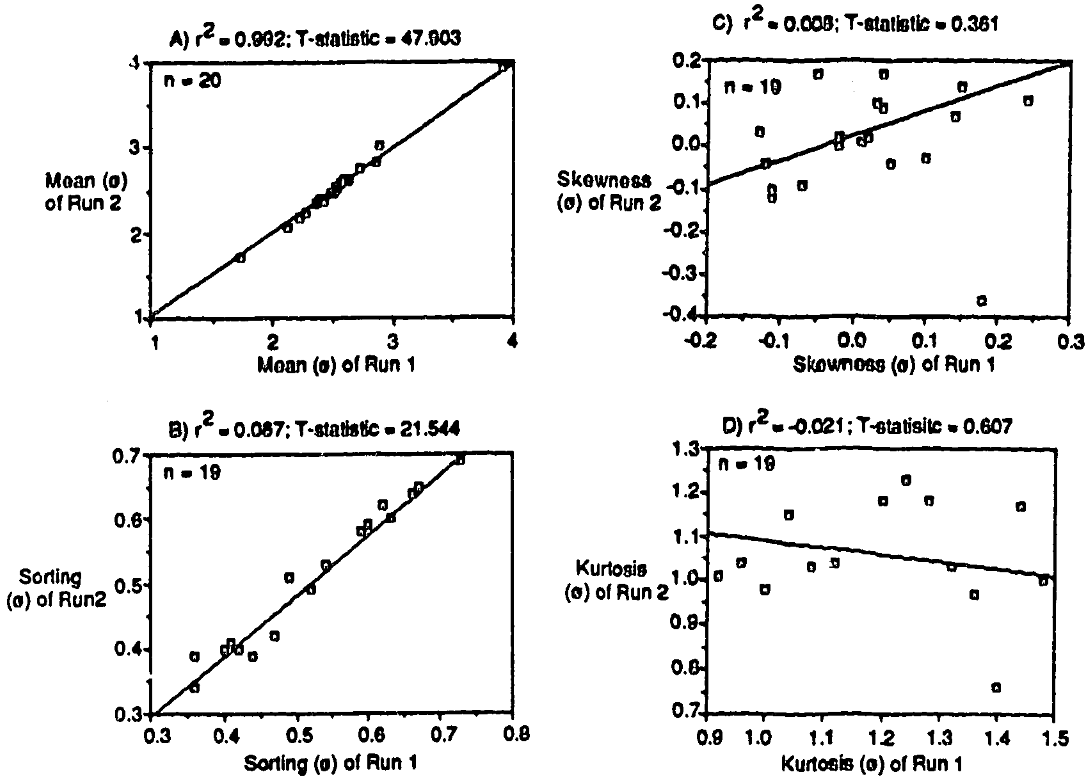

Skewness and kurtosis are not repeatable due to an error factor of +/- 0.5 g in the accuracy of the weigh scale used. This error factor resulted in smaller volumes of sediment which are present at the finest and coarsest ends of the grain size range to be weighed inaccurately. As the calculations for skewness and kurtosis are dependent on the tails of the grainsize distribution, whereas mean and sorting are not, they are not repeatable. Outliers for skewness and kurtosis occurred for some samples which were very well sorted as a result of this factor.

Mineralogical and shape analyses of medium grained sand from both terrace and dune sediments were performed on six samples using a binocular microscope. This was done to examine the similarities and differences between these two sediment types. One hundred grains were counted for each sample.

CHAPTER THREE: GEOMORPHOLOGY OF THE GRANDE PRAIRIE DUNE FIELD

Introduction

Dune development and morphology are controlled by a number of factors. The most important of these factors include surface airflow and sediment mobility (Wasson and Hyde 1983). Surface airflow is mainly controlled by wind direction(s) and velocity(s) and topography. Sediment mobility is dominantly controlled by the characteristics of the particles (eg. size, shape, and specific gravity), surface moisture, the thickness and lateral extent of the source deposit, and vegetation cover. Temporal and/or spatial changes in these controls will cause a variation in dune morphology.

Parabolic dunes

In the Grande Prairie dune field two geomorphic forms of parabolic dunes are present (Table 1) (Figure 7). These two geomorphic forms are gradational to each other (Figure 7). The first type of parabolic dune, designated type 1, is composed of long, narrow dunes which are present at elevations of 660m - 690m and tend to be located along the upwind and southern edges of the dune field (Figure 5). Type 1 parabolic dunes are low (5 - 10 m in height), have long arms (300 - 900 m), and short nose widths (45 - 100 m) (Appendix 2). The second type of parabolic dune, designated type 2, is composed of

Table 1: Table summarizing the differences between the two end member geomorphic forms of parabolic dunes present in the study area.

Parabolic dune type	Type 1	Type 2
Elevation	660 - 690 m	600 - 660 m
Dune height	5 - 10 m	15 - 20 m
Arm length	300 - 900 m	90 m^{+}
Nose width	45 - 100 m	50 m^{+}

Figure 7: Graph showing the two geomorphic forms of parabolic dunes present in the Grande Prairie dune field. The two different dune types have been distinguished here on the basis of the width of the dune crest and the sum of the length of both dune arms. Some overlap is present between the two dune types which is due to dune asymmetry. Type 1 parabolic dunes are represented by open squares, while type 2 parabolic dunes are represented by diamonds.

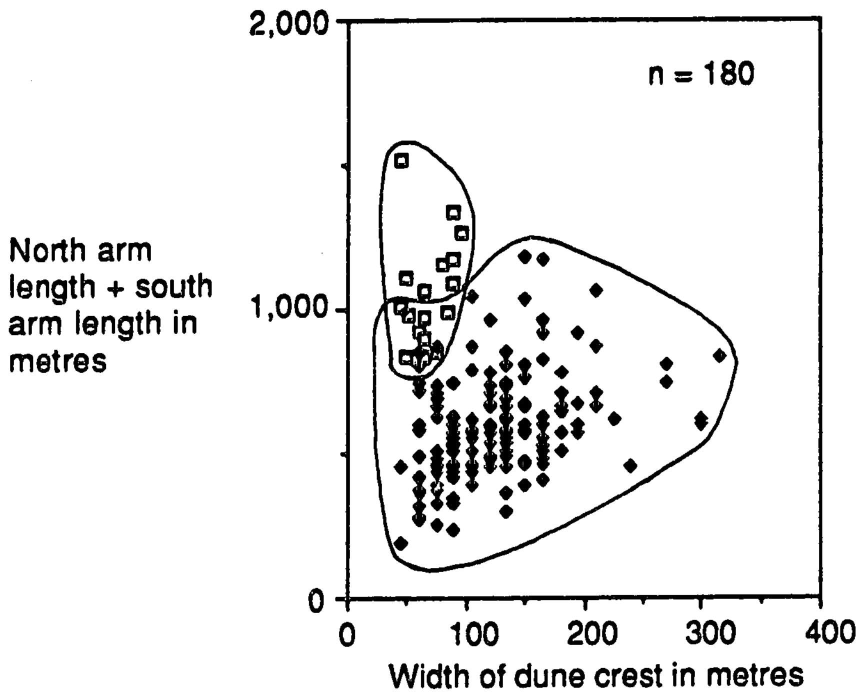

short, open dunes which are present at elevations of 600 - 660m. The second type of dune is high (15 - 20 m in height), has short arms (90 m^+), and wide nose widths (50 m^+) (Appendix 2).

The variation in geomorphology of the parabolic dunes of the Grande Prairie dune field is due to spatial and temporal differences in the environmental conditions under which they developed. Since the nose of a parabolic dune migrates while the arms remain relatively stationary, parabolic dune length is proportional to the amount of migration. For this reason, parabolic dunes in the Grande Prairie dune field with longer arms must have had a faster migration rate or have been active for a longer time period than dunes with shorter arms.

The migration rate of a dune is generally controlled by the directions and velocity of the wind, dune height, sediment supply, and the sediment budget of the dune (McKee and Douglass 1971, Cooke and Warren 1973). The stronger and more consistent in direction the surface wind is, the faster a dune will migrate in a given direction (Fryberger 1979). Dune height is also an important controlling factor in dune migration. Under the same conditions larger dunes will migrate at a slower rate than smaller dunes, as larger dunes require more sediment (Hasenrath 1967, Long and Sharp 1964, Norris 1966). In general, when sediment supply is high a dune will migrate at a faster rate as more sediment will be deposited on its lee side (Cooke and Warren 1973).

Dune height was probably an important factor in governing migration rates in the Grande Prairie dune field. Higher dunes require more sediment to migrate at the same rate as lower dunes. Higher parabolic dunes (type 2) have much shorter arms than low parabolic dunes (type 1), suggesting this factor affected dune morphology in the study area.

The sediment budget of a dune is also an important consideration (Mainguet and Chemin 1983, Marzolf 1988). Sediment budget can be defined as the retention capability of sediment on a dune. As the sediment budget of a dune not only depends on how much sediment is removed but on how much sediment is originally deposited, sediment supply should also control dune geomorphology. Dune migration is more efficient when more sediment is removed from the upwind portion of a parabolic dune than is deposited (negative sediment budget). Parabolic dunes develop negative sediment budgets and will migrate faster when the dune deflates easily (eg. has a dry surface) and/or has a low sediment supply. Parabolic dunes will migrate at a slower rate when the dune does not deflate easily (eg. has a wet surface) and/or has a high sediment supply. This implies that type 1 parabolic dunes may have had a lower sediment budget and supply than type 2 parabolic dunes.

In the Grande Prairie dune field both parabolic dune types may be asymmetrical, with north and south arms differing in length by as much as 500m. There was no tendency noted for northern of southern arms to be longer (Figure 8). Dune asymmetry may be generated by several mechanisms. These mechanisms include an asymmetry in the sand supply (Rim 1958), a sloping or irregular depositional surface (Long and Sharp 1964, Lettau and Lettau 1969), or an asymmetry in the wind pattern (King 1918, Melton 1940, Holm 1960, Norris 1966). As there is no preference for northern or southern arms to be longer in the study area, a regional asymmetry in sand supply, or a variation in the regional slope of the depositional surface can not be responsible for dune asymmetry. It is also unlikely that dune asymmetry was generated by an irregular depositional surface as the dunes have developed on fluvial terraces and glaciolacustrine sediments which are generally flat.

Measurement made on arm length and dune orientation showed a weak correlation; with the correlation coefficient $r^2 = 0.44$ (Figure 8). Dunes with longer northern arms tended to be oriented in a more northerly direction than the mean orientation (85.5°) (Figure 8). Conversely, dunes with longer southern arms tended to be oriented in a more southerly direction than the mean orientation (Figure 8). As parabolic dune orientation can be used as a predictor of surface airflow (Marrs and Gaylord 1982), this relationship suggests that secondary airflow generated by the dunes probably played a major role in developing dune asymmetry. This occurs because secondary airflow will generate uneven erosion and deposition. For example, when surface airflow is deflected to the north, the southern arm of a dune will be preferentially eroded, resulting in a parabolic dune with a longer northern arm.

Figure 8: Relationship of parabolic dune orientation and asymmetry. The relationship shows that dune asymmetry can be correlated to dune orientation with dunes that have longer north arms being oriented north of the mean orientation, and dunes with longer south arms being oriented south of the mean orientation. This relationship is statistically significant.

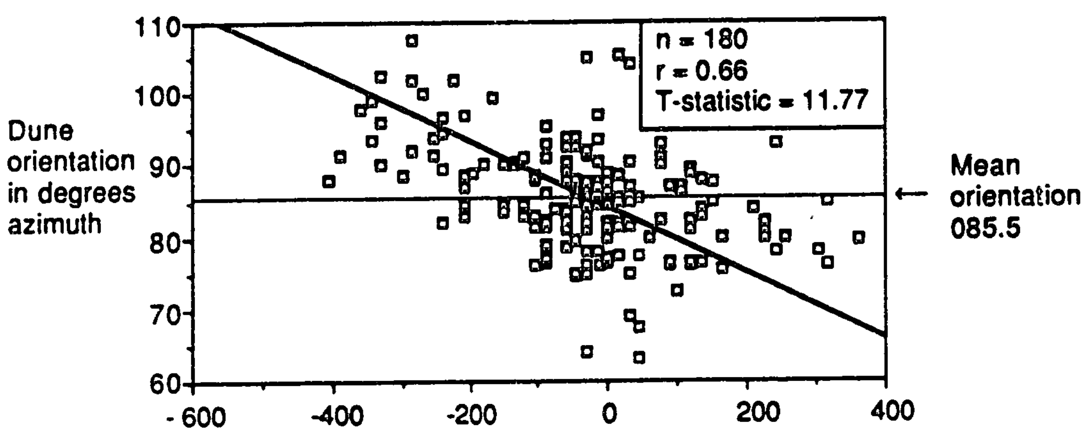

Dome dunes

Dome dunes in the Grande Prairie dune field are low (3 - 7 m in height), and vary in width from approximately 20 - 200 m. They are present on the downwind northern end of the dune field at elevations of 600m - 630m. The relatively smaller volume of sediment which composes dome dunes as opposed to parabolic dunes in the study area, suggests that they either had a much lower sedimentation rate, or that they developed over a shorter time period.

Fine sand present in dome dunes tends to be more poorly sorted than fine sand present in parabolic dunes with similar mean grain sizes (Figure 9). This suggests that less reworking has occurred in dome dunes. Thus, dome dunes probably had a larger positive sediment budget than parabolic dunes. This is also suggested by the geomorphic configuration of dome dunes which implies that they underwent very little migration. Moisture may have been an important factor in controlling the sediment budget of dome dunes.

Factors controlling dune type in the study area

The differing morphologies of the dunes present in the Grande Prairie dune field, as well as the variations in mean grain size and sorting, suggests that sediment supply, the duration of aeolian activity, and the sediment budget of the dunes may all have played a major role in controlling dune development.

Figure 9: Grain size and sorting for samples taken from parabolic and dome dunes in the study area. The squares represent samples taken from parabolic dunes, whereas the diamonds represent samples taken from dome dunes. A) This graph represents a scatter plot, B) This graph represents the regression lines for grainsize and sorting for both parabolic and dome dunes.

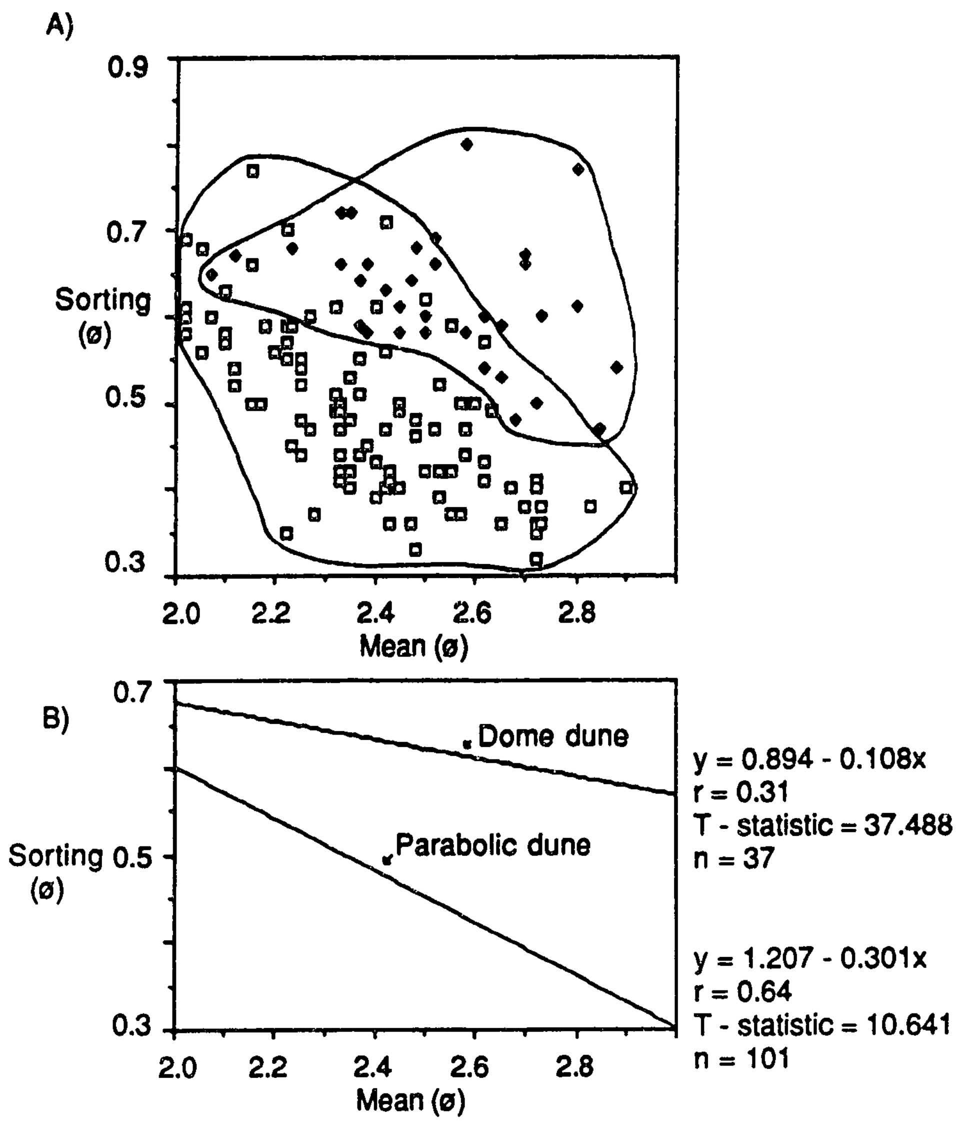

In general type 1 parabolic dunes migrated efficiently suggesting that they had a lower sediment budget and/or were active for a longer time period (Figure 10).

Type 2 parabolic dunes had a higher sediment budget and/or were active for a shorter time period as they did not migrate efficiently (Figure 10). As these type 2 dunes are significantly larger than those of type 1, they probably had a greater sediment supply (Figure 10). In contrast, dome dunes either had a much lower sediment supply and/or were active for a much shorter time period than either type of parabolic dune (Figure 10). Dome dunes also had a higher sediment budget than parabolic dunes (Figure 10).

Figure 10: Schematic diagram showing the relationship of the three main dune types to sand supply, time period of aeolian activity, and dune sediment budget (moisture). Dome dunes may develop over a short time period with a low sediment supply and budget, or with a high sediment budget. Type 1 parabolic dunes will develop over a long time period when there is a low sediment supply and budget. Type 2 parabolic dunes will develop when the sediment supply and budget is transitional to type 1 parabolic dunes and dome dunes.

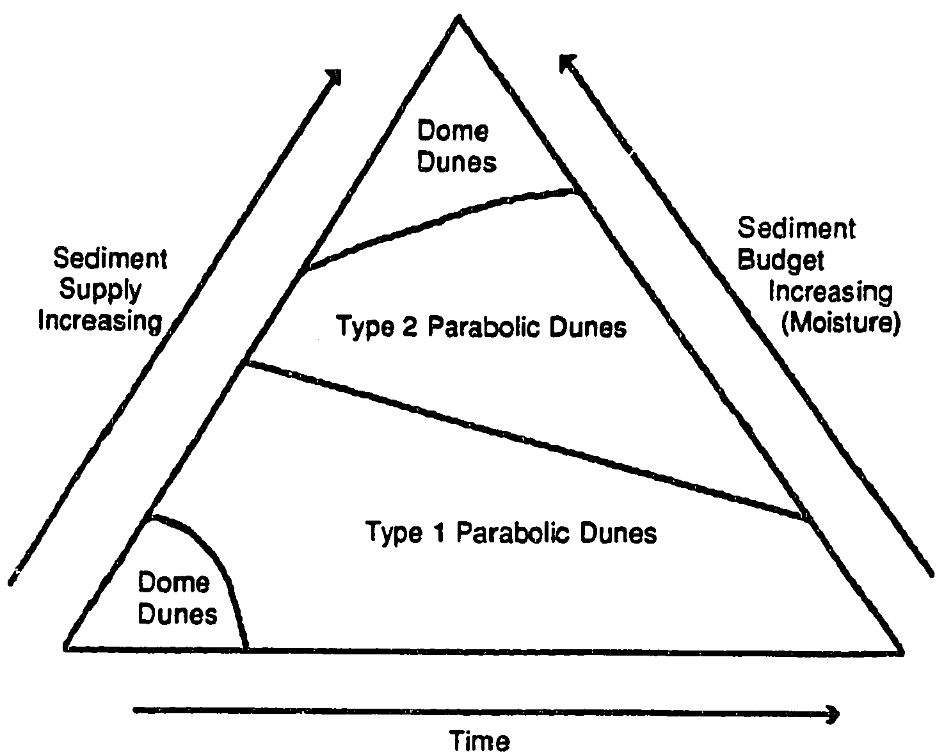

CHAPTER FOUR: SEDIMENTOLOGICAL ANALYSIS

Introduction

In the Grande Prairie dune field, sediments present in the sand dunes have been subdivided into ten facies and eight subfacies on the basis of sedimentary structures, and unit morphology. The results are summarized in Table 2 (in pocket). The general location of each facies in the dune types examined is given in Table 3. One additional facies overlying the sand dunes has been recognized. Each facies and subfacies is described and the processes responsible for their deposition are interpreted. The relative percentages of the occurrence of each facies and subfacies were calculated by measuring the thickness of each facies and subfacies examined in all sections and comparing them to the total thickness of all sections.

Facies A: Tabular medium to fine sand beds

Description

Facies A is composed of moderate to well-sorted tabular beds of sand which drape over the underlying topography. The beds are not present as sets, being always isolated from each other. Internal structures are not visible in the field. This facies has been subdivided on the basis of grain size (Figure 11).

Table 3: Summary table of facies associations and characteristics of the dune types present in the Grande Prairie dune field.

DUNE TYPE	DOME DUNE	SOLITARY PARABOLIC DUNE		COMPOUND PARABOLIC DUNE	
		TYPE 1	TYPE 2	TYPE 1	TYPE 2
SPREAD OF DIP DIRECTIONS	360°	170°	130°	300°	360°
LEE SIDE DEPOSITS	Facies C dominates. Facies B may be present. Preservation potential is moderate.	Subfacies B.1 dominates. Facies C may be present. Preservation potential is high.	Subfacies B.1 dominates. Facies C may be present. Preservation potential is high.	Facies C represents lee deposits at the intersection point. Preservation potential is high.	Facies C and D and subfacies B.2 represent deposits at the intersection point. Preservation potential is high.
BOTTOMSET OR DOWNWIND DUNE DEPOSITS	Facies C and D are present. Subfacies A.2 may be present. Preservation potential of bottomset deposits is high.	Facies C and D are present. Subfacies A.2 may be presesent. Preservation potential is high.	Facies C and D are present. Subfacies A.2 and J may be present. Preservation poteridal is high.	Preservation potential of downwind dune is low.	Preservation potential of downwind dune is high.
TOPSET DEPOSITS	Subfacies E.2 dominates. Subfacies A.1, E.1, and facies H, I, and J may also be present. Preserbation potential is high,	Facies E.2 dominates. Subfacies A.1 and facies D may also be present. Facies C is present on arms only. Preservation potential is low.	Facies E.2 dominates. Subfacies A.1, A.2, and E.1, and facies F G, H, I, and J may be present. Preservation potential is high	Facies E.2 dominates. with facies D also present. Preservation potential is low.	Facies E.2 dominates. Subfacies A.1, A.2, and E.1, facies F, G, H, I, and J may be present. Preservation potential is high.
STOSS DEPOSITS	Subfacies E.3. Preservation potential is moderate.	None observed. Preservation potential is assumed to be very low.	None observed. Preservation potential is assumed to be very low.	None observed. Preservation potential is very low.	Subfacies E.3 is present. Preservation potential is moderate.
STACKING ORDER	Topset / Stoss deposits Lee / Bottomset deposits Bottomset deposits	Topset deposits Lee / Bottomset deposits Bottomset deposits	Topset deposits Lee / Bottomset deposit Bottomset deposits	Topset deposits Lee deposits Downwind dune deposits	Topset deposits Lee / Stoss deposits Downwind dune deposits

Figure 11: Grain size and sorting variation of facies A. Subfacies A.1 is represented by diamonds, and subfacies A.2 by open squares.

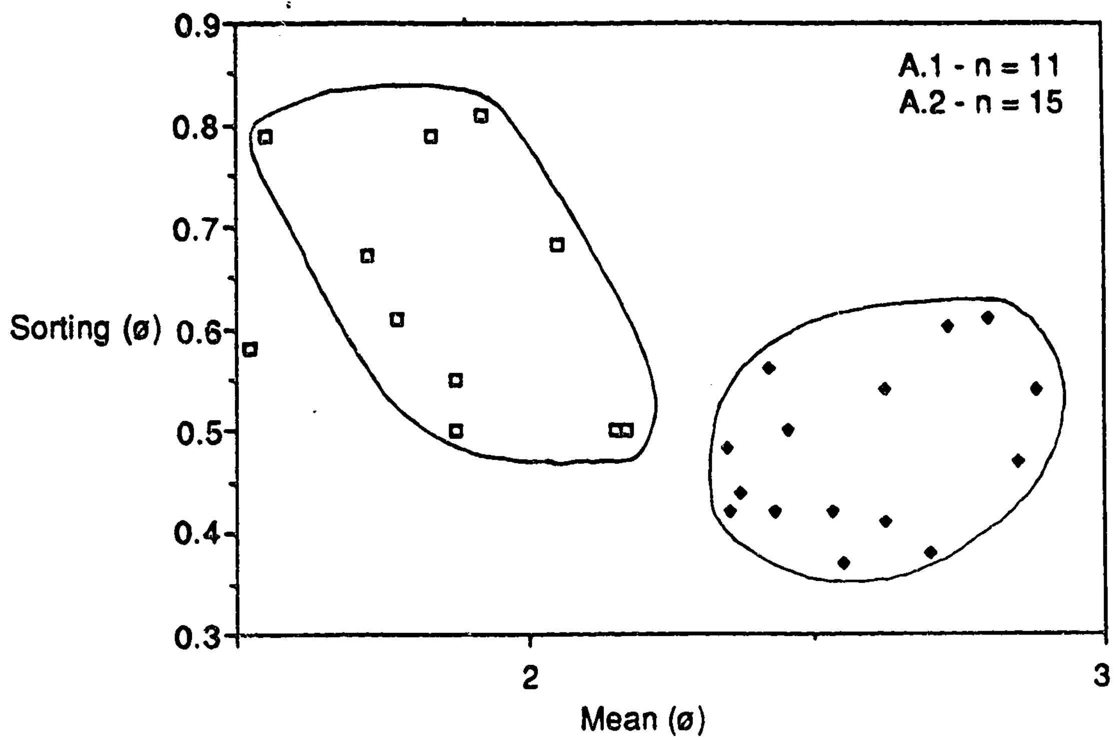

Subfacies A.1: Tabular fine sand beds

Beds of subfacies A.1 are 1.1 - 7.0 cm thick and dip 0° - 10°. Calcareous root tubules are rarely associated with subfacies A.1. Where they are present, they are spaced laterally every 90 - 150 cm and appear to slightly disrupt the beds. Upper bed surfaces of subfacies A.1 may be smooth (5%), rough and uneven (1%) (Plate 4a), or rippled (1%). Rippled upper bed surfaces have a (RI) ripple index of wavelength/height (Tanner 1967) of approximately 20-40. One bed has an upper surface with truncated ripples.

Subfacies A.1 may grade into laminated sediment of facies E or corrugated laminations of facies I. Subfacies A.1 is found in topset deposits of dome and type 2 parabolic dunes (Table 3). Subfacies A.1 represents approximately 7% of the sediments examined

Subfacies A.2: Tabular medium sand beds

Subfacies A.2 is characterised by tabular beds of medium sand which vary from 0.8 - 7.0 cm in thickness. These beds dip 0° - 18° with a dip direction of 000 - 245 (mean 056). In general, higher angle beds (10° - 18°) have a more easterly dip direction than lower angle beds (0° - 9°). Individual beds vary in orientation and dip where they conform to curved underlying contacts (Plate 4b). These contacts may be concave-upwards or concave-downwards.

The upper bed surfaces vary from flat, to irregularly undulating to rippled.

Plate 4 : Photographs of facies A. A) Massive bed of fine sand which represents subfacies A.1. The lower contact grades from indistinct corrugated laminations of facies I. Note the rough uneven nature of the upper bed surface. The camera lens is 5 cm in diameter

B) Massive tabular bed of medium sand classified as subfacies A.2. This bed varies in dip as it conforms to a curved concave-downwards lower contact. The upper contact becomes irregular where the dip decreases. The field note book is 18.5 cm high. Subfacies A.2 is overlain by facies B.2 / C. Arrows point to wedge-shaped strata interpreted as avalanche deposits and to high angle asymmetrical folds.

A)

B)

Where the upper surface is rippled, the RI ranges from 20 - 50 (mean 33.3), with the trough width of the ripples always being greater then the width of the ripples. Beds conforming to curved concave-upwards surfaces become more irregular, and slightly thicker where the dip of the bed becomes shallower (Plate 4b).

Subfacies A.2 occurs in bottomset deposits of all dune types and topset deposits of type 2 parabolic dunes (Table 3). Subfacies A.2 represents approximately 5% of the sediments examined.

Interpretation

Tabular beds of fine sand similar to those of subfacies A.1 are deposited in the aeolian environment when ripple migration is inhibited by the process of grainfall (Hunter 1977a). Grainfall occurs when the particle falls below the fluid threshold (A). Greeley and Iversen (1985) define the fluid threshold as:

$$A = (U^*)^2 p_F/p_p g D_p$$

Where: U^* is the surface friction speed
p_F is the density of the fluid
p_P is the density of the particle
g is acceleration due to gravity
D_p is the diameter of the particle.

The low angle of dip of facies A suggests that deposition occurred on shallow slopes. Grainfall will occur on shallow slopes when the surface friction speed is decreased by topographic obstacles such as vegetation (Glennie and Evamy 1968, Hummel and Kocurek 1984). Calcareous root tubules are found associated with subfacies A.1. Slightly disrupted beds of subfacies A.1 surround calcareous root tubules. This suggests that vegetation was present when the sediments were deposited. Thus, vegetation may have reduced the fluid threshold resulting in grainfall and the deposition of some beds of subfacies A.1.

Grainfall can also occur on shallow slopes when oblique winds with relatively low shear velocities transport large amounts of sediment (Hunter 1977a). High sedimentation rates dampen ripple formation limiting grain segregation and thus the development of laminations (Rim 1951, Yaalon 1967, Goldsmith 1973). The presence of ripples on upper surfaces of some beds of subfacies A.1 suggests that a temporary increase in sedimentation resulted in the deposition of a bed. Ripples subsequently developed when the sedimentation rate decreased and/or the potential for ripple migration increased. Ripple truncation probably developed when moist rippled surfaces were deflated by the wind. This occurs as coarser grained ripple crests will be less cohesive, drying faster and resulting in the removal of the relatively coarser grains present at the ripple crest (Gaylord 1982).

Other factors besides shear velocity affect the fluid threshold, and thus grainfall deposition (see Belly 1964, Borowka 1980, Hotta *et al.* 1984). Adhesion of a raindrop or snow particle to a sediment particle will increase the diameter of the grain lowering the fluid threshold. Local grain movement should theoretically occur for only a short period at the initiation of rainfall before the entire surface becomes saturated. This should result in abrupt upper bed surfaces which are not gradational. As sediment must be moving prior to deposition by wet grainfall, massive beds lain down by this mechanism should be gradational to underlying strata or have nonerosional lower bed surfaces. Some beds of subfacies A.1 meet these criteria.

The peculiar rough uneven appearance of the upper surface of some beds of subfacies A.1 can be explained if deposition was by wet grainfall. Soluble salts dissolved in rainwater will act as a cement when the sediment dries (Nickling and Ecclestone 1981). Exchangeable cations, such as Na^+, K^+, Ca^{2+} and Mg^{2+}, are present in the soils developed on the dunes (Twardy and Corns 1980). When saltation resumes erosion of the bed by grain impact will result, generating the rough uneven upper bed surfaces of subfacies A.1. Erosion may also result from the impact of hail stones. Small troughs associated with calcareous root tubules on upper bed surfaces of subfacies A.1 result from scouring at the base of vegetation (see Fryberger *et al.* 1979).

Subfacies A.1 is interpreted to have been deposited by grainfall. Various mechanisms were required to generate a decrease in the fluid threshold which resulted in the deposition of subfacies A.1. For beds associated with calcareous root tubules grainfall appears to have been generated in part by the presence of vegetation. For beds with rough uneven bed surfaces the fluid threshold was decreased from moisture adhering to the sediment resulting in wet grainfall

The variation in the upper bed surfaces of subfacies A.2 can be readily explained if movement of waterlogged sediment was important in its deposition. Movement of sediment downslope during liquefaction will lead to compression and contortion resulting in a higher degree of irregularity on the upper bed surface (Ahlbrandt and Andrews 1978, Steidtmann 1982). This can be related to the higher degree of irregularity of the upper bed surfaces of subfacies A.2, where the dip of a bed becomes shallower and explains the tendency for the beds to thicken. Movement of water logged sediment will also destroy any previous structures resulting in the deposition of a structureless bed (Ruegg 1983, Schwan 1986, 1987). The deposition of subfacies A.2 occurred after heavy rains or during snow melt.

The high RI of ripples present on the upper surface of some beds of subfacies A.2 can be attributed to wide trough widths. Sharp (1963) lists three factors which will increase trough width: high shear velocity, reduced sand supply, and resistance to erosion of the surface under the ripple (eg. a wet or frozen surface). When liquefaction occurs, sediment will be saturated, resisting erosion and reducing sand supply.

Facies B: Sets of high-angle cross-strata

Description

This facies consists of solitary and compound sets of cross-strata. Sets are tabular to wedge shaped and may interfinger with or grade laterally into other facies. Strata dip at high angles (22° - 36°) (Plate 5a), and are bounded by planar to curved surfaces which dip at lower angles (0° - 20°). Deformation structures such as normal faults, drag folds, and brecciated blocks are present but are rare (Plate 5b). Subfacies have been designated on the basis of the shape of the cross-strata present in a set.

Subfacies B.1: Sets of high-angle, concave-downwards cross-strata

Sets of high-angle, concave-downwards cross-strata may be solitary or compound (Plate 5b). Solitary sets are 0.4 - 12.0 m in thickness and are highly variable in shape as the nature of the lower bounding surface varies. Solitary sets have curved to planar lower bounding surfaces which vary in dip from 0° - 20° with a dip direction of 045 - 240. Upper bounding surfaces are generally planar and near horizontal. Solitary sets are present in the lee of both type 1 and type 2 parabolic dunes (Table 3) and represent approximately 6% of the sediments examined. Compound sets are 2.5 - 15 m in thickness and are tabular in shape. Lower and upper bounding surfaces of compound sets are planar and dip 0° - 5° with a dip direction of 070 - 125. Thick compound sets of subfacies B.1 were only observed in two sections (P.5 and GP.5) and represented 85% of the sediment in these two sections.

Sets of subfacies B.1 contain interbedded wedge and tabular shaped, concave-downwards cross-strata. Strata have a maximum dip of 26° - 33° with a dip direction of 060 - 135. Strata are abrupt to slightly asymptotic to lower bounding surfaces and are truncated by upper bounding surfaces.

Plate 5: Photographs of facies B. A) Section through the crest of a parabolic dune showing a thick sequence of high-angle cross-strata. B) Sets of high- angle, concave- downwards cross-strata of facies B.1. Arrows point to a deformation structure.

A)

B)

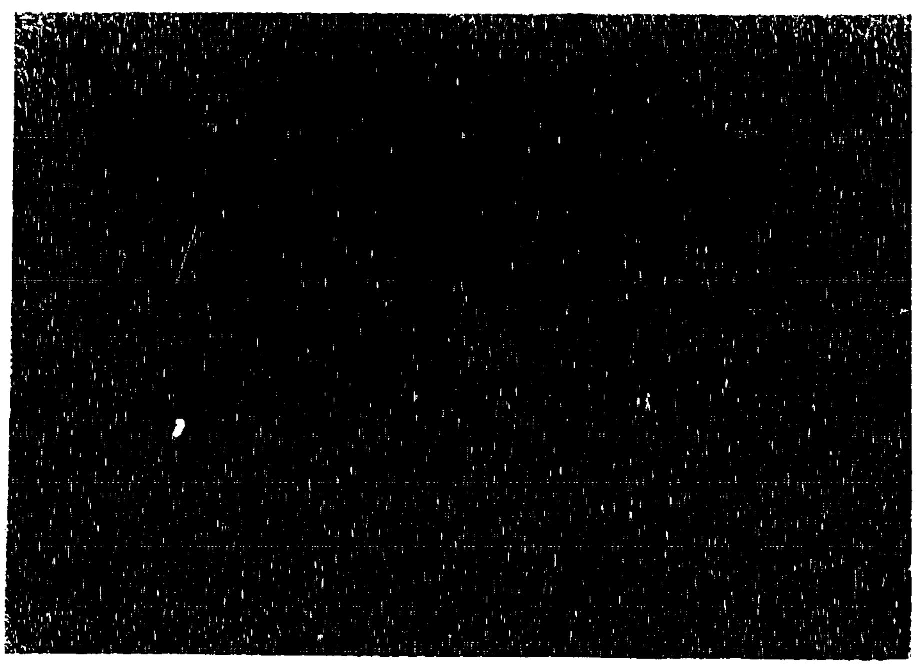

Sediments of subfacies B.1 are fine grained and well to moderately sorted (Table 2).

Tabular concave-downwards cross-strata compose 60-80 % of solitary sets and 90% or more of compound sets. As a set thickens the proportion of tabular strata increases. In solitary sets, tabular strata are 0.5 - 3.0 cm thick, whereas in compound sets the thickness varies from 1.3 - 8.0 cm. Tabular, concave-downwards cross-strata may thin to the west as the dip of the bed decreases, grading into finely laminated sediments of facies E. Wedge shaped, concave-downwards cross-strata have a maximum thickness of 0.3 - 0.8 cm and pinchout to the east. High-angle, asymmetrical folds are found on some upper bed surfaces forming a staircase-like topography (Plate 4b).

Subfacies B.2: Sets of high-angle, concave-upwards cross-strata

Solitary, tabular sets of interbedded high-angle, concave-upwards, wedge-shaped and tabular cross-strata characterise subfacies B.2. Sets are 1.0 - 1.7 m thick and are bounded by planar, near horizontal lower and upper bounding surfaces.

Wedge-shaped, concave-upwards cross-strata are 0.4 - 3.0 cm thick and pinchout to the east or to the west. The maximum dip of these strata vary from 28° - 33° with a dip direction of 040 - 115. Strata which pinchout to the west decrease in dip towards the east (22° - 25°) as they become asymptotic to lower bounding surfaces. A series of high-angle, asymmetrical-rounded folds are present on some upper bed surfaces of strata which pinchout to the east, resulting in a staircase-like topography (Plate 4b). Biconvex lenses, 40 - 60 cm wide and 0.3 - 0.5 cm thick are present and represent the basal portion of wedge-shaped cross-strata cut at an oblique angle. Tabular, concave-upwards laminae are 0.1 - 0.6 cm thick and conform to the underlying topography. Thicker laminae can be normally graded or inversely graded. Sediments of subfacies B.2 are fine grained and moderately to well sorted (Table 2).

Subfacies B.2 is present in the lee of type 2 parabolic dunes which are migrating onto a downwind dune. Subfacies B.2 may also be occasionally present in the lee of dome dunes. This subfacies represents approximately 8% of the total sediments examined.

Subfacies B.3: Set of high-angle, planar-tabular cross-strata

Subfacies B.3 is characterised by a solitary small scale tabular set of high-angle, planar-tabular cross-strata. The set is 40 cm in thickness and is bounded by planar surfaces which dip 5° - 10° with a dip direction of 045 - 060. Strata are truncated by the upper bounding surface.

Cross-strata are planar tabular and range in thickness from 0.1 - 0.6 cm. Individual strata are abrupt to slightly asymptotic to lower bounding surfaces and are usually ungraded. Some laminations are normally graded. Strata dip 33° - 36° with a dip direction of 055. No deformation structures were noted. Sediments of subfacies B.3 are fine grained and well sorted (Table 2).

Subfacies B.3 is found only in the lee of section P.2 which is a type 1 parabolic dune. Subfacies B.3 represents less than 1% of the total sediments examined.

Interpretation

The high angle of dip of cross-strata of facies B (22° - 36°) and their location in the lee of dunes suggests that avalanching was involved in their deposition. Avalanching occurs on the slipface of a dune as grainflows in noncohesive sand, or slumps in cohesive sand when the angle of repose of the dune slipface is surpassed (Hunter 1977a). Grainflow was the dominant mechanism of avalanching as deformation structures which are generated during slumping (eg. brecciated blocks) are rare.

On the dune slipface the angle of repose may be exceeded by several mechanisms. Variations in these mechanisms produced the different configurations of facies B. Brink accumulation is one such mechanism, and involves a larger accumulation of sediment at the brink of the dune compared to the rest of the slipface (Hunter 1981). Preferential accumulation of sediment at the dune brink occurs from grainfall and results in the development of a concave-downward dune profile. The concave-downwards shape of cross-strata of subfacies B.1 suggests that preferential grainfall accumulation at the dune brink played a major role in avalanche generation for this subfacies.

The angle of repose of the slipface may also be exceeded by undercutting due to crosswinds, lee eddies, or other mechanisms (McKee 1945, 1966). Crosswinds and lee eddies transport sediment up or along the slipface and deposit strata which pinchout upslope (Hunter 1981). The presence of wedge cross-strata which pinchout up the slipface in sets of subfacies B.2 indicates that lee eddies or crosswinds were responsible for deposition, and may have, in part, induced avalanching.

The presence of high-angle, asymmetrical folds on upper bed surfaces of cross-strata of subfacies B.1 and B.2 suggests that compressional deformation occurred. Similar results have been produced in labs (McKee *et al.*1971), and have been observed in the field (Bigarella 1975). Noncohesive sand in the aeolian environment may be either dry or saturated (Bigarella *et al.* 1969). Folds tend to occur mainly in saturated noncohesive sand as a response to deformation during avalanching (McKee and Bigarella 1972). Water adds additional weight and decreases frictional resistance resulting in slumping at lower angles (Hack 1941, Pye 1983). This process has been observed as a result of heavy rains on dune slipfaces by Hack (1941), Ward (1977), and Pye (1982, 1983). As many of the strata which have high-angle, asymmetrical folds on upper surfaces dip at angles considerably below the angle of repose of dry sand (26° - 30°), the sediment was saturated during avalanching.

Subfacies B.3 is composed of a high proportion of cross-strata which have dip angles at or above the angle of repose of dry, well sorted, fine sand (see Allen 1970, 1984; Statham 1974). Cross-strata above the angle of repose of dry sand can not have avalanched regardless of initial moisture conditions (Allen 1970; Carrigy 1970). As strata of subfacies B.3 generally dip at or greater than 34° a high degree of cohesion must have been present to prevent failure. Therefore the depositional surface and/or the sediment must have been damp to wet when subfacies B.3 was being deposited. The tabular nature and steep dip of the cross-strata suggests that deposition was by wet grainfall in the lee of parabolic dunes.

Facies C: Tabular sets of low-angle cross-laminae

Description

Solitary and compound tabular sets of low-angle cross-laminae characterise facies C. Sets vary in thickness from 0.1 - 1.5 m and dip 0° - 10° with a dip direction of 040 - 180. Sediments range from fine to medium grained and may be moderately to well sorted. Laminae are abrupt to slightly asymptotic to lower bounding surfaces and are truncated by upper bounding surfaces (Plate 4b). Laminae are tabular and consistently parallel to each other within individual sets. They range in dip from 6° - 26° (average of 11°) with a dip direction of 035 - 150. Thicker sets generally have a higher angle of dip. Laminae range in thickness from 0.1 - 0.8 cm, and average 0.2 - 0.4 cm. Laminae are typically ungraded, though approximately 10 - 20 % appeared inversely graded in cuts at low angles to the laminae. Thicker laminae may be normally graded.

Facies C commonly grades into cross-strata of facies B or laminated sediments of facies E. Facies C is present in lee side and bottomset deposits of type 1 and type 2 parabolic dunes and also in dome dunes (Table 3). Facies C represents approximately 25% of the total sediments examined.

Interpretation

Sets of cross-strata are abrupt to slightly asymptotic to lower bounding surfaces, suggesting they were deposited as a bedform. The low to moderate dip of the cross-strata within a set (average 11°), suggests that the bedforms responsible for their deposition did not develop slipfaces. Tabular sets of low-angle cross-strata are commonly recognized in modern aeolian deposits (eg. McKee 1966, 1979), and have been related to the migration or buildup of bedforms without the development of slipfaces (Gaylord 1982). The low angle of dip of cross-strata of facies C, and the tabular configuration of the sets suggest that it was deposited in this manner.

Facies D: Wedge sets of low-angle cross-laminae

Description

Facies D is composed of wedge sets of low-angle laminae. Sets vary in thickness from 2 - 30 cm thinning to the east. Lower bounding surfaces may be planar or curved and range in dip from 2° - 28° with a dip direction of 045 - 150. Upper bounding surfaces are near horizontal and truncate underlying laminae. Facies D may interfinger with cross-strata of facies B or grade laterally into laminated sediments of facies E. Sediments are fine grained and well sorted.

Laminae range in thickness from 0.1 - 0.5 cm and are inversely graded or ungraded. The dip of laminae varies from 0° - 12°, becoming slightly shallower upwards within an individual set. Laminae always dip at lower angles than underlying bounding surfaces resulting in individual laminae pinching out upslope. The dip directions of these laminae range from 340 - 250, with none dipping towards the west.

Facies D is present in bottomset deposits of type 1 and type 2 parabolic dunes and dome dunes (Table 3) . Facies D may also be present in topset deposits of type 1 parabolic dunes (Table 3). Facies D represents approximately 10% of the total sediments examined.

Interpretation

Thin, low-angle, inversely-graded laminae similar to those of facies D are generally produced by the migration of climbing ripples during net deposition from the saltation and traction load (Hunter 1977a, 1977b). The wedge shaped configuration of facies D results from preferential net deposition of sediment in the downslope direction during ripple migration. This occurs as the direction of ripple migration is largely a function of the orientation of the wind relative to the depositional surface and the gradient of that surface (Howard 1977). When wind flow is oblique to the depositional surface, gravity will deflect the orientation of the ripple migration in the direction of dip of the depositional surface resulting in the deposition of laminae which pinchout upslope (Figure 12). This process of preferential downslope deposition during ripple migration has been documented in wind tunnels (eg. Fryberger and Schenk 1981). Thus laminae of facies D, which pinchout upslope, are diagnostic of deposition from ripple migration on a sloping surface by winds which are oblique to, or in the opposite direction of the slope.

Facies E: Sets of near horizontal strata

Description

Facies E is characterised by sets of near horizontal strata (Plate 6). Upper bounding surfaces dip at very low angles and truncate underlying strata. This facies locally grades into stratified sediments of facies A, B, C, D, G, H, and I. Facies E has been subdivided on the basis of the type of grading present in individual strata and on the dip direction of the strata.

Subfacies E.1: Sets of normally-graded, near horizontal strata which dip easterly

These normally-graded, near horizontal strata conform to lower bounding surfaces which may be planar or curved, and smooth, undulatory, or rippled. Deposition of these strata over undulatory and rippled lower bounding surfaces acts to progressively subdue the relief up section. Upper bounding surfaces dip at very low angles and truncate underlying strata. Sets vary in thickness from 3 - 100 cm and commonly grade vertically into subfacies E.2 in

Figure 12: Schematic diagram of translatent strata deposited on a moderately dipping surface by oblique winds. Saltating grains are deflected downslope by gravity, resulting in the direction of ripple migration being oblique to windflow. The sets are wedge shaped and pinchout upslope.

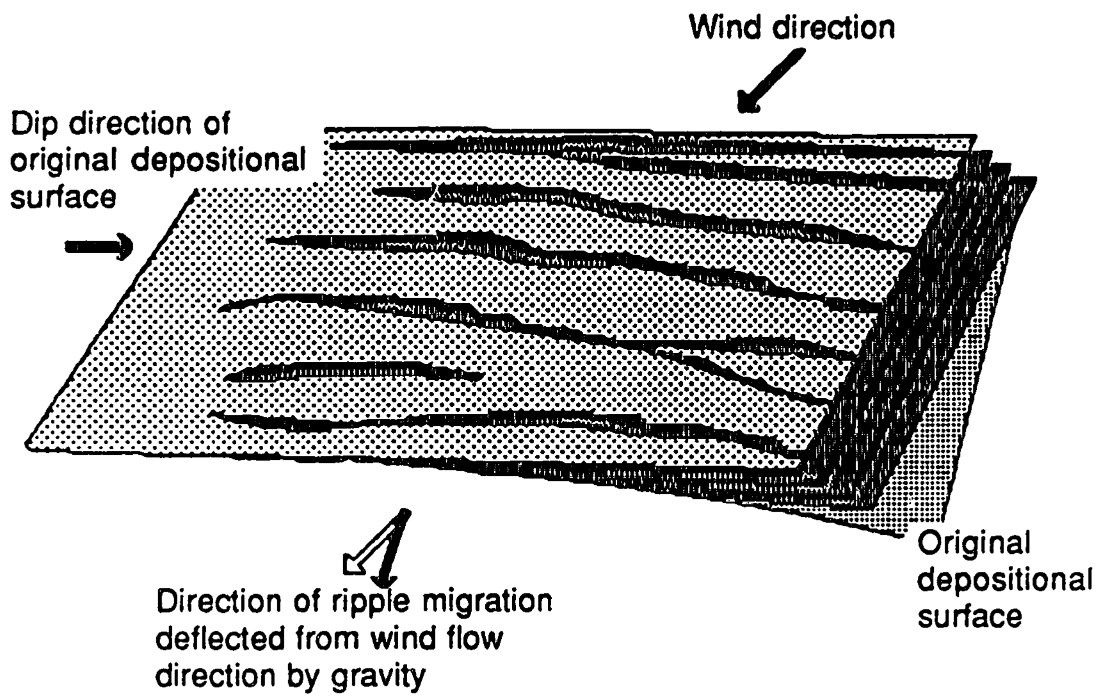

Plate 6: Photographs of facies E. A) Sets of subfacies E.2. Arrows indicate isolated ripple forms. The camera lens is 5 cm in diameter. B) Facies E.2 is overlain by facies E.3. The arrow points to the east in the direction of palaeowind flow inferred from the morphology of the parabolic dunes. The field book is 18.5 cm high and is inverted.

A)

B)

thicker sets. Sets are solitary or compound and are tabular in shape.

Strata range in thickness from 0.1 - 1.2 cm and average 0.6 - 0.7 cm. Strata dip 0° - 14° with a dip direction of 035 - 150. Sediments of subfacies E.1 are fine grained and well to moderately well sorted (Table 2).

Subfacies E.1 is present in topset deposits of type 2 parabolic dunes and is rarely present in topset deposits of dome dunes (Table 3). This subfacies represents 3% of all the sediments examined.

Subfacies E.2: Sets of ungraded to inversely-graded, near horizontal laminae which dip easterly

Subfacies E.2 is characterised by ungraded to inversely-graded, near horizontal laminae which conform to lower bounding surfaces. Ungraded laminae dominate, comprising 60 - 80 % of this subfacies. Lower bounding surfaces are smooth and may be planar or curved. Upper bounding surfaces truncate laminae and dip at very low angles. Some upper bounding surfaces are rippled with an RI of 20 - 30. Small troughs 0.4 - 1.3 cm deep and 5 - 14 cm wide which truncate underlying laminae may be present on upper bounding surfaces. Some troughs may have calcareous root tubules running through their centers Sets vary in thickness from 3 - 150 cm and may be solitary or compound. Thicker sets grade vertically into subfacies E.1.

Laminae range in thickness from <0.1 - 0.5 cm and dip 0° - 5° with a dip direction of 000 - 200. Ripple foreset cross-laminae may be present and dip 8° - 15° (Plate 6a). Sediments of subfacies E.2 are medium to fine grained and moderately to well sorted (Table 2). Medium grained laminae with isolated ripple forms up to 0.3 - 0.5 cm in height may be present (Plate 6a). Medium grained laminae are laterally discontinuous, extending no more than a metre in length.

Subfacies E.2 is present in topset deposits of all dune types (Table 3), and represents 30% of the total sediments examined.

Subfacies E.3: Ungraded, near horizontal laminae which dip westerly

Ungraded, laminae which conform to westerly dipping lower bounding surfaces characterise subfacies E.3. Lower bounding surfaces are smooth and planar as are upper bounding surfaces. Upper bounding surfaces dip at very low angles and truncate underlying laminae. Sets vary in thickness from 5 - 80 cm and are tabular.

Laminae range in thickness from <0.1 - 0.5 cm and dip 3° - 15° with a dip direction of 245 - 340 (Plate 6b). Sediments of subfacies E.3 are medium to fine grained and moderately to well sorted (Table 2). This subfacies is present in stoss deposits of all dune types and represents 3% of the sediments examined.

Interpretation

Sets of near horizontal strata which are separated by low-angle truncation surfaces similar to those of facies E develop from deposition followed by erosion (Kocurek 1986). Deposition of consistently parallel strata of facies E which conform to lower bounding surfaces will occur when that surface is in "equilibrium" with wind flow. Deposition of a set of facies E will continue on this surface (intermittently or continuously) as long as the effective sand transport direction does not vary significantly. As the morphology of the dune surface is mainly aerodynamically controlled it will respond rapidly to a shift in wind direction, resulting in erosion (Nielson and Kocurek 1987). Erosion will occur when the shear velocity of the wind is sufficient to transport sediment and the wind has an excess carrying capacity developing a set bounding surface of facies E. This occurs when the source of sediment is moist, or when grainfall or some other factor causes a local increase in the shear velocity of the wind (Hunter 1977a, Gaylord 1982).

Deposition of sets of strata on low-angle surfaces equivalent to those of facies E may occur from grainfall, ripple migration, or from the saltation and traction load at shear velocities too high for ripple formation (Hunter 1977a). Strata which drape over and progressively subdue the underlying topography, as in the case of subfacies E.1, are produced by grainfall. Individual strata are distinguishable due to upwind sorting of the sand during transport (Otto 1938, Hunter 1977a). Normal grading of subfacies E.1 laminae is produced during periods of decreasing shear velocity.

The presence of ripple foreset cross-laminae and inverse grading in subfacies E.2 suggests it was deposited from ripple migration. Inverse grading tends to develop as aeolian ripples are generally coarser grained at their crests (Hunter 1977a). Sets with well-sorted laminae of facies E.2 are equivalent to Fryberger *et al.*'s (1979) type "a" low-angle sand sheet deposit. Fryberger *et al.* (1979) considered sets of type "a" laminae to have been deposited during a single depositional phase of ripple migration. The sand supply must have been relatively uniform so that net deposition was continuous (Kocurek 1981). The shear velocity of the wind must have varied enough, however, to generate the grain size segregation required to distinguish ripple foreset cross-laminae.

Some ungraded strata with no distinguishable ripple foreset cross-laminae may have been deposited by grainfall. Subfacies E.2 also has some sets of laminae which have bulk sample means in the medium sand range (Table 2). The wind speeds required to move medium sand (20 - 40 m/s) can result in net deposition of sediment from the saltation and traction load without the formation of ripples (Hunter 1977a).

Laminated sets of subfacies E.2 which contain ripple forms of relatively coarse sand are equivalent to Fryberger *et al.* 's (1979) type "b" low-angle sand sheet deposit. Laminae develop from ripple migration with coarser grained sediment being deposited as a response to a decrease in sand supply or an increase in the shear velocity of the wind (Kocurek 1981). Coarser grained laminae may also result from deflation, although truncation will not occur since the dune surface is still in "equilibrium" with wind flow.

Rippled upper bounding surfaces of subfacies E.2 are preserved as they are buried by grainfall deposits or because they are cohesive, resisting erosion. Cohesion will occur when the surface is wet (Hummel and Kocurek 1984). Small troughs, associated with calcareous root tubules, result from scouring at the base of vegetation (see Fryberger *et al.* 1979).

Westerly dipping near horizontal strata of subfacies E.3 can be interpreted to represent deposition on the stoss slopes of dunes based on the dip direction. The grain size of stoss slopes is generally coarser than that of lee slopes (Cornish 1927, Folk 1971). This is due to the fact that the shear velocity of the wind increases on windward slopes as a result of flow compression (Mason and Sykes 1979, Bradley 1980, Lancaster 1985), and decreases down lee slopes as a result of flow expansion (Allen 1984). Variations in the shear velocity will be minimized when wind flow is oblique to the dune (Lancaster 1985). Thus, when wind flow is oblique to a dune, stoss and lee slopes should be roughly equivalent in grain size. Subfacies E.3 overlaps the grain size range of lee slope deposits (Table 2) suggesting that oblique winds played an important role in sediment deposition. Laminae may have developed from ripple migration, grainfall, and/or from the saltation and traction load at shear velocities too high for ripple migration.

Facies F: Coarse sand rich laminations

Description

Facies F is composed of a single lamina of medium sand which contains a high proportion of coarse sand (Appendix 3). Facies F has an upper bed surface which is ridged (Plate 7). Ridges are defined to have wavelengths greater than 20 cm (Cornish 1914, Sharp 1963, Ellwood *et al.* 1975). Facies F is near horizontal and has a lower contact which is abrupt and smooth. This lamina ranges from 2 to 3 grains in thickness to 1 cm, laterally thickening to the east. Ridges range from 2 - 3.5 cm in height and have a wavelength of 30 - 50 cm. Some ridges have lenses of fine sand in their lee side approximately 1cm in height and 3cm in width.

Facies F is represented by one lamina which extends the entire exposure of section GP.1 (approximately 30m) (Appendix 1). It occurs as a topset deposit in this type 2 parabolic dune.

Interpretation

Ridges, such as those of facies F, are only considered to develop in the aeolian environment during net removal under the saltation and traction load (Bagnold 1954). As deflation occurs the surface becomes progressively coarser until there are no grains which can be moved directly by the wind. As facies F represents the coarsest grained sediment present in the dunes (Appendix 3), it seems likely that some deflation occurred during its development. As deflation occurs coarser grains will be driven by the impact of finer grains up and over surface irregularities and will build up on the lee side (Bagnold 1954) (Figure 13). Very few grains will impact on the lee side of the irregularity as the angle of incidence will be low compared with the

Plate 7: Photograph of facies F. Note large ridge of medium sand in the center of the photo. Facies F is overlain by facies C/E.2. The arrow is pointing to a low-angle ripple foreset which has been preserved. The fieldbook is 18.5 cm high.

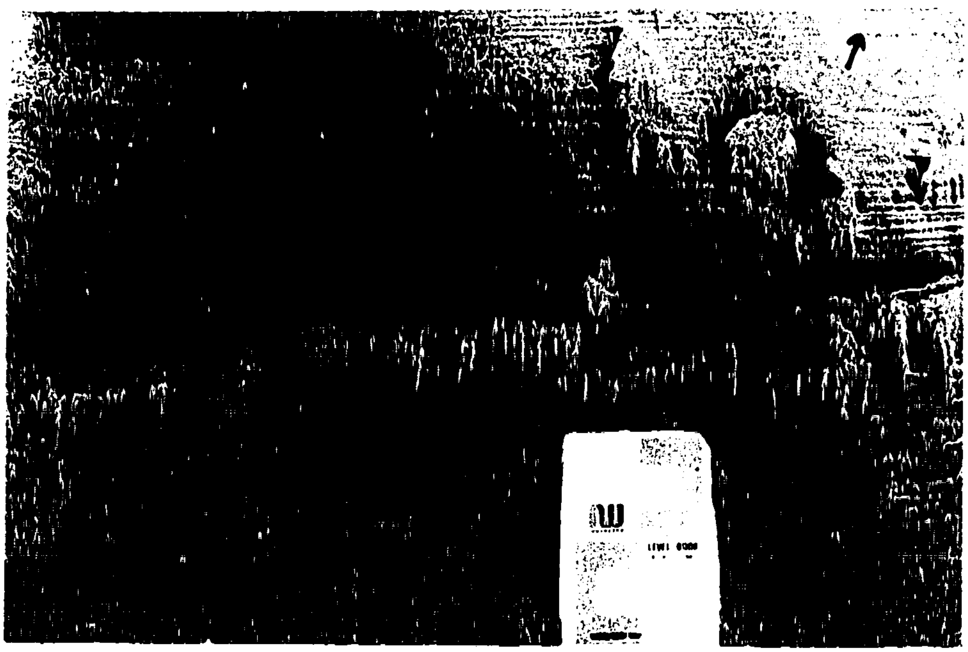

Figure 13: Schematic diagram showing the development of facies F. A) Saltating grains tend to accumulate on the stoss slope of an irregularity as it has a higher angle of incidence with the trajectory of a saltating grain. When grains move by creep to the lee slope they will not be removed by saltating grains, and the irregularity will grow. B) A decrease in the shear velocity of the wind or an increase in sediment supply will result in deposition of fine sand. C) When the shear velocity of the wind increases this fine sediment will be removed. If the ridge is large enough a zone of flow separation may be present in its lee, preserving a lens of fine sand.

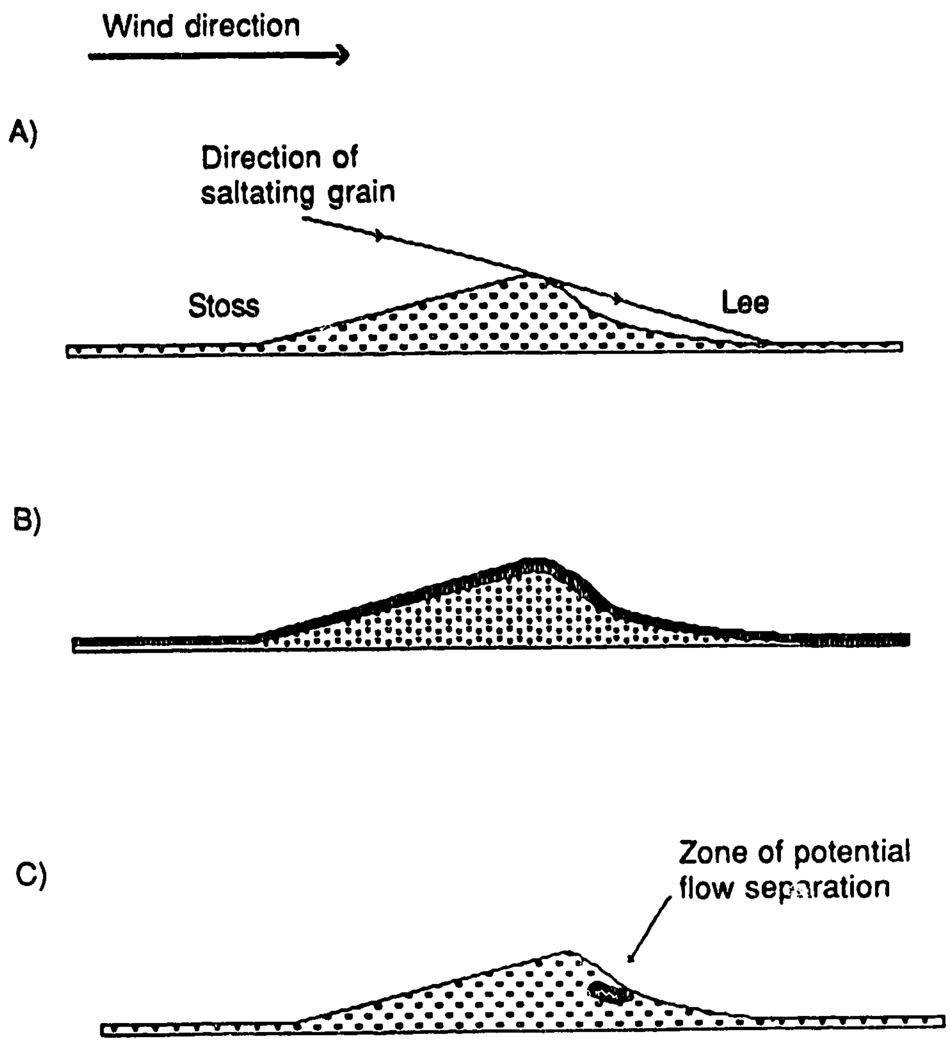
Wind direction
A)
Direction of
saltating grain
Stoss
Lee
B)
C)
Zone of potential
flow separation

trajectory of the saltating grains (Bagnold 1954) (Figure 13). Thus, there will be a net accumulation of coarser grains and the irregularity will grow in size producing ridges of facies F.

Fine sand in the lee of ridges of facies F may have been deposited when the saltation and traction load was large enough to impart a sufficient drag on the shear velocity of the wind such that net deposition occurred. When the saltation and traction load decreased, or when the shear velocity of the wind increased, fine sand would be removed. If the ridge is large enough a zone of flow separation may be present in the lee, and the fine sand will not be removed here (Figure 13). Moisture may also assist in limiting removal. This mechanism may have generated the lenses of fine sand present in the lee of some ridges of facies F.

Facies G: Plano-convex lenses of sand associated with calcareous root tubules

Description

Facies G is composed of plano-convex lenses of well to moderately well sorted, fine sand. The plano-convex lenses of sand have a maximum height and width which may range from 1.0 - 60.0 cm and 0.05 - 3.0 m. These plano-convex lenses of sand are associated with calcareous root tubules in their thickest and widest part, or have a very small amount of organic debris present.

Facies G grades laterally and vertically into horizontal strata of Facies E. Facies G is present in topset deposits of type 2 parabolic and dome dunes (Table 3). Facies G represents approximately 1% of the sediments examined.

Interpretation

The presence of organic debris and calcareous root tubules in facies G suggests that these plano-convex lenses were deposited as a result of the interaction of the saltation and traction load with vegetation. The accumulation of large mounds of sediment in and to the lee of vegetation on interdune and sand sheet deposits has commonly been reported (Frere 1870; Hefley and Sidwell 1945; Cooke and Warren 1973; Goldsmith 1977, 1985; McKee 1982). Deposition of facies G began as vegetatively induced grainfall resulting in the deposition of a mound of sediment. The size of these large mounds is a function of the original size and shape of the shrub or clump of vegetation and the rate of growth and/or regeneration of the vegetation in relation to sediment deposition (Melton 1940, Olson 1958, Hesp 1981). The mound becomes buried when the rate of sediment deposition exceeds plant growth progressively decreasing the amount of grainfall. Laminae began to develop as the vegetation was covered, reducing grainfall and increasing ripple migration resulting in facies G to grade into facies E.

Facies H: Plano-convex lenses of sand which are not associated with calcareous root tubules

Description

This facies is composed of small, plano-convex lenses with a maximum height of 0.5 - 2.0 cm and a width of 2.0 - 3.0 cm (Plate 8a). Facies H is composed of well to moderately sorted, fine sand. These small, plano-convex lenses are irregularly spaced along individual bedding planes at intervals of 15 - 70 cm. Calcareous root tubules or organic debris are not associated with these plano-convex lenses (Plate 8a).

Facies H is present in topset deposits of type 2 parabolic dunes (Table 3). Facies H represents less that 1% of the total sediments examined.

Interpretation

Small, plano-convex lenses are similar, though considerably larger, to the adhesion warts described by Kocurek and Fielder (1982). Reineck (1955) experimentally developed adhesion warts on a wet surface subjected to strong, shifting winds. Kocurek and Fielder (1982) were unable to duplicate these results and suggested that the formation of these structures by fluctuating wind conditions would be rare in nature. They suggested two more probable mechanisms which could have generated small, plano-convex lenses similar to facies H. These include wind sculpturing and grainfall over

Plate 8: Photographs of subfacies H and facies I. A) Photograph of facies H. Arrows point to the outline of the plano-convex lens. The topography of this feature is progressively subdued by overlying tabular strata. The quarter is 1.3 cm in diameter. B) Photograph of facies I. Camera lens is 5cm in diameter.

A)

B)

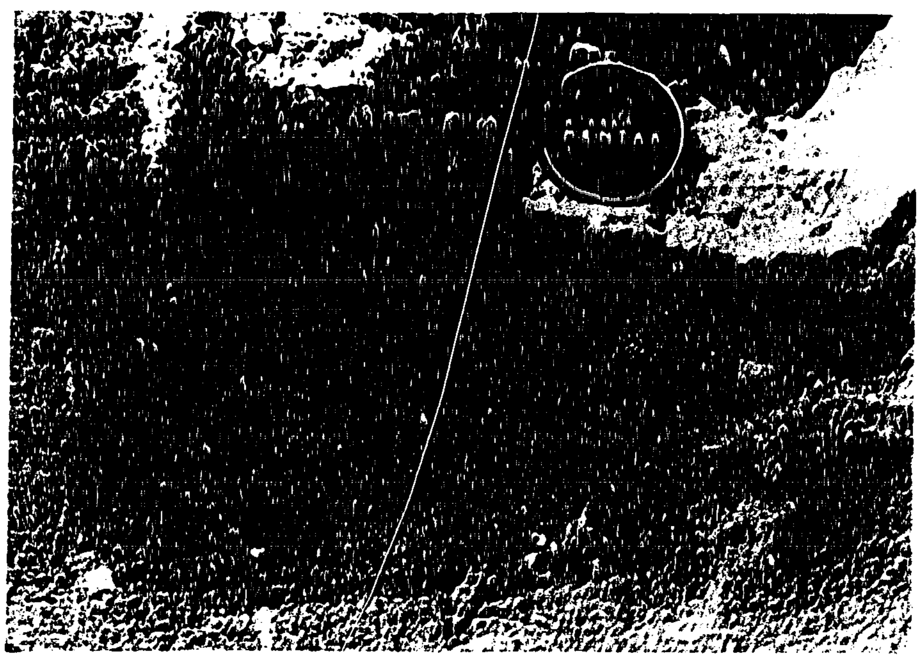

microtopographical features.

Wind sculpturing of some topographic feature (eg. a ripple) may have generated these small, plano-convex lenses of sand. Erosion of low cohesive sediments around a topographic feature of high cohesion by low velocity winds would accentuate the relief of the feature. Differences in cohesion would be initiated by slight textural differences, and thus variations in moisture retention. Similar results have been noted during ripple truncation on modern sand sheets. The irregularity in the spacing of these plano-convex lenses could have resulted from complete removal of some ripples.

A topographical feature could also have been produced by either initial irregularities in deposition, or by the erosion of areas of low cohesion by low-velocity winds. Slight textural differences in an initially planar surface could lead to differences in moisture retention, and thus cohesion. Low cohesive areas would then be preferentially deflated by low-velocity winds, resulting in a topographical obstruction to flow in the form of more cohesive areas, maybe only a few millimeters in height. This could be sufficient to initiate the development of small, plano-convex lenses of facies H by grainfall.

Regardless of whether subfacies H was initially generated from a moist planar surface or from a moist rippled or irregular surface, wind sculpturing was important in its formation.

Facies I: Sets of corrugated laminae of fine sand

Description

Facies I is composed of 2 - 5 cm thick sets of indistinct corrugated laminae of moderately to well sorted, fine sand (Plate 8b). Laminae are near horizontal and undulate irregularly on the millimetre scale. Laminae range in thickness from <0.1 - 0.3 cm and conform to the lower bounding surfaces or grade from units below. Facies I may grade into facies A, E, or J. Upper bounding surfaces may undulate irregularly.

Facies I is present in topset deposits of type 2 parabolic dunes and dome dunes (Table 3). Facies I represents less than 5% of the total sediments examined.

Interpretation

The thinness, indistinctness, and corrugated nature of laminae of facies I suggest they were deposited by some process other than grain segregation from ripple migration. Corrugated laminae which appear to be similar to facies I have been termed adhesion laminae by Hunter (1973, 1980). Kocurek and Fielder (1982) suggest that adhesion laminae will tend to develop during gusty winds from adhesion induced grainfall. A wind gust will deposit a thin layer of sediment which will adhere to the damp surface. Small irregularities on the deposition surface will generate the corrugated nature of laminae of facies I. Capillary action drawing moisture from below may also enhance the corrugated nature of facies I. Successive wind gusts will deposit other thin layers of sediment developing a set of facies I. Given that the wind continues to blow the process will repeat itself until capillary action can no longer draw moisture to the new depositional surface, or the surface becomes saturated from rainfall. Adhesion laminae are not known to develop on saturated surfaces (Kocurek 1981, Kocurek and Fielder 1982). Thus, facies I developed from sediment adhering to a damp surface under gusting winds.

Facies J: Sets of irregularly undulating laminae of fine sand

Description

Facies J is composed of 10 - 30 cm sets of indistinct irregularly undulating laminae of well to moderately well sorted, fine sand 0.1 - 1.0 cm in thickness. Laminae are relatively tabular in nature and dip 0° - 9° with a dip direction of 055 - 180. The undulations of the laminae have an amplitude of 0.1 - 0.5 cm and a wavelength of 0.2 - 6.0 cm. Laminae do not appear to truncate each other. Thinner laminae may be very indistinctly laminated internally, with internal laminae being approximately 0.2 cm thick and dipping 45° - 70°. Thinner laminae may grade vertically into facies I. Upper bounding surfaces may be planar to irregularly undulating .

Facies J is present in topset deposits of type 2 parabolic dunes and dome dunes (Table 3). Facies J may also be present in bottomset deposits of type 2 parabolic dunes. This facies represent less than 5% of the sediments examined.

Interpretation

Hunter (1981), Kocurek and Fielder (1982), Hummel and Kocurek (1984) and Schwan (1986) suggested mechanisms for generating irregularly undulating laminae similar to facies J. Those potentially applicable to the Grande Prairie dune field include:

1) adhesion ripple deposition
2) dewatering / small scale loading
3) niveo-aeolian deposition

Sets of facies J which grade into facies I were probably deposited as adhesion ripples. The extremely high-angle internal laminae present in some laminae of facies J are typical of adhesion ripples (Van Straaten 1953, Hunter 1973, Kocurek and Fielder 1982). Adhesion ripples develop as sediment adheres to an irregular surface (Kocurek and Fielder 1982). Facies J commonly develops on bedding planes which truncate underlying laminations, providing an irregular depositional surface. Extremely high-angle internal laminae will form as the saltating sand grains adhere to the stoss side of these truncated laminations . Adhesion ripples will only develop when the depositional surface has a saturation level greater than 80% (Kocurek and Fielder 1982). A change from adhesion ripple deposition of facies J to adhesion laminae deposition of facies I represents a drying-upwards sequence.

Irregularly undulating laminae thicker than a few millimeters do not develop from adhesion ripple deposition (Kocurek and Fielder 1982). Sets of thicker laminae of facies J are restricted to areas near the base of dune sections, some directly below avalanche beds of facies B. Their stratigraphic position suggests that loading and dewatering may have played a role in their formation.

Other thicker irregularly undulating laminae of facies J may also have developed as a result of niveo-aeolian deposition. Successive depositional episodes of texturally distinct sediment on a patch of snow will result in a laminated niveo-aeolian deposit (Schwan 1986). Movement of fine sand in such an environment could conceivably occur in the fall or spring when the upper surface was not frozen but isolated patches of snow were present. Variations in the moisture content of the surface and the shear velocity of the wind would produce successive depositional episodes of texturally distinct sediment. Lateral variations in the snow/sediment concentration would result in the deposition of irregular undulating laminae such as those of facies J which successively drape over each other as snow melting takes place.

Facies K: Plano-convex, lens-shaped set of laminated clay

Description

Facies K is composed of a plano-convex, lens-shaped set of laminated clay. The set thins to the north, overlapping adjacent parabolic dune sediments, and is truncated to the south (Plate 9). The maximum thickness of

Plate 9: Photograph of facies K which overlies a brunisolic palaeosol. The palaeosol is exposed on a parabolic dune surface to the north.

the set is 5m. Laminations average 0.6 cm in thickness with a range from 0.2 - 0.8 cm. Laminations also thin to the north. The set overlies a 30cm thick Bm horizon which is exposed on the parabolic dune surface to the north (Plate 9). The Bm horizon is capped by a 1 cm thick Ah horizon (humic organic layer). The organic layer contains abundant gastropods and wood fragments (identified as *Pinus contorta* by (R. Mott, Geological Survey of Canada, personal communication, 1985).

Interpretation

The fine grained sediment of facies K suggests it was deposited in a low energy environment. As facies K is located adjacent to the north arm of a parabolic dune in an interdune area, and is plano-convex, lens-shaped in morphology, it is interpreted to represent an interdune pond deposit. Finely laminated clays are typical of interdune deposits (Gaylord 1982). The Bm horizon and overlying organic layer represent a brunisolic palaeosol which developed when the adjacent parabolic dune became stabilised. As the laminated clays overlie this palaeosol, the interdune pond represented by facies K developed after dune stabilisation

Summary

A descriptive and interpretive summary of the aeolian facies and subfacies discussed in this chapter is given in Table 2 (in back pocket). The variation in sedimentary structures observed in the Grande Prairie dune field can be

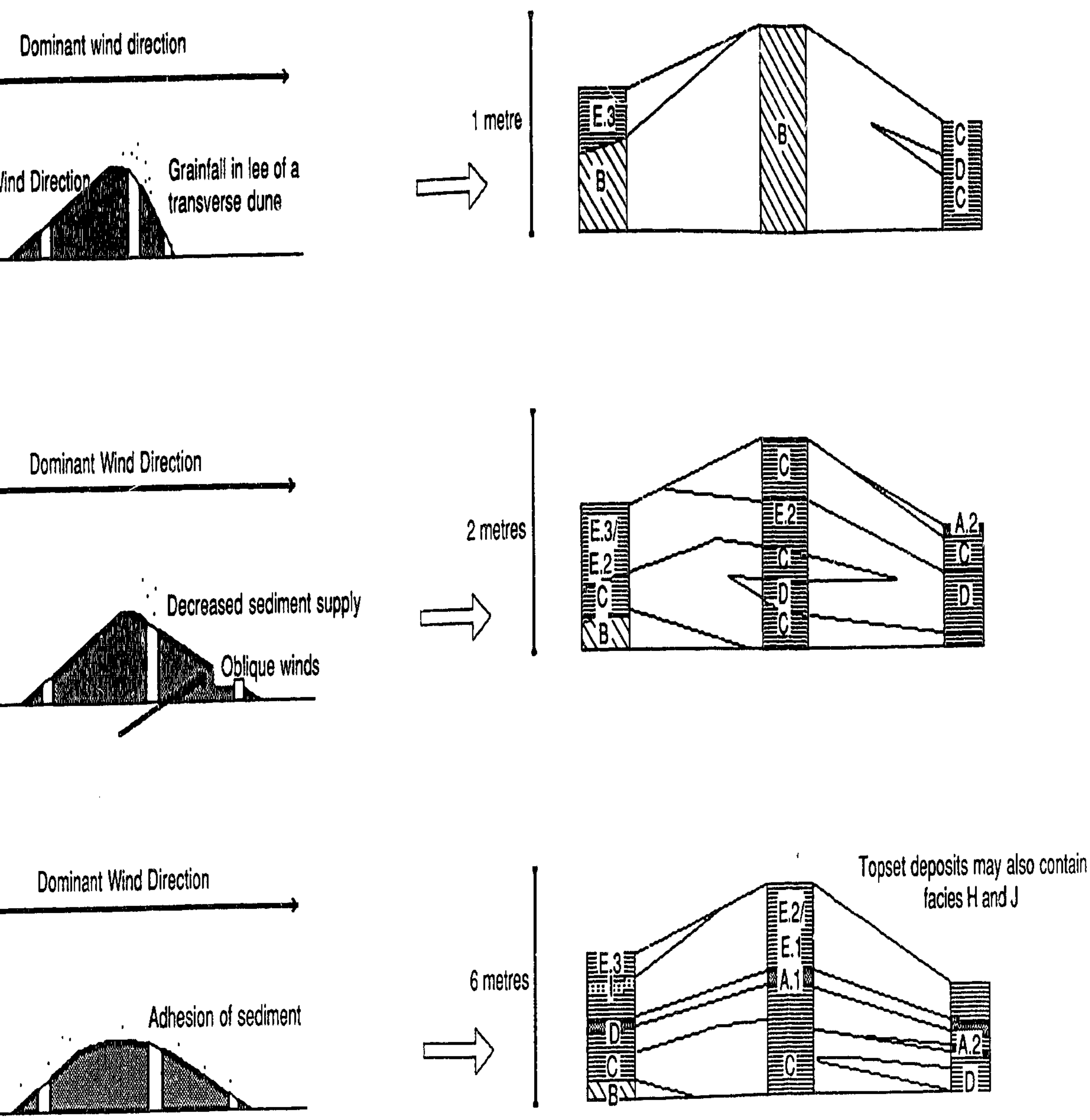
Dominant wind direction
Grainfall in lee of a transverse dune
1 metre
E.3
B
B
C
D
C
Dominant Wind Direction
Decreased sediment supply
Oblique winds
2 metres
E.3/
E.2
C
B
C
E.2
C
D
C
A.2
C
D
Dominant Wind Direction
Adhesion of sediment
6 metres
E.3
D
C
B
E.2/
E.1
A.1
C
A.2
D
Topset deposits may also contain facies H and J

mainly attributed to differences in:

1) geomorphology of the depositional surface
2) surface airflow (direction and velocity)
3) moisture conditions of the depositional surface
4) sediment supply
5) vegetation cover.

The geomorphology of the depositional surface is the most important factor in controlling the distribution of facies in the Grande Prairie dune field. Lee side deposits are primarily composed of facies B and C (Table 3). Lee side deposits grade laterally into bottomset deposits of facies C and D, with subfacies A.2 and J representing minor components (Table 3). Topset deposits drape the dune surface and grade laterally into lee side deposits in a downwind direction and into stoss side deposits of subfacies E.3 in an upwind direction. The different facies which comprise topset deposits are controlled by the moisture of the depositional surface (subfacies A.1, A.2, and facies H, I and J), sediment supply (subfacies E.1), and vegetation cover (facies G). The relationship between these controlling factors and the facies associations deposited in the different dune types will be examined in chapter 5.

CHAPTER FIVE: FACTORS CONTROLLING DUNE DEVELOPMENT IN THE GRANDE PRAIRIE DUNE FIELD

INTRODUCTION

Variations in aeolian depositional and erosional processes occur both spatially and temporally in a dune field due to changes in surface airflow and sediment availability. As surface airflow is directly affected by changes in topography, specific processes will tend to dominate in certain parts of a dune (eg. Howard *et al.* 1978, Barndorff-Nielsen *et al.* 1982). This spatial variation in depositional processes will produce a relatively consistent lateral sequence of sedimentary units in any given dune. As dunes behave as bedforms (Wilson 1972, Sweet *et al.* 1988), this preferred lateral sequence of sedimentary units should theoretically be translated into a preferred vertical sequence (Brookfield 1984). The geometry and behavior of the dune (eg. migration rate and angle of climb) will control the generation of the vertical sequence (Nielson and Kocurek 1987).

Facies models which presently exist for dunes are mainly based on theoretical models of bedform behavior (see Brookfield 1984). Dunes which have been trenched, though in part conforming to these theoretical models, show a high degree of variability. It seems likely that just as the short term processes which deposit aeolian sediments are gradational, long term variations in dune behavior will also be gradational. For any given dune type a spectrum of preferred vertical sequences will exist that reflects the spatial and temporal changes in surface airflow and sediment availability which existed during the time of dune development.

Facies associations are presented in this chapter for dome and parabolic dunes. A summary table of facies associations for the different solitary and compound dunes is given in Table 3 (in back pocket).

DOME DUNES

Introduction

Dome dunes present in the vicinity of Grande Prairie are located on the downwind northern margin of the dune field (Figure 5). Previously described dome dunes (see McKee 1966, Bigarella and Popp 1966, Bigarella *et al.* 1969, Bigarella 1972, Ahlbrandt 1973) are generally located on the upwind margins of coastal and inland dune fields. One exception is a dome dune located downwind of a large interdune corridor, described by McKee (1982).

The dome dunes which have been described by previous workers can be separated into two end members based on their internal structures. Dome dunes present along the upwind margin of inland dune fields are typically composed of high-angle, planar tabular cross-strata which dip downwind, suggesting deposition initially formed transverse dunes (see McKee 1966, Ahlbrandt 1973). These cross-strata are draped by a thin layer of near horizontal topset strata which grade downwind into low-angle cross-strata. Cut-and-fill structures which parallel the dominant wind direction are also present (see McKee 1966). The change in depositional style probably resulted from strong winds beveling the dune, impeding slipface development

(McKee 1979).

Dome dunes present along the upwind margin of coastal dune fields contain near-horizontal to low-angle cross-strata separated by concave-downwards bounding surfaces. Very few slipface deposits are present (see Bigarella and Popp 1966, Bigarella *et al.* 1969, Bigarella 1972). The dune morphology is attributed to variation in wind flow direction, with erosion being inhibited by moisture and vegetation. As dome dunes in the Grande Prairie dune field differ in their relative location from previously described dome dunes, the factors which controlled their development may have differed.

Facies associations of Grande Prairie dome dunes

In general, strata in dome dunes of the Grande Prairie dune field tend to decrease in dip upsection. The spread of dip directions of strata also increases upsection. Where the dip directions span 360°, individual strata conform to curved contacts which develop the dome morphology of the dune.

Cross-strata tend to have the highest dip in the basal, upwind, central area of dome dunes (Figure 14). The dip direction of high-angle cross-strata of facies B is tightly clustered to the east (Figure 15). Easterly dipping cross-strata which dip at high angles are interpreted to represent slipface deposits. A tight unimodal dip direction of slipface deposits suggests deposition occurred in the lee of a straight crested dune oriented normal to the wind (transverse dune) (McKee 1979). As windward dipping deposits are not associated with facies B, migration of the initial transverse dune must have occurred.

Figure 14: Schematic diagram showing growth of a dome dune in relation to the sedimentary structures deposited. A) Dunes begin as either transverse dunes or dome dunes with facies B and C being deposited in the lee and grading downwind into facies D and subfacies A.2. B) When sedimentation rates decrease, slipface development is inhibited and the dome morphology is established. The deposition of sediment by oblique winds contributes to constructing the dome morphology of the dune. C) Adhesion of sediment on the dome dune surface results in a buildup of the dune. Topset deposits become much more diverse.

Figure 15: Orientation of strata in dome dunes plotted on a schmidt equal area projection. Facies B is represented by circles, facies C is represented by squares, and other facies are represented by dots. All points are directly plotted.

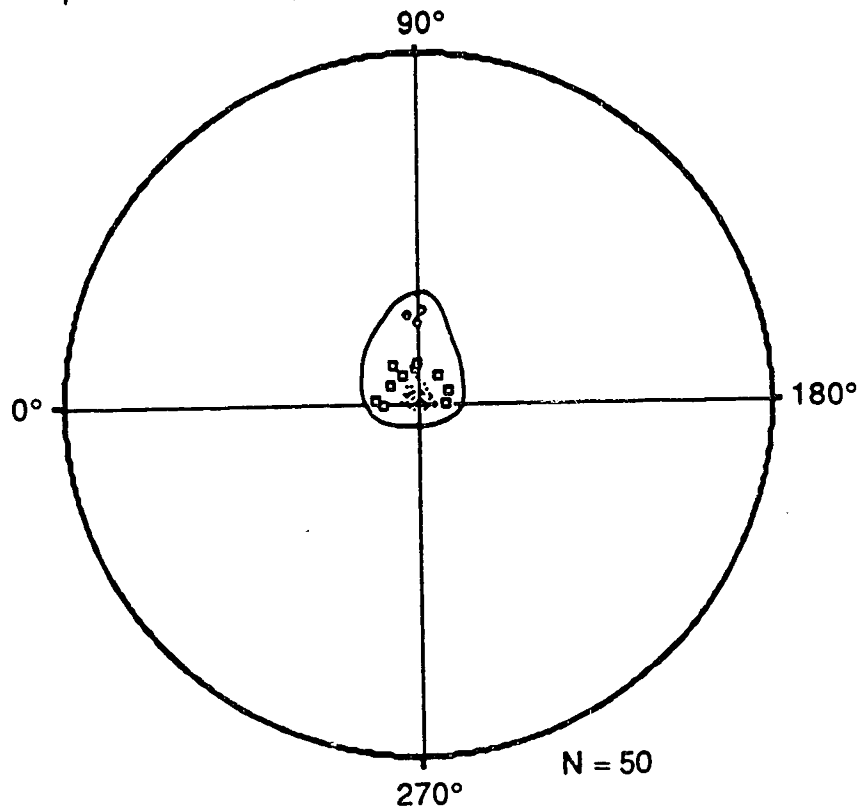

Basal strata become progressively lower in dip downwind and towards the dune margins (Table 3). In dome dunes which contain slipface deposits, these high angle cross-strata of facies B grade into low-angle cross-strata of facies C (Figure 14). The presence of contorted and folded strata in slipface deposits indicates that avalanching occurred in part as wet sand flows (McKee *et al.* 1971), which acted to subdue relief (Pye 1983). The subdued relief of the lee side of the dune allowed for the deposition of facies C. Avalanching did not reoccur, as the angle of the lee side of the dune never reached or approximated the angle of repose.

As dome dunes in the study area are located only at the downwind margin of the dune field, they had a low sedimentation rate. This is indicated by the rare occurrence of sedimentary structures indicating deposition by dry grainfall (Subfacies E.1) . Slipface development may have been hindered by this low sedimentation rate, resulting in the deposition of low-angle lee side deposits of facies C (Figure 14).

For those dome dunes which do not contain slipface deposits, easterly dipping low-angle cross-strata of facies C are present. Dome dunes which do not contain slipface deposits may also have been initiated as transverse dunes. The absence of slipface deposits may be due to upwind sediment removal during dune migration, or from low sedimentation rates at the initiation of dune building, thus inhibiting slipface development.

The dip direction of low-angle, basal cross-strata diverges from an easterly direction downwind and towards the dune margins spanning approximately

180° (Figure 15). Sets of low-angle cross-strata are generally restricted to the base of dome dunes and mark a transition from transverse dune deposition. As no slipface is present, a shallow cone of sediment is constructed. This shallow cone of sediment in the lee of the dune establishes the incipient morphology of the dome dune.

Wedge sets of low-angle cross-strata (facies D) are found interbedded with facies C along the margins of dome dunes (Figure 14) (Table 3). Laminae of facies D which pinchout upslope are indicative of deposition from ripple migration on a sloping surface by oblique winds. The deposition of facies D results in a decrease in the dip of the dune margin and an increase in the spread of dip directions around the dune margin. Deposition of sediment by oblique winds aids in the development of the dome dune morphology. Medium sand beds of subfacies A.2 may also be present in bottomset deposits as liquified sediments move downslope (Figure 14).

Bounding surfaces vary from planar near the base of the dune separating sets of cross-strata, to concave-downwards towards the top of the dune. Concave-downwards bounding surfaces separate sets of near horizontal laminae which conform to lower bounding surfaces (facies E). Concave-downwards lower bounding surfaces have dip directions which span 360°, conforming to the morphology of the present dune surface. Bounding surfaces and laminae decrease in dip upsection, responding to the growth of the dune. Bounding surfaces develop as a result of shifting wind directions and local variations in wind strength, rather than from dune migration.

Sets, dominated by the near horizontal laminae of facies E, also include facies G (plano-convex lenses of sand associated with calcareous root tubules), facies I (corrugated laminae), and facies J (irregular undulating laminae) (Figure 14) (Table 3). Sets of corrugated to irregularly undulating laminae, which are indicative of deposition under high moisture conditions, are thicker and more frequent towards the dune margin. Some sets of near horizontal laminae grade into solitary beds of fine sand (subfacies A.1) (Figure 14). Beds of fine sand which grade from underlying laminae are interpreted as having been deposited by wet grainfall. These beds also tend to be more frequently preserved at the dune margins.

The abundance of sedimentary structures indicative of deposition under high moisture conditions in the upper parts of dome dunes suggests that moisture played an important role during dome dune development. Moisture results in the deposition of sediment by adhesion to the dome dune surface, and impedes dune migration and erosion.

Summary

The dome dunes in the Grande Prairie dune field appear to exhibit characteristics of both inland and coastal dune fields. The basal parts resemble previously described inland dome dunes, whereas the upper parts resemble previously described coastal dome dunes.

Some or all of the dome dunes are considered to have been initiated as transverse dunes. As the sedimentation rate decreased, slipface development was impeded and the dome morphology was developed. Sedimentation rates may have decreased as a result of an increase in the moisture of the surface, an increase in the vegetation cover, or a combination of both factors. Continued sedimentation resulted in the buildup of sediment on the dome dune, mainly by adhesion.

SOLITARY PARABOLIC DUNES

Introduction

Parabolic dunes which have been previously described show a general sequence of strata decreasing in dip from the dune base (eg. McKee 1966, McKee and Bigarella 1972, Ahlbrandt and Andrews 1978, Bigarella 1975, 1979). Basal cross-strata commonly have a concave-downwards configuration representing slipface deposition at the dune nose (McKee 1966). Concave-downwards cross-strata are considered to be characteristic of parabolic dunes (McKee 1979). As the nose migrates downwind the deposition of concave-downwards cross-strata is subsequently replaced by shallow-dipping topset strata grading laterally downwind, into slipface deposits, increasing the spread in dip direction (McKee 1966). As migration continues, sediments which were originally deposited at the dune nose will be removed or stabilised along the sides to form the arms (McKee 1966, Andrews 1979, Bigarella 1979). Continued deposition on the sides of dune arms will result in an increase in the spread of dip directions, sometimes encompassing up to 270° (Bigarella 1979).

Vegetation has long been considered essential in the development of parabolic dunes, as it acts to stabilize dune arms (eg. Steenstrup 1894, Enquist 1932, Melton 1940, Hack 1941). Warping or disturbance of strata by vegetation has been commonly noted in parabolic dune sections (eg. McKee 1966, Nielsen 1986), and is considered to be unique to parabolic dunes (McKee 1979).

Facies associations of Grande Prairie solitary parabolic dunes

In general, strata in solitary parabolic dunes of the Grande Prairie dune field tend to decrease in dip upsection. The spread in dip directions of strata increases upsection as the dip decreases (Figure 16).

Initial deposition at the base of a parabolic dune nose is represented by subfacies B.1 (high-angle, concave-downwards cross-strata) (Figure 17). The concave-downwards configuration is attributed to oversteepening of the dune slipface by preferential accumulation of sediment directly downwind of the brinkline. Formation and preservation of these strata requires a high but fluctuating rates of sediment supply, coupled with fluctuating low to moderate wind velocities. If the wind velocities were high and the sand supply was constant, redistribution of sand from the brinkline would proceed more consistently, and would result in the construction of a shallow cone of sand in the lee of the dune. This would produce the low-angle cross-strata observed in dome dunes formed by strong winds (McKee 1966).

Both the low, long armed, type 1 and high, short armed, type 2 parabolic dunes contain high-angle, concave-downwards cross-strata of subfacies B.1 at their bases (Table 3). This suggests that initially sedimentation rates were at least sufficient to generate brinkine accumulation for each of the dune

Figure 16: Orientation of strata in solitary parabolic dunes of the Grande Prairie dune field plotted on a schmidt equal area projection. All data has been directly plotted. The area was extrapolated on the assumption that these dunes have bilateral symmetry.

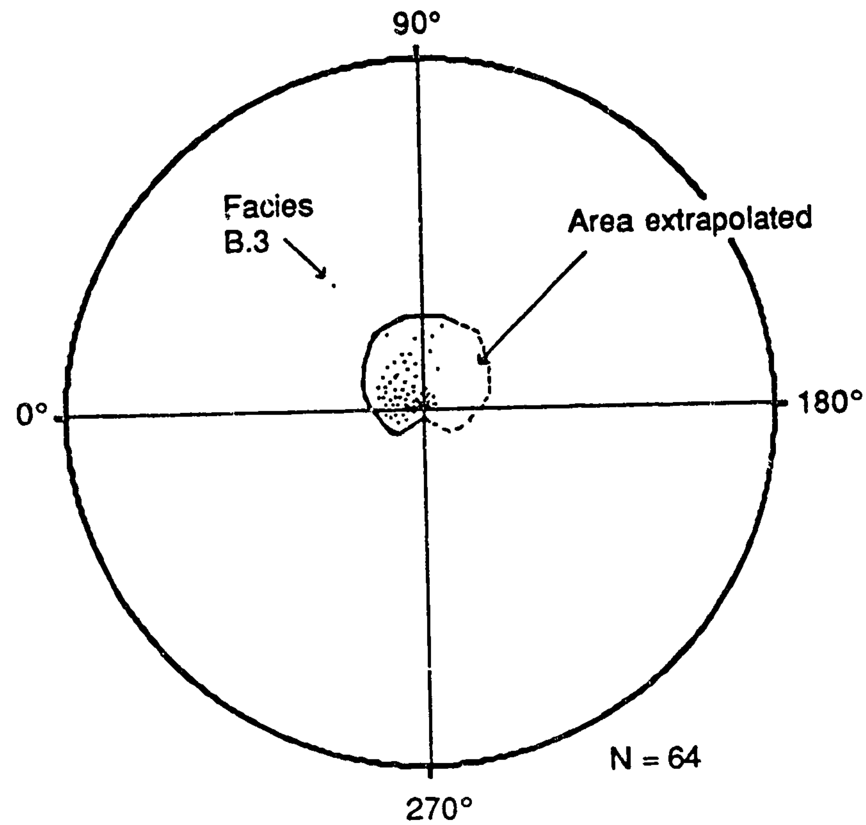

Figure 17: Schematic diagram showing growth of a solitary parabolic dune. A) Parabolic dunes are initiated by preferential accumulation of sediment at the brinkline resulting in the deposition of subfacies B.1. Facies C may also be deposited when the angle of the slipface decreases. B) Migration of the dune results in deposition of topset deposits. Variations in sedimentation rates and the sediment budget control the thickness and type of strata which are deposited. Dunes with a higher sedimentation rate and sediment budget will develop thicker topset deposits with a more diverse group of sedimentary structures. C) Deposition at the base of dune arms will deposit strata of facies C and D which increase the spread in dip direction. Subfacies A.2 is also occasionally deposited.

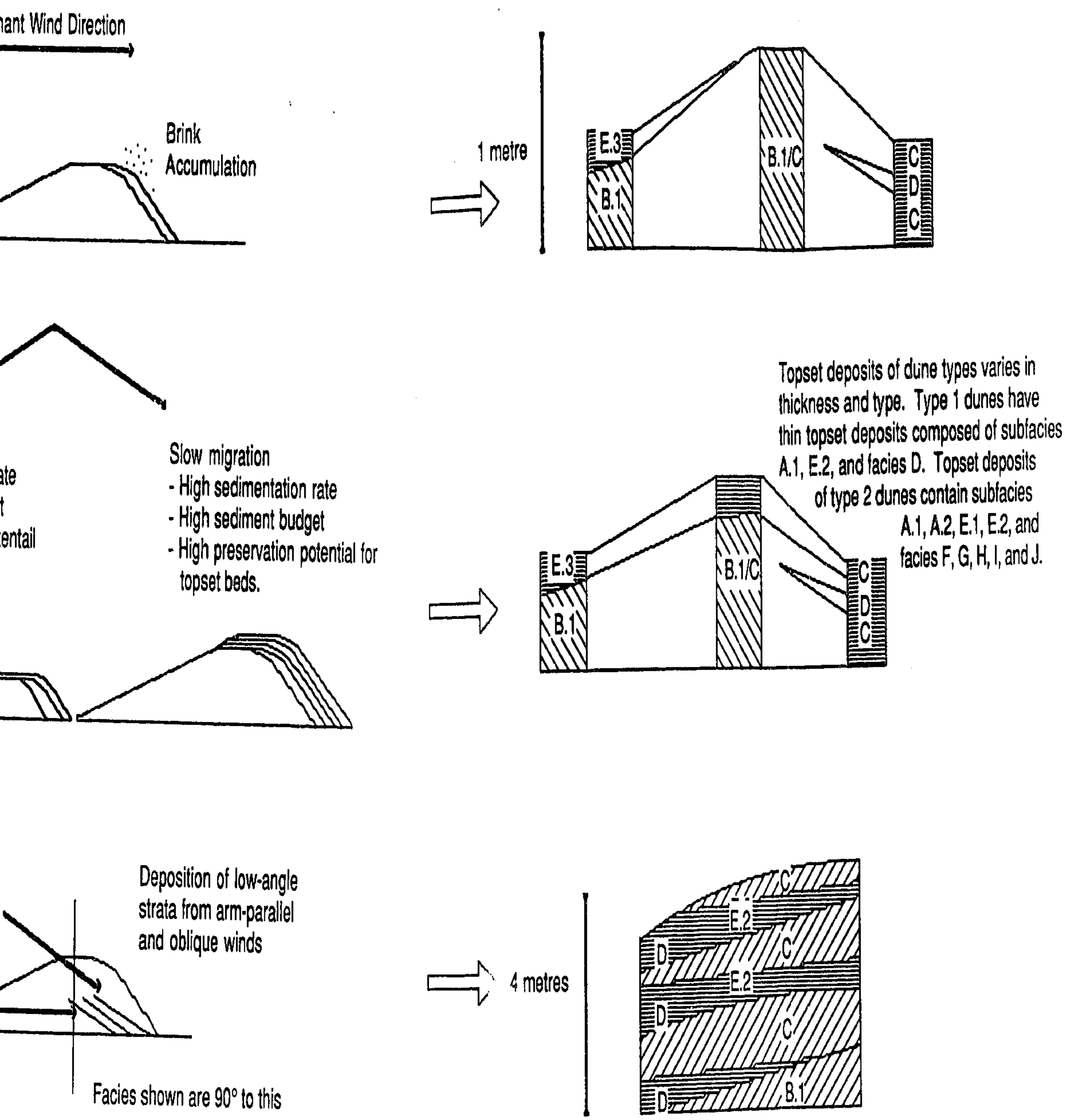

nant Wind Direction
Brink
Accumulation
1 metre
E.3
B.1
B.1/C
C
D
C
Topset deposits of dune types varies in thickness and type. Type 1 dunes have thin topset deposits composed of subfacies A.1, E.2, and facies D. Topset deposits of type 2 dunes contain subfacies A.1, A.2, E.1, E.2, and facies F, G, H, I, and J.
ate
t
entail
Slow migration
- High sedimentation rate
- High sediment budget
- High preservation potential for topset beds.
E.3
B.1
B.1/C
C
D
C
Deposition of low-angle strata from arm-parallel and oblique winds
Facies shown are 90° to this
4 metres
C
E.2
D
C
E.2
D
C
D
B.1

types (Figure 17).

Subfacies B.1 grades laterally into low-angle cross-strata of facies C for those concave-downwards strata of subfacies B.1 having high-angle asymmetrical folds present on their upper surfaces (Figure 17). High-angle asymmetrical folds are interpreted to result from avalanching of saturated noncohesive sand. The angle of repose of saturated noncohesive sand is much lower (6° - 8°) than that of dry sand. This results in the deposition of facies C when the sediment becomes dry. Unlike the sequences observed in dome dunes, low-angle cross-strata of facies C will grade laterally downwind into facies B (Figure 17) (Table 3). This occurs where slipface deposits are reestablished in the lee of the dune. Reestablishment of slipface deposits by brinkline accumulation is essential in maintaining the parabolic configuration of the dune.

As the dune migrates, successive vertical and lateral accumulation of sediment acts to decrease the angle of repose. This results in the deposition of strata which conform to the dune surface, forming shallow dipping topset beds (Figure 17). As deposition proceeds on the expanding slipface, bounding surfaces become more closely spaced due to an increase in surface area (Table 3). Low, long armed, type 1 parabolic dunes generally contain only interbedded topset deposits of wedge sets of low-angle cross-strata which pinchout upslope (facies D), and sets of ungraded to inversely graded laminae which conform to lower bounding surfaces (subfacies E.2) (Figure 17) (Table 3). Sets of these facies are interpreted to form mainly by the migration of climbing ripples during net deposition from the saltation and traction load. The interbeddding of these sets can be attributed to changes in wind flow direction. Topset deposits in type 1 parabolic dunes rarely exceed 1m in thickness.

Some beds of subfacies A.1, are interpreted to have been deposited by grainfall and are rarely present in topset deposits of type 1 parabolic dunes (Figure 17). Other facies resulting from grainfall, or related to moisture or vegetation are not present. Preservation of a set of strata on the crest or arms of a dune will be largely fortuitous. The predominance of strata deposited from ripple migration therefore suggests that this was the dominant process occurring at the dune crest and on the arms.

A much more diverse group of sedimentary structures is preserved in thick topset deposits (6m+) of high, short armed, type 2 parabolic dunes (Figure 17) (Table 3). Sets of subfacies E.2 are most commonly found in sections of type 2 parabolic dunes (Table 3). This suggests that deposition from ripple migration was the most important process occurring at the dune crest and on dune arms. Unlike topset deposits of parabolic dune type 1, no sets of facies D were found in topset deposits of parabolic dune type 2 (Table 3). This implies that the effective sand transport direction was rarely oblique at the dune crest. This would be expected for high (15-20m) features such as the type 2 dunes in the Grande Prairie area. Other sedimentary structures present in topset deposits of type 2 parabolic dunes include:

Subfacies A.1: Tabular fine sand beds

Subfacies A.2: Tabular medium sand beds

Subfacies E.1: Sets of normally graded low-angle to horizontal strata which dip easterly

Facies F: Coarse sand rich lamina

Facies G: Plano-convex lenses of sand associated with calcareous root tubules

Subfacies H: Plano-convex lenses of sand which are not associated with calcareous root tubules

Facies I: Corrugated laminae of fine sand

Facies J: Irregularly undulating laminae of fine sand

The presence of beds and sets of strata which are interpreted to have been deposited by grainfall (subfacies A.1, E.1, and facies G), suggests that the sedimentation rates were high. The rarity or absence of these subfacies in type 1 parabolic dunes indicates that type 2 parabolic dunes had a higher sedimentation rate (Figure 17).

The occurrence of sedimentary structures which are indicative of development under moist conditions (subfacies A.2, and facies H, I and J) suggests that moisture played an important role in the development of type 2 parabolic dunes. As these facies are not present in type 1 parabolic dunes, type 2 parabolic dunes had a higher sediment budget (Figure 17).

Little warping or disturbance of strata was noted in topset deposits with the exception of facies G, in contrast with the parabolic dunes described previously (eg. McKee 1966, Nielsen 1986). This implies that vegetation was not the primary agent stabilising the parabolic dune arms in the study area. The occurrence of sediments which require moisture for deposition suggests that moisture was the primary stabilising agent for parabolic dune arms.

Högbom (1923) and David (1977, 1979, 1981) have suggested that moisture acts as the primary agent in stabilising parabolic dunes. Vegetation also probably contributed to stabilization, but was of only secondary importance when the dunes were active.

Low-angle cross-strata of facies C which are oriented normal to the dominant wind direction, are commonly found associated with topset deposits on the dune arms (Figure 17). Strata of facies C represent deposition at the base of dune arms by winds which are both parallel and oblique to the arms. Sets of low-angle cross-strata which pinchout upslope (facies D) are found interbedded with facies C, representing deposition from oblique winds (Figure 17). Deposition at the base of dune arms increases the spread in dip directions of strata preserved in parabolic dunes.

Summary

The facies associations preserved in both types of parabolic dunes in the Grande Prairie dune field are similar to the general sequences of parabolic dunes described previously. Important differences exist between type 1 and 2 dunes (Table 3). These differences can be attributed to spatial variations in sediment availability and budget.

Sedimentation rates and sediment budget control the migration rate of a parabolic dune. Type 1 dunes migrated much more rapidly then type 2 parabolic dunes, because they had a lower sedimentation rate and a smaller sediment budget. For this reason, topset deposits are thin and have a low preservation potential on type 1 parabolic dunes (Table 3). Type 2 parabolic dunes migrated much more slowly than type 1 parabolic dunes, because they had a higher sedimentation rate and a greater sediment budget. This resulted in the deposition of thick topset deposits which have a higher preservation potential (Table 3).

COMPOUND PARABOLIC DUNES

Introduction

Compound parabolic dunes develop as a result of downwind migration when the dunes behave as climbing bedforms. The stacking of these climbing bedforms documents the extent to which strata deposited on dunes are preserved. This represents an important record as it provides the potential to develop facies models for dunes which can be more directly applied to the ancient record than solitary dunes. The sedimentary sequences preserved in compound parabolic dune sections have not been described in detail previously.

Facies associations of Grande Prairie compound parabolic dunes

The general sequence of sedimentary structures present in compound parabolic dunes of the Grande Prairie dune field is composed of stacked cosets of strata which decrease in dip upsection in individual cosets. Complexities arise in compound parabolic dune sequences from the generation of secondary airflow and lee eddies, and from the preservation of stoss deposits.

Type 1 compound parabolic dunes have a low angle of climb due to their low sedimentation rate and sediment budget. The low angle of climb results in the truncation of the majority of the upwind dune arm. For this reason, only basal strata present in the dune arm will be preserved with stoss and topset deposits being removed (Figure 18). Basal strata consist of bottom set arm deposits of low-angle cross-strata of facies C and D and high-angle, concave-downwards cross-strata of subfacies B.1, originally deposited on the dune slipface (Figure 18).

Basal strata of the upwind dune are overlain by low-angle cross-strata of facies C which are deposited on the lee of the downwind dune (Figure 18). Low-angle cross-strata of facies C are deposited instead of slipface deposits because brinkline accumulation is overshadowed by winds parallel and oblique to the arms (Figure 18). These winds deposit sediment at the intersection point between the two dunes as there is a morphologically generated flow expansion (Figure 18). The deposition by winds parallel and oblique to the arms limits the angle of repose as brinkline accumulation is not sufficient to generate avalanching. This results in the deposition of low-angle cross-strata of facies C.

When the downwind dune migrates over the upwind dune, the entire complex behaves as the arm of the upwind dune. Topset deposits of facies D and subfacies E.2 are therefore deposited over low-angle cross-strata of facies C (Figure 18). Deposition of topset deposits occurs when the nose of the intersection point between the two dunes is filled in.

Type 2 compound parabolic dunes have a high angle of climb due to their

Figure 18: Initial deposition of sediment in compound parabolic dunes. Preferential brinkline accumulation is overshadowed by the deposition of sediment by secondary airflow. A) Type 1 parabolic dune is truncated. Deposition by arm-parallel and oblique winds overshadows preferential brinkline accumulation in type 1 parabolic dunes as a morphologically generated flow expansion is created when the two dunes intersect. This results in the deposition of facies C. Typical topset deposition of type 1 parabolic dunes continues when the intersection point is filled in. B) Type 2 parabolic dunes have a high angle of climb resulting in the majority of the upwind dune being preserved including stoss deposits of subfacies E.3. In type 2 parabolic dunes oblique winds, cross-winds and lee eddies overshadow brinkline accumulation resulting in the deposition of facies C and B.2. When the intersection point is filled in typical topset deposits of type 2 parabolic dunes are laid down.

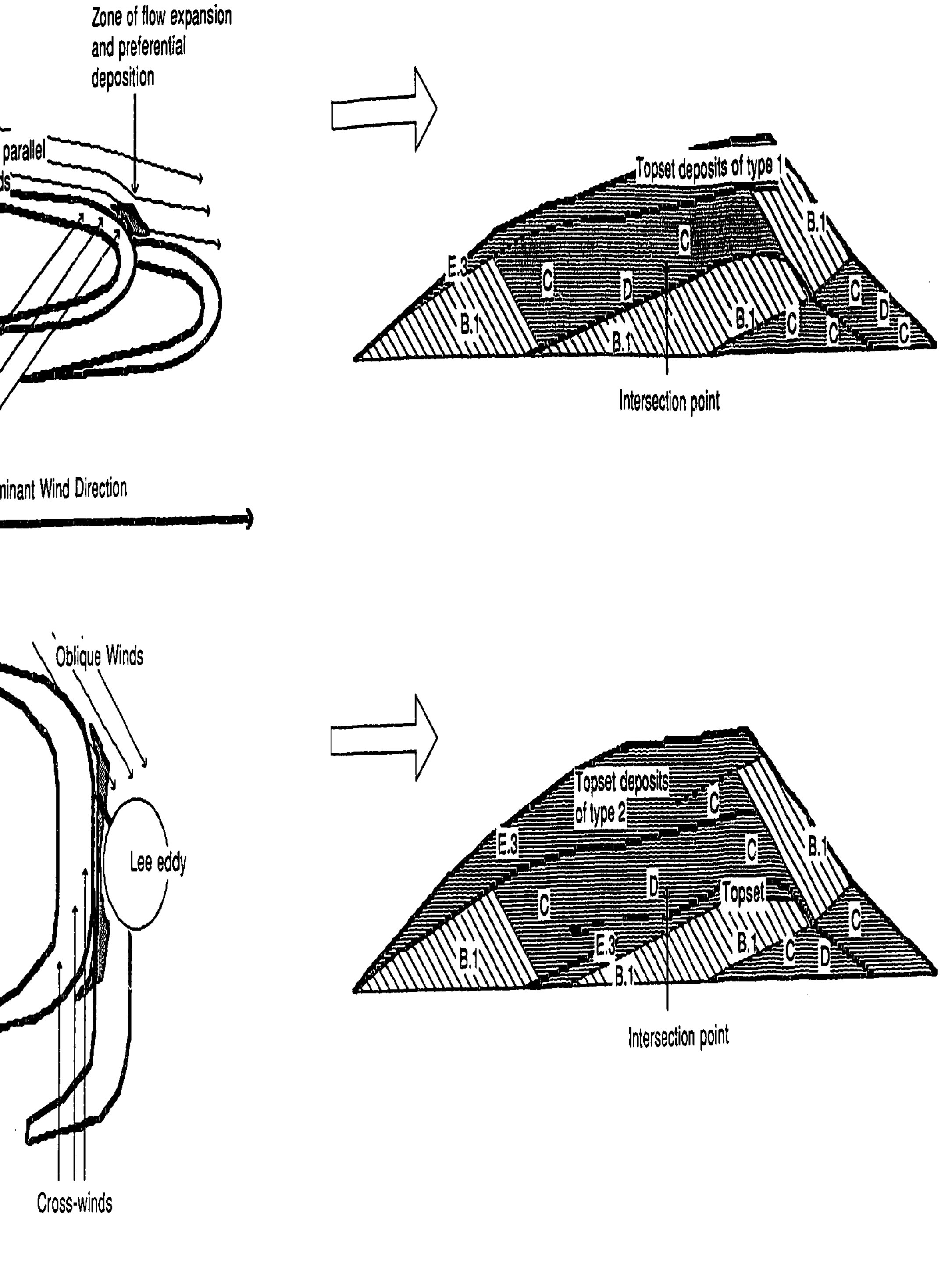
Zone of flow expansion
and preferential
deposition
parallel
ds
Topset deposits of type 1
E.3
C
D
B.1
Intersection point
ninant Wind Direction
Oblique Winds
Lee eddy
Cross-winds
Topset deposits
of type 2
Topset
E.3
Intersection point

high sedimentation rate and sediment budget. The high angle of climb results in the preservation of the majority of the upwind dune arm (Figure 18). High-angle, concave-downwards cross-strata of subfacies B.1 and bottom set deposits of low-angle cross-strata (facies C and D) will be preserved as will overlying topset deposits. Topset deposits will follow the general sequence of strata preserved in solitary type 2 parabolic dunes (Figure 18). Stoss deposits may also be preserved at the top of the upwind arm sequence (Figure 18). Preservation of stoss deposits results in a spread of dip directions which span 360^{o} (Figure 19) (Plate 10).

Strata of the upwind dune are mainly overlain by low-angle cross-strata of facies C and D and beds of subfacies A.1 (Figure 19). These strata represent deposition in the lee of the downwind dune. Low-angle cross-strata of facies C are deposited on the lee of the downwind dune instead of slipface deposits, as brinkline accumulation is overshadowed by deposition from oblique winds, cross- winds, and lee eddies. Winds parallel to the arms were probably not too important in depositing low-angle cross-strata in the lee of the downwind dune due to the width of type 2 parabolic dune noses (Figure 18). Sedimentation rates must have remained relatively high as grainfall deposits (subfacies A.1) are present.

Facies C may grade laterally into high-angle, concave-upwards cross-strata of subfacies B.2 (Appendix 1). Strata of subfacies B.2 were deposited from avalanching when lee side deposits reached the angle of repose due to undercutting by cross-winds or lee eddies (Figure 18). The lateral association of facies C and D with subfacies B.2 supports the interpretation that cross-

Figure 19: Orientation of strata plotted directly onto a schmidt equal area projection for compound type 2 parabolic dunes of the Grande Prairie dune field.

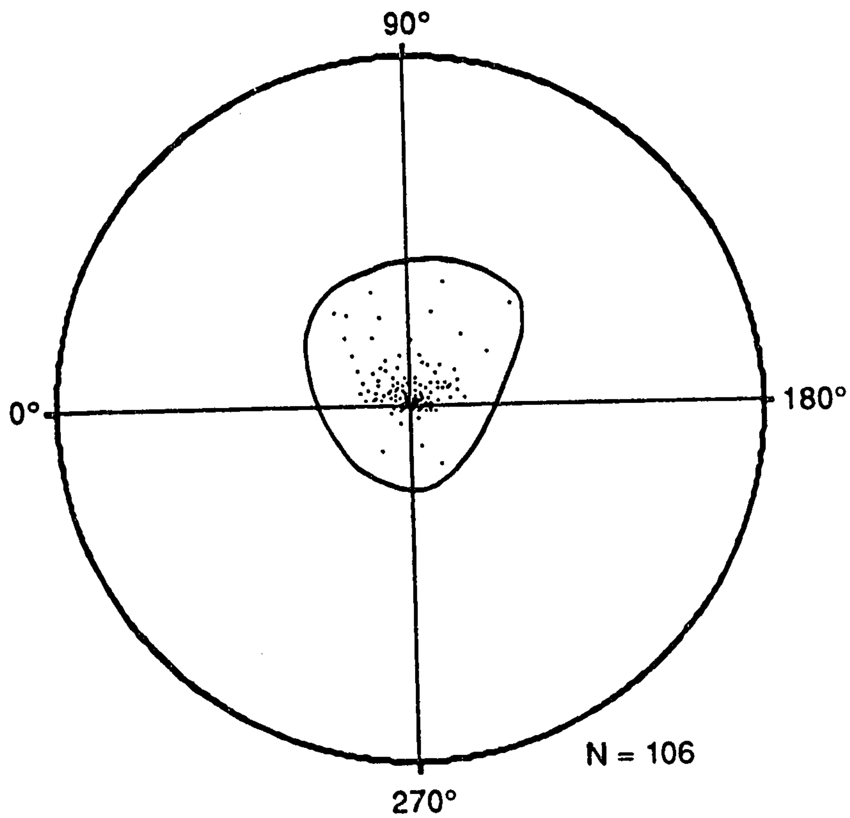

Plate 10: Photograph of a section through a type 2 compound parabolic dune. Strata of the upwind dune are marked as dune 1 and strata of the downwind due are marked as dune 2. Arrows point to preserved stoss side deposits.subfacies B.2 (Appendix 1). winds and lee eddies were important in the deposition of these strata.

Strata which are deposited on the lee side of the downwind dune are interbedded with sets of low-angle laminae which dip upwind (subfacies E.3), representing stoss deposits of the upwind dune. Sets of lee side and stoss side strata continue to be deposited until the intersection point between the two dunes is filled in.

When the intersection point between the compound type 2 parabolic dune is filled in, the entire complex behaves as the arm of the upwind dune. For this reason thick topset deposits composed of strata equivalent to topset deposits of solitary type 2 parabolic dunes will be deposited.

Summary

The general sequence of sedimentary structures, preserved in compound parabolic dunes of the Grande Prairie dune field, depends on the migration rate of the dune. Type 1 parabolic dunes have a low angle of climb resulting in the truncation of most of the upwind dune (Table 3). Type 2 parabolic dunes have a high angle of climb resulting in the preservation of most of the upwind dune including stoss side deposits (Table 3). For both dune types, low-angle cross-strata overlie the upwind arm deposits (Table 3). For type 1 parabolic dunes, low-angle cross-strata are deposited mainly by winds both parallel and oblique. For type 2 parabolic dunes low-angle cross-strata are deposited mainly by oblique winds, cross-winds, and lee eddies. These cross-strata are interbedded with stoss side deposits of the upwind dune. When the intersection point between the two dunes is filled in, the entire complex acts as the arm of the upwind dune resulting in the deposition of topset beds.

Traditionally aeolian dune deposits were considered to be mainly composed of high-angle cross-strata (eg. Bigarella 1972, Brookfield 1984). Recent work on a variety of modern desert dunes (transverse, oblique, cresentic, linear, and star) has shown that due to low angles of climb, low-angle deposits comprise a large portion of dune sediments (eg. Kocurek 1986, Nielson and Kocurek 1987). This occurs as apron and plinth deposits are preferentially preserved (Kocurek 1986). Compound parabolic dunes of the Grande Prairie dune field also contain a high proportion of low-angle to horizontal strata. Preservation of low-angle cross-strata is interpreted to result not so much from a low angle of climb, but from the infilling of the intersection point of the dunes by apron deposits.

CHAPTER SIX: DEVELOPMENT OF THE GRANDE PRAIRIE DUNE FIELD

The Grande Prairie dune field developed during the Holocene, after glacial lakes impounded by the Laurentide Ice Sheet, drained from the area *via* the valley of Lesser Slave Lake (St. Onge 1972, Mathews 1980). Glacial lake drainage is interpreted to have occurred by about 11,000 years based on a basal date on gyttja from Lofty Lake, Alberta of 11,700 +/- 90 years BP (GSC-1049) (St. Onge 1972), and a basal date on gyttja from Boone Lake, Alberta of 11,700 +/- 90 years BP (SFU 223) (White *et al.* 1985) (Figure 20).

Dune orientation indicates that a westerly wind flow was the dominant agent of formation. The mean direction of transport during dune formation in the Grande Prairie dune field was found to be 085.5 azimuth based on 180 measurements (Figure 21). Sedimentary structures preserved in the dunes indicate that winds diverging both to the north and south of the dominant wind direction were also responsible for the transport of sediment.

The primary source of sediment for the dune field was terrace sands of the Wapiti and Smoky Rivers, as advocated by Odynsky (1958). Mineralogy and shape of terrace sands were found to be similar to sands present in the dunes (Figure 22). Also, the dune field extends only slightly outside the limits of old river terraces.

Figure 20: Diagram showing the chronological control on aeolian activity in the Grande Prairie dune field.

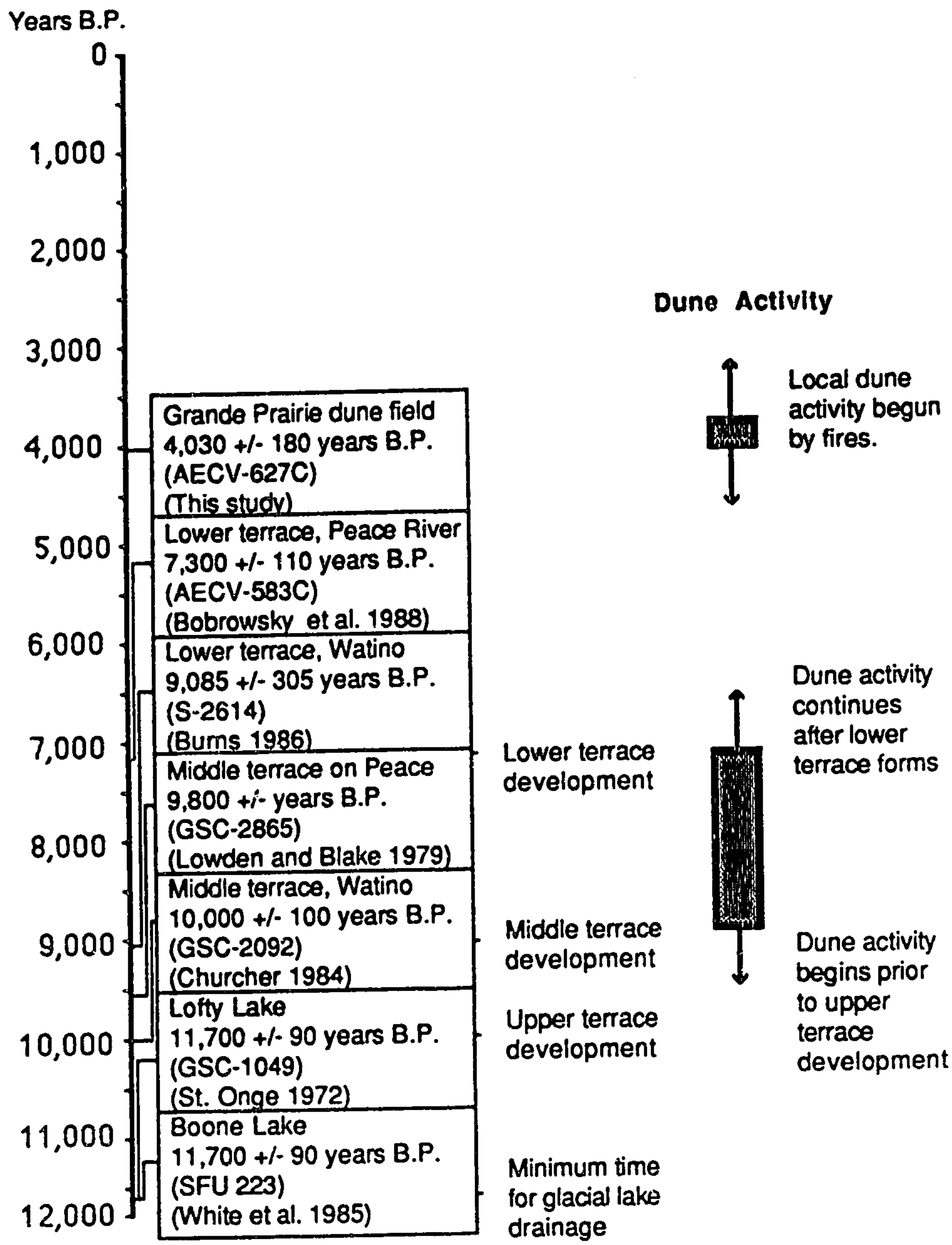

Figure 21: Histogram showing the distribution of dune orientation in the Grande Prairie dune field. The mean orientation is 085.5 degrees azimuth with a standard deviation of 7.5.

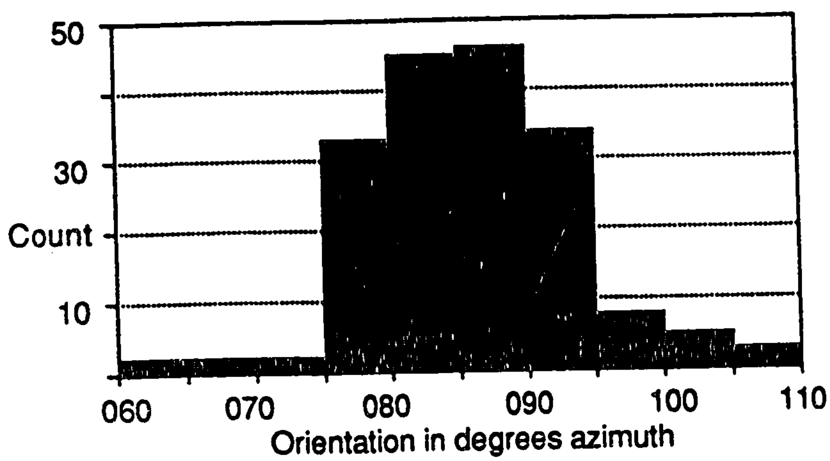

Figure 22: Triangular diagrams comparing terrace and dune sands. Terrace sands are represented by closed circles, while dune sands are represented by open circles. A) Mineralogy, and B) Shape.

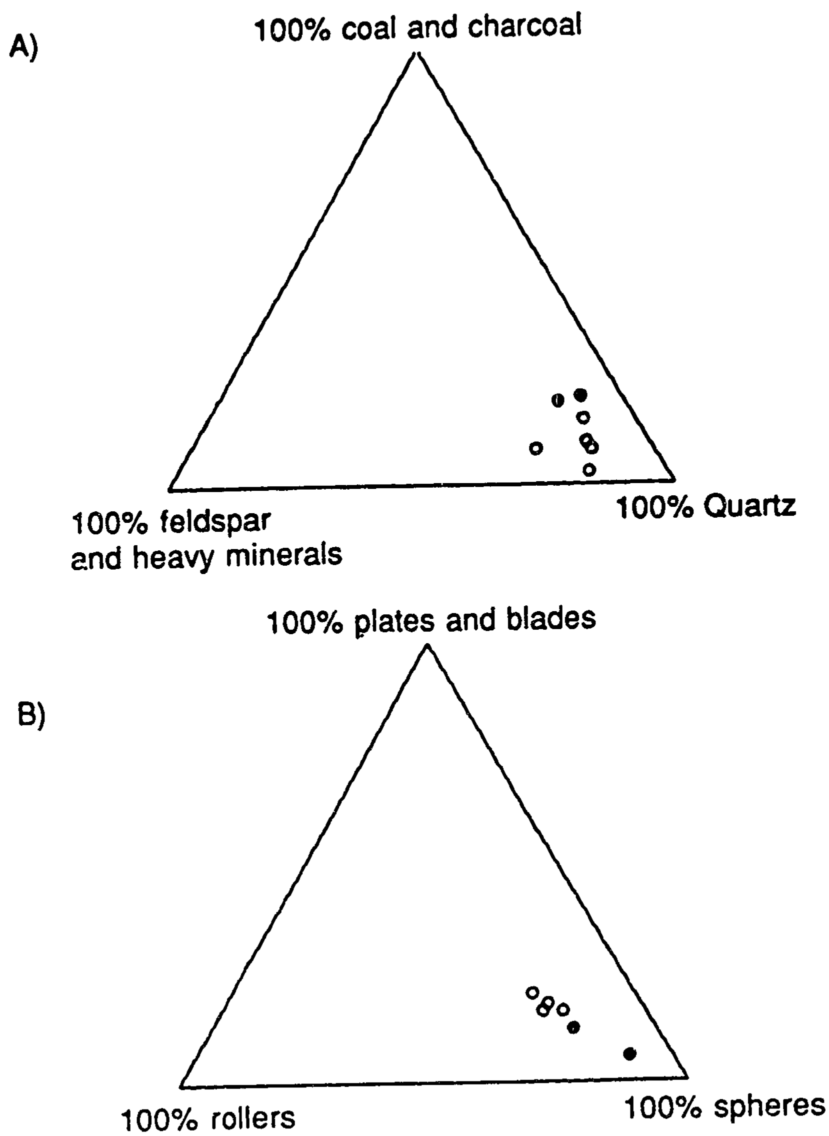

Dunes are present on all three terraces of the Wapiti River. In some areas, dunes present on the upper terrace have migrated onto the middle terrace or have been truncated by the development of the middle terrace (Plate 11). Dunes present on the lower terrace have been truncated by the development of the flood plain (Plate 11). This implies that aeolian activity began prior to the formation of the middle terrace and continued after the lower terrace was developed (Figure 20). This does not imply that dune formation continued throughout the entire dune field over this period. It is quite common for localized areas of dune activity to occur in a largely stabilised field (eg.Hack 1941, Gaylord 1982).

The upper terrace of the Peace River is estimated to date at 10,500 years BP on the basis of a chronocline of variation on *Bison* sp. dates and from St. Onge's (1972) chronology (Churcher and Wilson 1979). The second terrace along the Peace River at Peace River, Alberta has yielded an allochthonous *Bison* sp. bone date of 9,800 +/- 130 years BP (GSC-2865) (Lowden and Blake 1979). Several dates have been obtained from the middle terrace of the Smoky River near Watino, Alberta. Allochthonous *Bison* sp. bones present in gravels have yielded collagen dates of 10,000 +/- 100 years BP (GSC 2092) (Churcher 1984). An autochthonous articulated *Cervas elapus* skeleton yielded a bone collagen date of 9075 +/- 305 years BP (S 2614) (Burns 1986). A date of 7,300 +/- 110 (AECV 583C) on a palaeosol has been obtained from the lower terrace of the Peace River 4km downstream of Peace River, Alberta (Bobrowsky *et al.* 1988). These dates suggest that terrace development in northwest-central Alberta occurred between approximately

Plate 11: Aerial photograph showing the relationship of the dunes to the terraces. Terraces are marked with a dotted line. Arrows point to truncated dunes and to dunes which have migrated onto lower terraces. Scale of aerial photograph is 1: 30,000.

10,500 -7,500 years BP. This implies that the Grande Prairie dune field was active over some or all of this time period beginning prior to 9,000 years BP (Figure 20).

Palaeoecological studies conducted throughout west-central Alberta indicate that maximum aridity occurred in the early Holocene prior to approximately 7,500-7,400 years BP (Vance 1986, White and Mathewes 1986, Schweger and Hickman in press). Climatic models based on orbital parameters and surface boundary conditions predict early Holocene aridity in central Alberta, generated mainly from high summer insolation (Kutzbach and Huetter 1986). Early Holocene aridity would favor the development of dune fields such as the Grande Prairie dune field as aeolian activity would be highly efficient. Low, long armed, type 1 parabolic dunes, which are interpreted to have had the most rapid migration of the dunes present in the study area are restricted to areas above the second terrace.

Fiddler's Pond, British Colombia, a 1m deep pond located approximately 160 km northwest of Grande Prairie, has a basal date of 7,250 +/- 120 years BP (WAT 380) (White 1982). Increasing moisture after 8,000 years BP, generated from increased seasonality, resulted in shallow basin flooding (Schweger and Hickman in press), and would have aided in dune stabilization.

One date has been obtained from a silty-clay layer containing organic detritus directly below a 20m high, compound, type 2 parabolic dune (GP.1) located on the middle terrace of the Wapiti River. This horizon yielded a date of 4,030 +/- 180 years BP (AECV 627C). This indicates that aeolian activity was still occurring locally in the area after c. 4,000 years BP. Lowden and Blake (1979) reported a date of 4,540 +/- 230 years BP (GSC 2802) on charcoal present below 3m of sand and silt also located on the second terrace of the Wapiti River. The sand and silt contained several thin soils and numerous fire bands. Fires would create fresh surfaces, allowing for aeolian activity. This implies that dune formation in the Grande Prairie dune field was initiated by surfaces devoid of vegetation.

CHAPTER SEVEN: SUMMARY

The Grande Prairie dune field developed during the early Holocene prior to c. 9,000 years BP. Aeolian activity continued throughout the Holocene as fresh surfaces became available from terrace development and from fires. The wind direction under which the dunes formed was roughly 085.5 azimuth, corresponding to the strongest and most frequent winds today. Dune asymmetry developed as a result of secondary airflow generated by downwind dunes.

Variations in sediment supply, sediment budget, and the time period of aeolian activity in the study area resulted in the development of three dune types. Dome dunes developed over a short time with a low sediment supply and budget, or with a high sediment budget. Low, long armed, type 1 parabolic dunes developed over a long time period with a low sediment supply and budget. High, short armed, type 2 parabolic dunes developed when the sediment supply was high and the sediment budget was transitional to type 1 parabolic dunes and dome dunes.

Detailed sedimentary analysis revealed the presence of ten facies and eight subfacies in dune sediments, distinguished on the basis of sedimentary structures, contacts, and morphology (Table 2). Variation in these facies and subfacies is interpreted to have resulted from differences in:

1) geomorphology of the depositional surface

2) sediment supply

3) vegetation cover

4) surface airflow (direction and velocity)

5) moisture condition of the depositional surface

Facies associations were established for solitary dome dunes and solitary and compound type 1 and type 2 parabolic dunes (Table 3).

Dome dunes present in the Grande Prairie dune field appear to exhibit characteristics of both inland and coastal dome dunes. The basal part resembles inland dome dunes, whereas the upper part resembles coastal dome dunes.

Some or all of the dome dunes present in the study area are considered to have been initiated as transverse dunes. Similar hypothesis have been put forth for inland dome dunes. As the sedimentation rate decreased, slipface development was impeded and the dome morphology was developed. Continued sedimentation resulted in the buildup of sediment on the dome dune, mainly by adhesion. Similar conditions exist for coastal dome dunes.

The facies associations preserved in both types of solitary parabolic dunes in the Grande Prairie dune field are similar to the general sequences of parabolic dunes. Important differences exist between type 1 and 2 dunes (Table 3). These differences can be attributed to spatial variations in sediment availability and budget.

Sedimentation rates and sediment budget control the migration rate of a parabolic dune. Type 1 dunes migrated much more rapidly then type 2 parabolic dunes, because they had a lower sedimentation rate and a smaller sediment budget. For this reason, topset deposits are thin and have a low preservation potential on type 1 parabolic dunes. Type 2 parabolic dunes migrated much more slowly than type 1 parabolic dunes, because they had a higher sedimentation rate and a greater sediment budget. This resulted in the deposition of thick topset deposits which have a higher preservation potential.

The general sequence of sedimentary structures, preserved in compound parabolic dunes of the Grande Prairie dune field, depends on the migration rate of the dune. Type 1 parabolic dunes have a low angle of climb resulting in the truncation of the majority of the upwind dune. Type 2 parabolic dunes have a high angle of climb resulting in the preservation of the majority of the upwind dune including stoss side deposits. For both dune types, low-angle cross-strata overlie the upwind arm deposits. For type 1 parabolic dunes, low-angle cross-strata are deposited mainly by winds both parallel and oblique to the slipface. For type 2 parabolic dunes low-angle cross-strata are deposited mainly by oblique winds, cross-winds, and lee eddies. These cross-strata are interbedded with stoss side deposits of the upwind dune. When the intersection point between the two dunes is filled in, the entire complex acts as the arm of the upwind dune resulting in the deposition of topset beds.

BIBLIOGRAPHY

AHLBRANDT, T. S., 1973. Sand dunes, geomorphology and geology. Killpecker Creek area, northern Sweetwater County, Wyoming. Ph. D., University of Wyoming Laramie, 174p.

AHLBRANDT, T. S., and ANDREWS, S., 1978. Distinctive features of cold climate eolian deposits, North Park Colorado. Palaeogeography, Palaeoclimatology, Palaeoecology, **25**: 327-351.

AHLBRANDT, T. S., and FRYBERGER, S. G., 1982. Eolian Deposits. *In* Sandstone depositional environments. *Edited by* P. A. Scholle and D. Spearing. American Association of Petroleum Geologists Memoir **31**: 11 -47.

ALLEN, J. R. L., 1970. The avalanching of granular solids on dune and similar slopes. Journal of Geology **78**: 326-351.

- 1984. Sedimentary structures volumes 1 and 2. Developments in Sedimentology **30**, 1256p.

AMERICAN SOCIETY FOR TESTING MATERIALS. 1964. Standard method for grainsize analysis of soils ASTM-0422-63. *In* Procedure for testing soils. pp. 95-106.

BIGARELLA, J. J., BECKER, R. D., and DUARTE, G. M., 1969. Coastal dune structures from Parana (Brazil). Marine Geology **7**: 5 -55.

BOBROWSKY, P. T., DAMKJAR, E. R., GIBSON, T. H., 1988. A geological and archaeological study of HcQh-6, Peace River, Alberta. Report of file. Archaeological Survey of Alberta, 79p.

BOROWKA, R. K., 1980. Present day dune processes and morphology on the Leba Barrier Polish Coast of the Baltic. Geografiska Annaler **62A**: 75-82.

BRADELY, E. F., 1980. An experimental study of the profiles of wind speed, shearing stress and turbulence at the crest of a large hill. Quarterly Journal of the Royal Meterological Society **106**: 101-123.

BROOKFIELD, M. E., 1984. Eolian facies. *In* Facies Models (2nd edition). *Edited by* R. G. Walker. Geoscience Canada Reprint Series **1**: 91-103.

BURNS, J. A., 1986. A 9,000-year old Wapiti (*Cervus elaphus*) skeleton from northern Canada, and its implications for the early Holocene environment. Géographie physique et Quaternaire **40**: 105-108.

CARRIGY, M. A., 1970. Experiments on the angle of repose of granular materials. Sedimentology **14**: 147-158.

COOKE, R. U., and WARREN, A., 1973. Geomorphology in deserts. Anchor

Press. London, 394 p.

COOPER, W. S., 1958. Coastal sand dunes of Oregon and Washington. Geological Society of America Memoir **72**,169p.

CORNISH, V., 1914. Waves of sand and snow. Fisher Unwin, London, 383p.

-1927. Waves in granular material formed and propelled by wind and currents. Royal Astronomical Society of London Supplemental**1**: 447-467.

CURCHER, C. S., 1984. Faunal correlations of Pleistocene deposits in western Canada. *In* Correlation of Quaternary chronologies. *Edited by* W. C. Mahaney, pp. 145-158.

CHURCHER, C. S., and WILSON, M. 1979. Quaternary mammals from the eastern Peace River district, Canada. Canadian Journal of Earth Sciences **19**: 555-570.

DAWSON, G. M., 1881. Report on an exploration from Port Simpson on the Pacific Coast, to Edmonton on the Saskatchewan, embracing a portion on the northern part of British Colombia and the Peace River country, Geological Survey of Canada Report of Progress for 1879-1880, 1B-142B.

DAVID, P.,1977. Sand dune occurrences of Canada: A theme and resource inventory study of eolian landforms of Canada. Indian and Northern Affairs

National Parks Branch Contract No. **74-230**,183p.

-1979. Sand dunes in Canada. Geos **8**:12-14.

-1981. Stabilized dune ridges in northern Saskatchewan. Canadian Journal of Earth Science **18**: 286-310.

ELLWOOD, J. M., EVANS, P. D., and WILSON, I. G., 1975. Small scale aeolian bedforms. Journal of Sedimentary Petrology **45**: 554-561.

ENQUIST, F., 1932. The relationship between dune-form and wind-direction. Geologiska Förenengins **54**: 19-59.

ENVIRONMENT CANADA, 1977 - 1982. Atmospheric Environment. Monthly record, meterological observations in Western Canada. Volumes 62 to 67.

FRYBERGER, S. G., 1979. Dune forms and wind regime. *In* A study of Global Sand Seas. *Edited by* E. D. McKee. United States Geological Survey Professional Paper **1052**: 137-169.

FRYBERGER, S. G., AHLBRANDT, T. S., and ANDREWS, S., 1979. Origin sedimentary features and significance of low-angle eolian sand sheet deposits, Great Sand Dunes National Monument and vicinity, Colorado. Journal of Sedimentary Petrology **49**: 733-746.

FRYBERGER, S. G., and SCHENK, C., 1981. Wind sedimentation tunnel experiments on the origins of aeolian strata. Sedimentology **28**: 805-821.

FOLK, R. L., 1971. Longitudinal dunes of the northwestern edge of the Simpson Desert, Northern Territory, Australia, 1. Geomorphology and grain size relationships. Sedimentology **16**: 5-54

FOLK, R. L., and WARD, W. C., 1957. Brazos River Bar, a study in the significance of grainsize parameters. Journal of Sedimentary Petrology **16**: 3-27.

FRERE, H. B. E., 1870. Notes on the Runn of Cutch and neighboring region. Journal of the Royal Geographical Society **40**: 181-207.

GAYLORD, D. R., 1982. Geologic history of the Ferris Dune Field, south -central Wyoming. *In* Interpretation of windflow characteristics from eolian landforms. *Edited by* R. W. Marrs and K. E. Kolm. Geological Society of America Special Paper **192**: 65-82.

GLENNIE, K. W., and EVAMY, B. D., 1968. Dikaka: Plants and plant-root structures associated with aeolian sand. Palaeogeography, Palaeoclimatology, Palaeoecology **4**: 7- 87.

GOLDSMITH, V.,1973. Internal geometry and origin of vegetated coastal dunes. Journal of Sedimentary Petrology **43**: 1128-1143.

-1977. The "VAMP" coastal dune classification. *In* Coastal processes and resulting forms of sediment accumulations, Currituck Spit, Virginia-North Carolina. *Edited by* V. Goldsmith. Special Report in Applied Marine Science and Ocean Engineering **143**: 383-402.

-1985. Coastal Dunes. *In* Coastal sedimentary environments (2nd. edition). *Edited by* R. A. Davies. Springer-Verlag, New York, pp. 303 - 378.

GRAVENOR, C. P., 1956. Air photographs of the Plains Region in Alberta. Alberta Research Council Preliminary Report **56-5**, 35p.

GRAVENOR, C. P., GREEN, R., and GODFREY, J. D., 1960. Air photographs of Alberta. Alberta Research Council Bulletin **5**, 38p.

GREELEY, R., and IVERSEN, J. D., 1985. Wind as a geological process. Oxford, Cambridge University Press, 333p.

HACK, J. T., 1941. Dunes of the western Navajo country. Geographical Review **31**: 240-263.

HASENRATH, S. L., 1967. The barchans of the Arequipa region, southern Peru. Zeitschrift für Geomorphologie **11**: 300-331.

HEFLEY, H. M., and SIDWELL, R., 1945. Geological and ecological observations of some high plains dunes. American Journal of Science

243: 361-376.

HENDERSON, E. P., 1959. Surficial geology of Sturgeon Lake Map-area Geological Survey of Canada Memoir **303**, 108p.

HESP, P. A., 1981. The formation of shadow dunes. Journal of Sedimentary Petrology **51**: 101-112.

HÖGBORM, I., 1923. Ancient inland dunes or northern and middle Europe. Geografiska Annaler **5**: 114-242.

HOLM, D. A., 1960. Desert geomorphology in the Arabian Peninsula. Science **132**: 1369-1379.

HOTTA, S., KUBOTA, S., KATORI, S., and HORIKAWA, K., 1984. Sand transport by wind on a wet sand surface. Proceedings of the 19th International Coastal Engineering Conference, New York, pp. 1265-1281.

HOWARD, A. D., 1977. Effect of slope on the threshold of motion and its application to orientation of wind ripples. Geological Society of America Bulletin **88**: 853-856.

HOWARD, A. D., MORTON, J. B., and MOHAMED, G.-E.-J., and PIERCE, D. B., 1978. Sand transport model of barchan dune equilibrium. Sedimentology **25**: 307-338.

HUMMEL, G., and KOCUREK, G., 1984. Interdune areas of the back-island dune field, North Padre Island, Texas. Sedimentary Geology, **39**: 1-26.

HUNTER, R. E.,1973. Pseudo-crosslamination formed by climbing adhesion ripples. Journal of Sedimentary Petrology **50**: 1125-1127.

-1977a. Basic types of stratification in small eolian dunes. Sedimentology, **24**: 361-387.

- 1977b. Terminology of cross-stratified sedimentary layers and climbing ripple structures. Journal of Sedimentary Petrology **47**: 697-706.

- 1980. Quasi-planar adhesion stratification - an eolian structure formed in wet sand. Journal of Sedimentary Petrology **50**: 31-43.

-1981. Stratification styles in eolian sandstones: some Pennsylvanian to Jurassic examples from the western interior U.S.A. *In* Recent and ancient nonmarine depositional environments: models for exploration. *Edited by* F. G. Ethridge and R. M. Flores. Special Publication of the Society of Paleontologists and Mineralogists **31**: 315-329.

- 1985. A kinematic model for the structure of lee-side deposits. Sedimentology **32**: 409-422.

HUNTER, R. E., RICHMOND, J. B., and ALPHA, T. R., 1983. Storm controlled oblique dunes of the Oregon Coast. Bulletin of the Geological Society of America **94**: 1450-1465.

JONES, J. F., 1961. Surficial geology and related problems of the Beaverlodge district northwestern Alberta. M. Sc. University of Western Ontario, London,

-1966. Geology and groundwater resources of the Peace River district, northwestern Alberta. Research Council of Alberta Bulletin **16**, 143p.

KING, W. J. H., 1918. The nature and form of sand ripples and dunes Geographical Journal **47**: 189-209.

KOCUREK, G.,1981. Significance of interdune deposits and bounding surfaces in aeolian dune sands. Sedimentology **28**: 753-780.

-1986. Origins of low-angle stratification in aeolian deposits. *In* Aeolian geomorphology. *Edited by* W. G. Nickling. Bingham Symposia in Geomorphology International Series **7**: 177-211.

KOCUREK. G., and DOTT, 1981. Distinctions and uses of stratification types in the interpretation of eolian sands. Journal of Sedimentary Petrology **51**: 579-595.

KOCUREK, G., and FIELDER, G., 1982. Adhesion structures. Journal of Sedimentary Petrology **54**: 1229-1241.

KOCUREK, G. and NIELSON, J., 1986. Conditions favorable for the formation of warm-climate aeolian sand sheets. Sedimentology **33**: 795-816.

KUTZBACH, J. E., and GUETTER, P. J., 1986. The influence of changing orbital parameters and surface boundary conditions on climate simulations for the past 18,000 years. Journal of the Atmospheric Sciences **43**: 1726 -1759.

LANCASTER, N., 1985. Variations in wind velocity and sand transport on the windward flanks of desert sand dunes. Sedimentology **32**: 581- 593.

LAND, L. S., 1964. Eolian cross-bedding in the beach dune environment, Sapelo Island, Georgia. Journal of Sedimentary Petrology **34**: 389-394.

LANG, A. H., BOSTOCK, H., S., and FORTIER, Y. O., 1947. Interim catalogue of the Geological Survey collections of outstanding air photographs. Geological Survey of Canada Paper **47-26**, 17p.

LETTAU, K., and LETTAU, H., 1969. Bulk transport of sand by the barchans of the Pampa La Joya in southern Peru. Zeitschrift für Geomorphologie **13**: 182-195.

LONG, J. T., and SHARP, R. P., 1964. Barchan-dune movement in the Imperial Valley, California. Geological Society of America Bulletin **75**: 149-156.

LOWDEN, J. A., and BLAKE, W., 1979. Geological Survey of Canada radiocarbon dates XIX. Geological Survey of Canada Paper **79-7**, 58 p.

MAINGIET, M., and CHEMIN, M. C., 1983. Sand seas of the Sahara and the Sahel: an explanation of their thickness and dune type by the sand budget principle. *In* Eolian sediments and processes. *Edited by* M. E, Brookfield and T. S. Ahlbrandt. Developments in Sedimentology **38**: 353-364.

MARRS, R. W., and GAYLORD, D. R., 1982. Techniques for interpretation of windflow characteristics from eolian landforms. *In*Interpretation of windflow characteristics from eolian landforms. *Edited by* R. W. Marrs and K. E. Kolm. Geological Society of America Special Paper **192**: 3-17.

MARZOLF, J. E., 1988. Controls on late Paleozoic and early Mesozoic eolian deposition of the western United States. *In* Late palaeozoic and mesozoic eolian deposits of the western interior of the United States. *Edited by* G. Kocurek. Sedimentary Geology **56**: 167-191.

MASON, P. J., and SYKES, R. I., 1979. Flow over an isolated hill of moderate slope. Quarterly Journal of the Royal Meterological Society **105**: 383-395.

MATHEWS, W. H., 1980. Retreat of the last ice sheets in northeastern British Columbia and adjacent Alberta. Geological Survey of Canada Bulletin **331**, 22p.

MCBRIDE, E. F., and HAYES, M. O., 1962. Dune cross-bedding on Mustang

Island, Texas. Bulletin of the American Association of Petroleum Geology **46**: 546-551.

MCKEE, E. D.,1945. Small-scale structures in the Cococino sandstone of northern Arizona. Journal of Geology **53**: 313-325.

-1966. Structures of dunes at White Sands National Monument, New Mexico (and a comparison with structures of dunes from other selected areas). Sedimentology **7**: 3-69.

- 1979. Sedimentary structures in dunes. *In* A study of global sand seas. *Edited by* E. D. McKee. United States Geological Survey Professional Paper **1052**: 83-113.

- 1982. Sedimentary structures in dunes of the Namib Desert, South West Africa. Geological Society of America Special Paper **188**, 64p.

-1983. Eolian sand bodies of the world. *In* Eolian sediments and processes. *Edited by* M. E. Brookfield and T. S. Ahlbrandt. Developments in Sedimentology **38**: 1-25.

MCKEE, E. D., and DOUGLASS, J. R., 1971. Growth and movement of dunes at White Sands National Monument, New Mexico. United States Geological Survey Professional Paper **750-D**: D108-D114.

MCKEE, E. D., DOUGLASS, J. R., and RITTENHOUSE, S., 1971. Deformation of lee-side laminae in eolian dunes. Geological Society of America Bulletin **82**: 359-378.

MCKEE, E. D., and BIGARELLA, J. J., 1972. Deformational structures in Brazilian Coastal Dunes. Journal of Sedimentary Petrology **42**; 670-681.

MELTON, F. A., 1940. A tentative classification of sand dunes: Its application to dune history in the Southern High Plains. Journal of Geology **48**: 113 -145.

NICKLING, W. G., and ECCLESTONE, M., 1981. The effects of soluble salt on the threshold shear velocity of fine sand. Sedimentology **28**: 505 - 510.

NIELSON, J. A., 1986. The surface processes, internal structure, and net deposits of eolian dune and sand sheets. Ph. D. University of Texas, Austin, Texas, 224p.

NIELSON, J. A., and KOCUREK, G., 1987. Climbing zibars of the Algodones. Sedimentary Geology **48**: 1-15.

-1987. Surface processes, deposits, and development of star dunes: Dumont dune field, California. Geological Society of America Bulletin **99**: 177 - 186.

NORRIS, R. M., 1966. Barchan dunes of Imperial Valley, California. Journal of Geology **74**: 292-306.

ODYNSKY, W., 1958. U-shaped dunes and effective wind directions in Alberta. Canadian Journal of Soil Science **38**: 56-62.

ODYNSKY, W., WYNNYK, A., NEWTON, J. D., 1956. Soil survey of the Grande Prairie and Sturgeon Lake Sheets, Alberta Soil Survey Report.**18**, 111p.

ODYNSKY, W., LINDSAY, J. D., REEDER, S. W., and WYNNYK, A., 1961. Soil Survey of the Beaverlodge and Blueberry Mountain Sheets, Research Council of Alberta Report. **20**, 123p.

OJAMAA, P., 1978. Ecological (Biophysical) land classification and use -limitation table Wapiti Sand Dune study area, Alberta Energy and Natural Resources Report **78A**, 39p.

OLSON, J. S., 1958. Lake Michigan dune development 2. Plants as agents and tools in geomorphology. Journal of Geology **66**: 345-351.

OTTO, G. J., 1938. The sedimentation unit and its use in field sampling. Journal of Geology **46**: 569-582.

PYE, K.,1983. Early post-depositional modification of aeolian sand dunes *In* Eolian sediments and processes. *Edited by* M. E. Brookfield and T. S. Ahlbrandt. Developments in Sedimentology **38**: 455-482.

-1982. Morphological development of coastal dunes in a humid tropical environment, Cape Bedford and Cape Flattery, North Queensland. Geografiska Annaler **64A**: 213-227.

REINECK, H. E., 1955. Haftrippeln und haftwarzen ablagerungsformen von flugsand. Senckenbergiana Lethaea **36**: 447-357.

RIM, M., 1951. The influence of geophysical processes on the stratification of sandy soils. Journal of Soil Science **2**: 188-195.

-1958. Simulation by dynamical model of sand tract morphologies occurring in Isreal. Bulletin of the Research Council of Isreal **7-G**: 123-133.

ROWE, J. S., 1972. Forest regions of Canada. Canadian Forestry Service Publication **1300**, 172 p.

RUEGG, G. H. J., 1983. Periglacial eolian evenly laminated sandy deposits in the late Pleistocene of N. W. Europe, a facies unrecorded in modern sedimentological handbooks. *In* Eolian sediments and processes. *Edited by* M. E. Brookfield and T. S. Ahlbrandt. Developments in Sedimentology **38**: 455-482.

RUBIN, D. M., and HUNTER, R. E., 1982. Bedform climbing in theory and nature. Sedimentology **29**: 121-138.

SCHENK, C. J., 1983. Textural and structural characteristics of some experimentally formed eolian strata. *In* Eolian sediments and processes. *Edited by* M. E. Brookfield and T. S. Ahlbrandt. Developments in Sedimentology **38**: 41-49.

SCHWAN, J., 1986. The origin of horizontal alternating bedding in Weichselian aeolian sands in Northwestern Europe. Sedimentary Geology, **49**: 73-108.

-1987. Sedimentological characteristics of a fluvial to aeolian succession in Weichselian Talsand in the Emsland (FGR). Sedimentary Geology **52**: 273-298.

SCHWEGER, C. E., and HICKMAN, M., in press. Holocene paleohydrology, central Alberta: testing the general circulation model climate simulations. Canadian Journal of Earth Sciences.

SHARP, R. T., 1963. Wind Ripples. Journal of Geology **71**: 617-636.

SMITH, H. T. U., 1949. Physical effects of Pleistocene climatic changes in nonglaciated areas: Eolian phenomena, frost action and stream terracing. Geological Society of America Bulletin **60**: 1485-1516.

STATHAM, I., 1974. The relationship of porosity and angle of repose to mixture proportions in assemblages of different sized materials. Sedimentology **21**: 149-162.

STEIDTMANN, J. R., 1982. Structures in the moist, cold-climate sand dunes of southern Wyoming. *In* Interpretation of windflow characteristics from eolian landforms. *Edited by* R. W. Marrs and K. E. Kolm. Geological Society of America Special Paper **192**: 83-87.

STEENSTRUP, K. J. V., 1894. Om klitterns vandrug. Meddelelser frä Dansk **1**: 1-14.

STONE, R. O. 1967. A desert glossary. Earth-Science Review **3**: 211-299.

ST. ONGE, D. A., 1972. Sequence of glacial lakes in north-central Alberta. Geological Survey of Canada **213**, 16p.

SWEET, M. L., NIELSON, J., HAVHOLM, K., and FARRALLEY, J., 1988. Algodunes dune field of southeastern California: case history of a migrating modern dune field. Sedimentology **35**: 939 - 952.

TANNER, W. F., 1967. Ripple mark indices and their uses. Sedimentology **9**: 89 - 04.

TWARDY, A. G., and CORNS, I. G. W., 1980. Soil Survey and interpretations of the Wapiti map area, Alberta. Alberta Institute of Pedology Bulletin **39**, 134p.

THORNBURY, W. D., 1954. Principles of geomorphology. John Wiley and Sons, New York, 618p.

VANCE, R. E., 1986. Aspects of postglacial climate of Alberta: calibration of the pollen record. Géographie physique et Quaternaire **40**: 153-160.

VAN STAATEM, L. M. J. U., 1953. Rhythmic pattern on Dutch North Sea beaches. Geologie en Mijnbouw **15**: 31-43.

WARD, W. T., 1977. Sand movement of Fraser Island. University of Queensland Occasional Papers in Anthropology **8**: 113-126.

WASSON, R. J., and HYDE, R,. 1983. Factors determining desert dune type. Nature **304**: 337-39.

WHITE, J. M., 1983. Late Quaternary geochronology and palaeoecology of the Upper Peace River district, Canada. Ph.D. Simon Fraser University, Burnaby, British Colombia, 149p.

WHITE, J. M., and MATHEWES, R. W., 1986. Postglacial vegetation and climatic change in the Upper Peace River district, Alberta. Canadian Journal of Botany **64**: 2305-2318.

- 1982. Holocene vegetation and climatic change in the Peace River district, Canada. Canadian Journal of Earth Sciences **19**: 555-570.

WHITE, J. M., MATHEWES, R. W., and MATHEWS, W. H., 1985. Late Pleistocene chronology and environment of the "Ice-free Corridor" of northwestern Alberta. Quaternary Research **24**: 173-186.

WILSON, I. G., 1972. Aeolian bedforms-their development and origins. Sedimentology **19**: 173-210.

YAALON, D. H., 1967. Factors affecting the lithification of eolianite and interpretation of its environmental significance in the coastal plain of Isreal. Journal of Sedimentary Petrology **37**: 1189-1199.

APPENDIX ONE: SCHEMATIC DIAGRAMS AND DESCRIPTIONS OF MAJOR SECTIONS

LEGEND

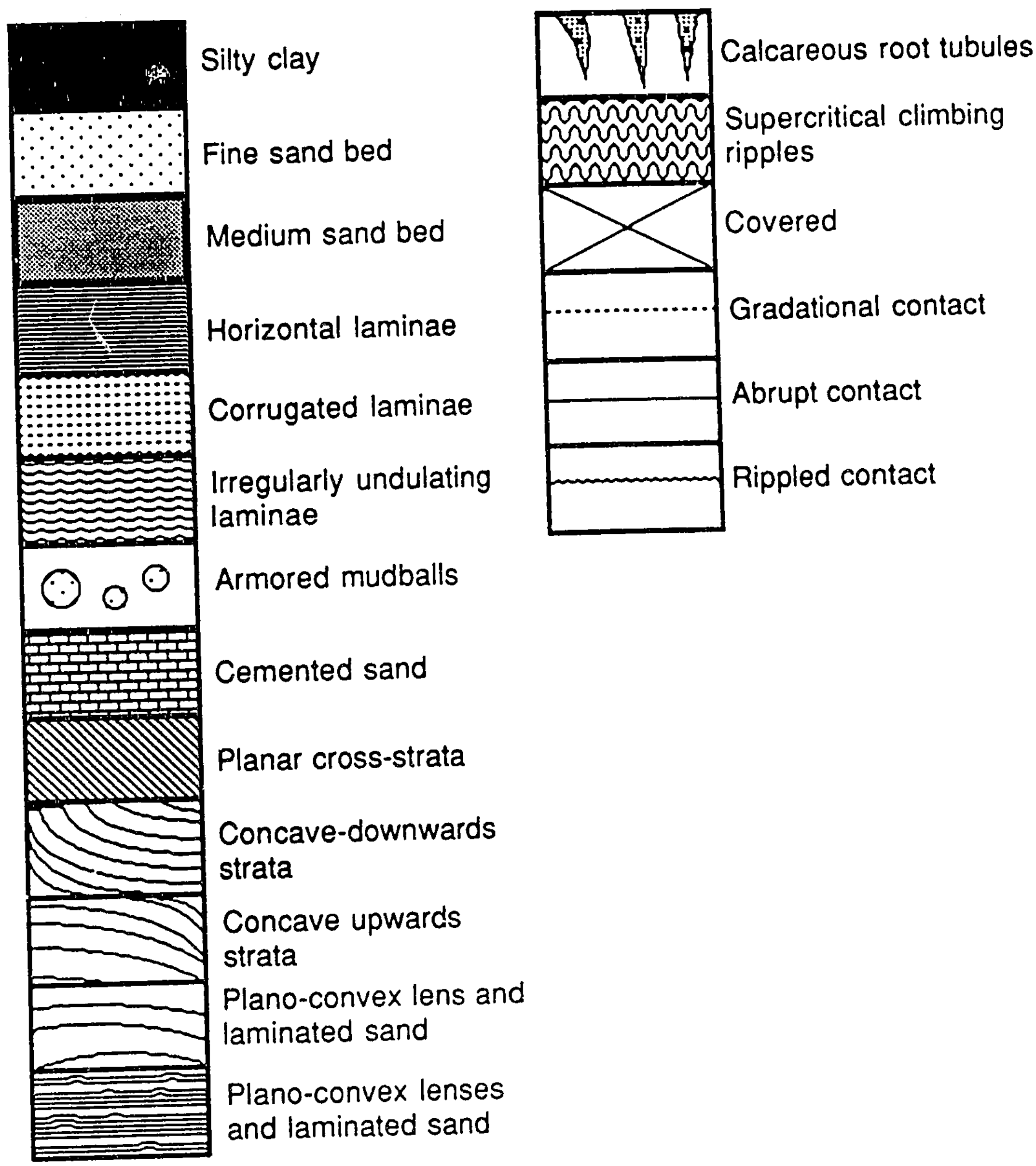

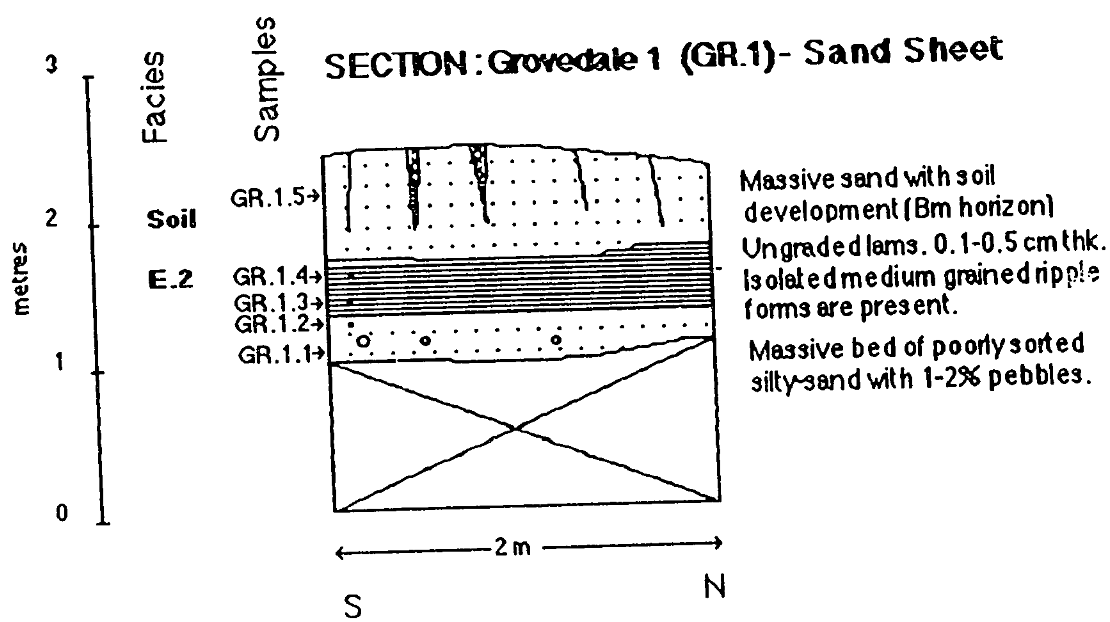
SECTION : Grovedale 1 (GR.1)- Sand Sheet
metres
3
2
1
0
Facies
Soil
E.2
Samples
GR.1.5
GR.1.4
GR.1.3
GR.1.2
GR.1.1
Massive sand with soil development (Bm horizon)
Ungraded lams. 0.1-0.5 cm thk. Isolated medium grained ripple forms are present.
Massive bed of poorly sorted silty-sand with 1-2% pebbles.
2 m
S
N

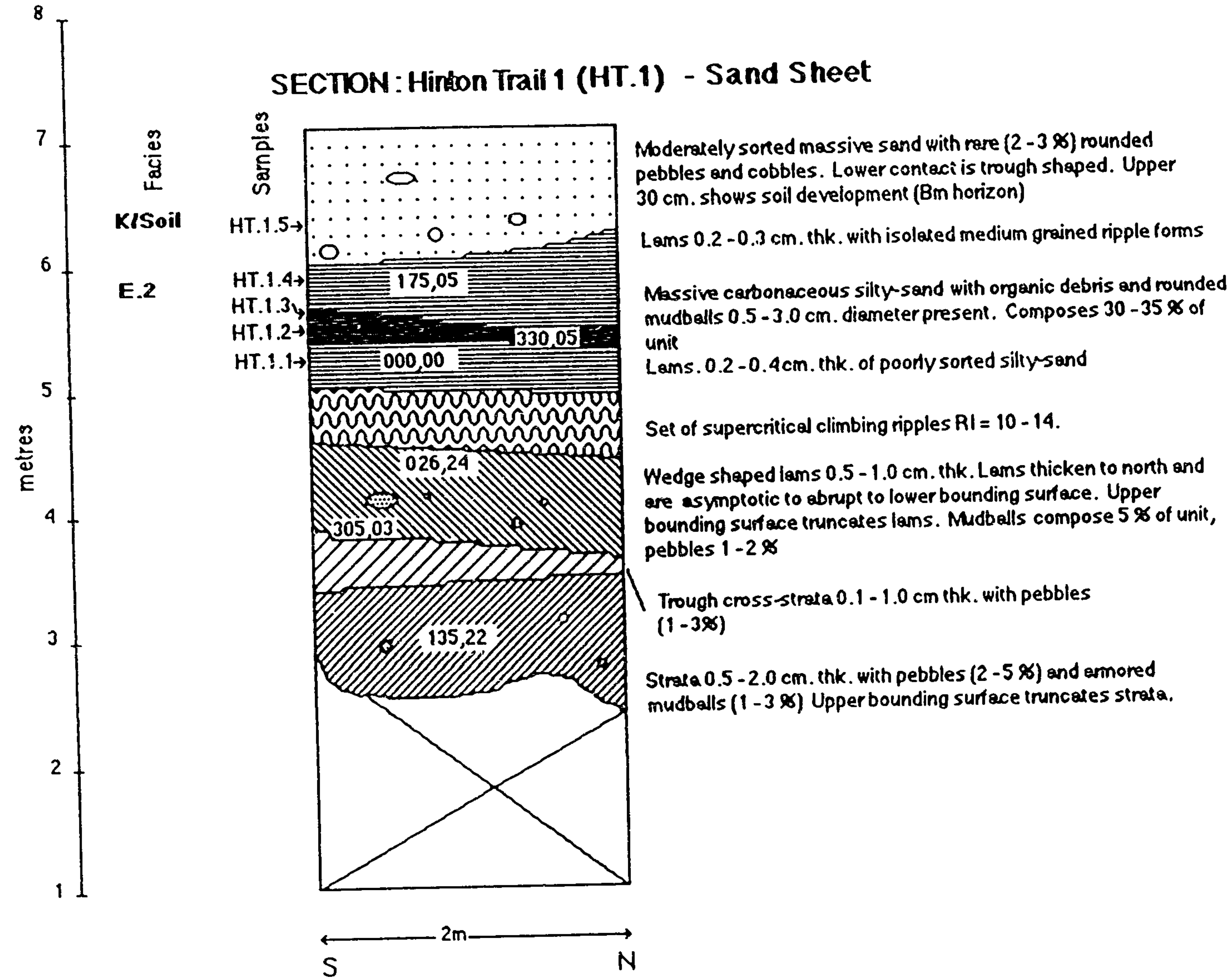

SECTION : Hinton Trail 1 (HT.1) - Sand Sheet
metres
8
7
6
5
4
3
2
1
Facies
K/Soil
E.2
Samples
HT.1.5→
HT.1.4→
HT.1.3
HT.1.2→
HT.1.1→
175,05
330,05
000,00
026,24
305,03
135,22
Moderately sorted massive sand with rare (2 - 3 %) rounded pebbles and cobbles. Lower contact is trough shaped. Upper 30 cm. shows soil development (Bm horizon)
Lams 0.2 - 0.3 cm. thk. with isolated medium grained ripple forms
Massive carbonaceous silty-sand with organic debris and rounded mudballs 0.5 - 3.0 cm. diameter present. Composes 30 - 35 % of unit
Lams. 0.2 - 0.4cm. thk. of poorly sorted silty-sand
Set of supercritical climbing ripples RI = 10 - 14.
Wedge shaped lams 0.5 - 1.0 cm. thk. Lams thicken to north and are asymptotic to abrupt to lower bounding surface. Upper bounding surface truncates lams. Mudballs compose 5 % of unit, pebbles 1 - 2 %
Trough cross-strata 0.1 - 1.0 cm thk. with pebbles (1 - 3%)
Strata 0.5 - 2.0 cm. thk. with pebbles (2 - 5 %) and armored mudballs (1 - 3 %) Upper bounding surface truncates strata.
2m
S
N

SECTION : Pipestone 1 (P.1) - Compound type 1 parabolic dune

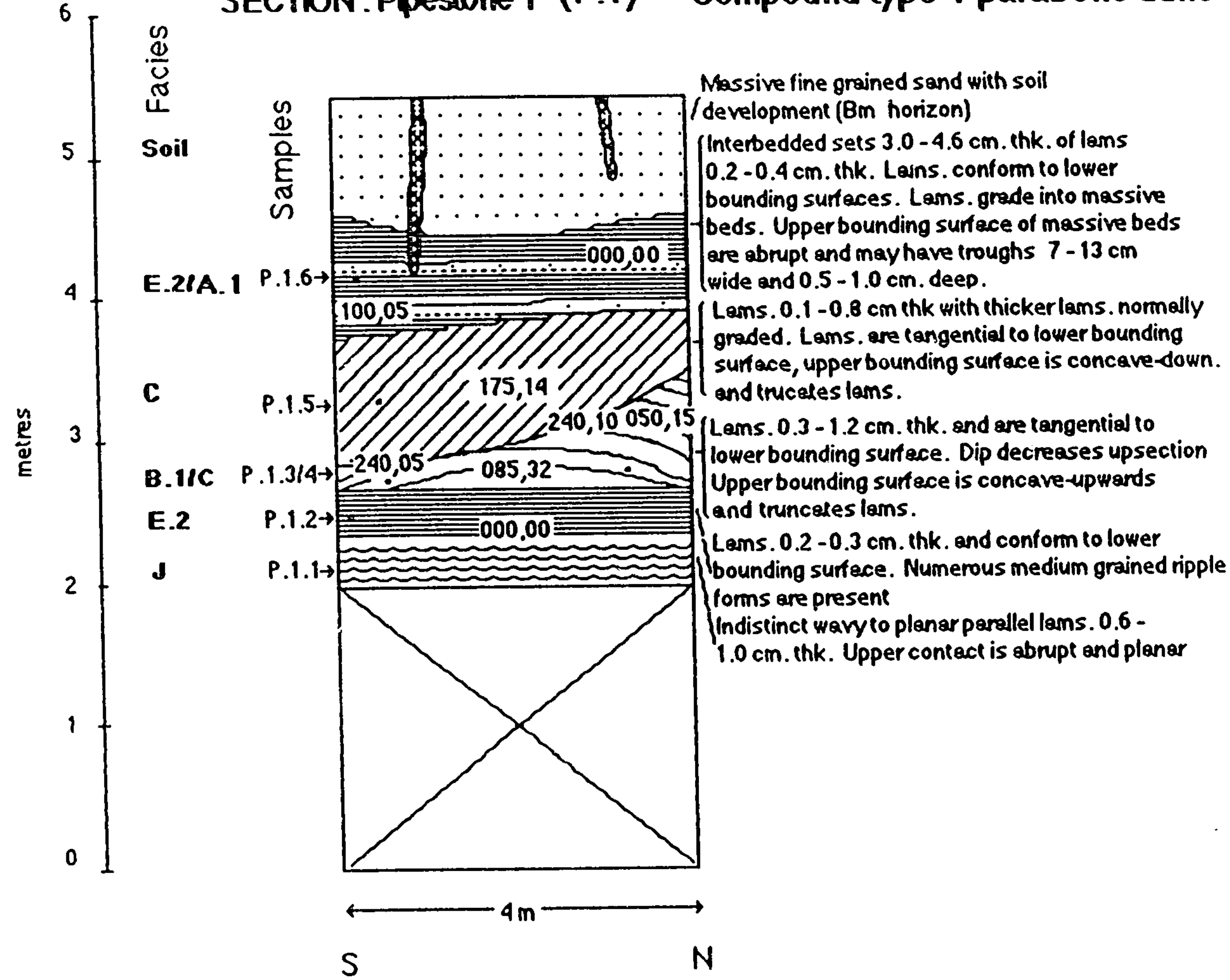

SECTION : Pipestone 2 (P.2) - Solitary type 1 parabolic dune

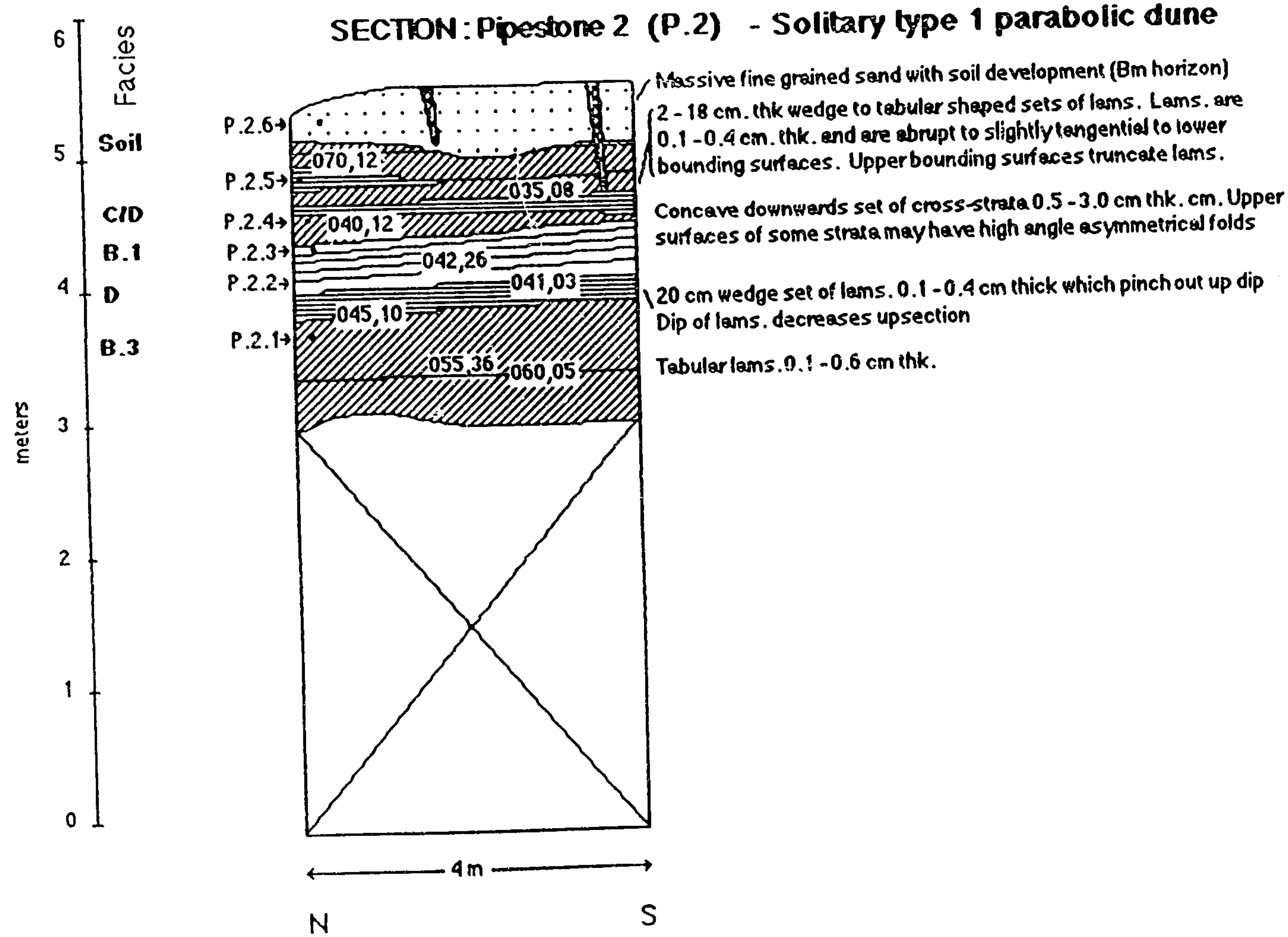

SECTION : Pipestone 3 (P.3) - Sand Sheet

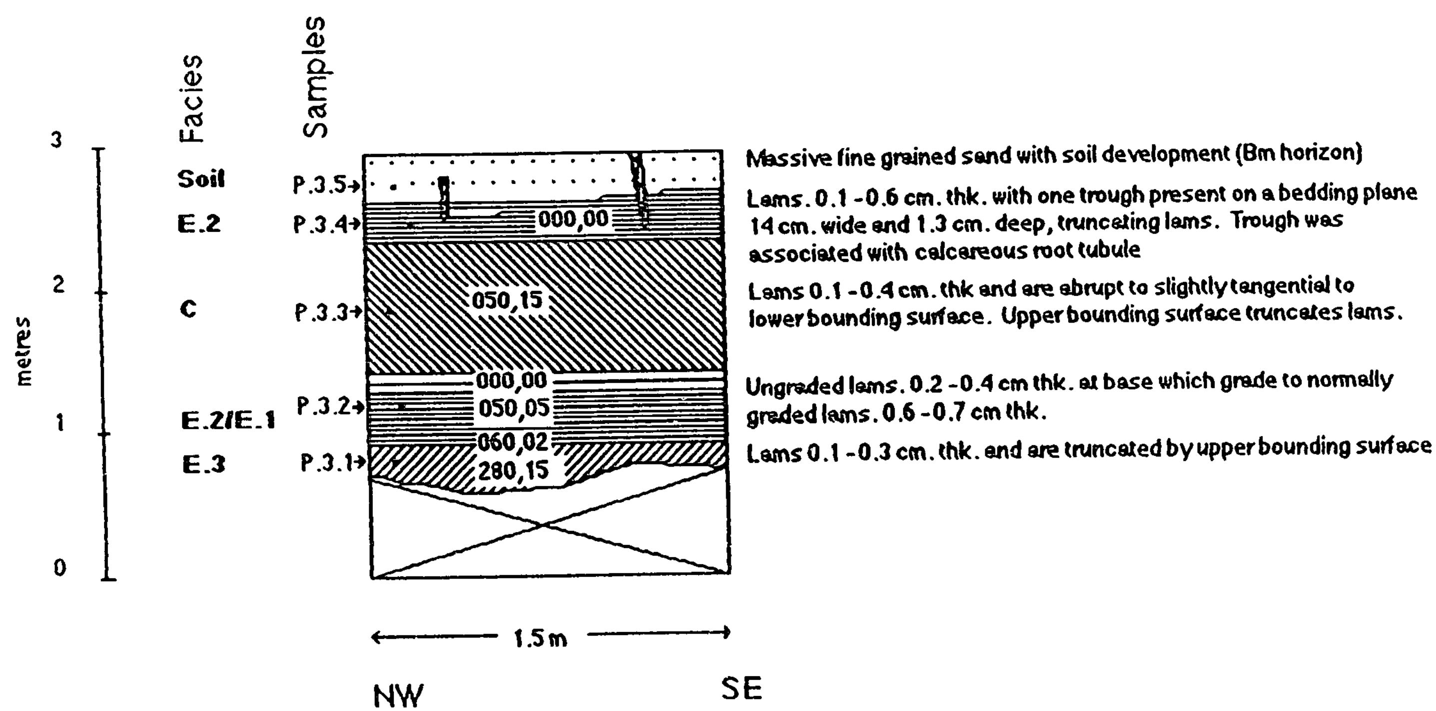

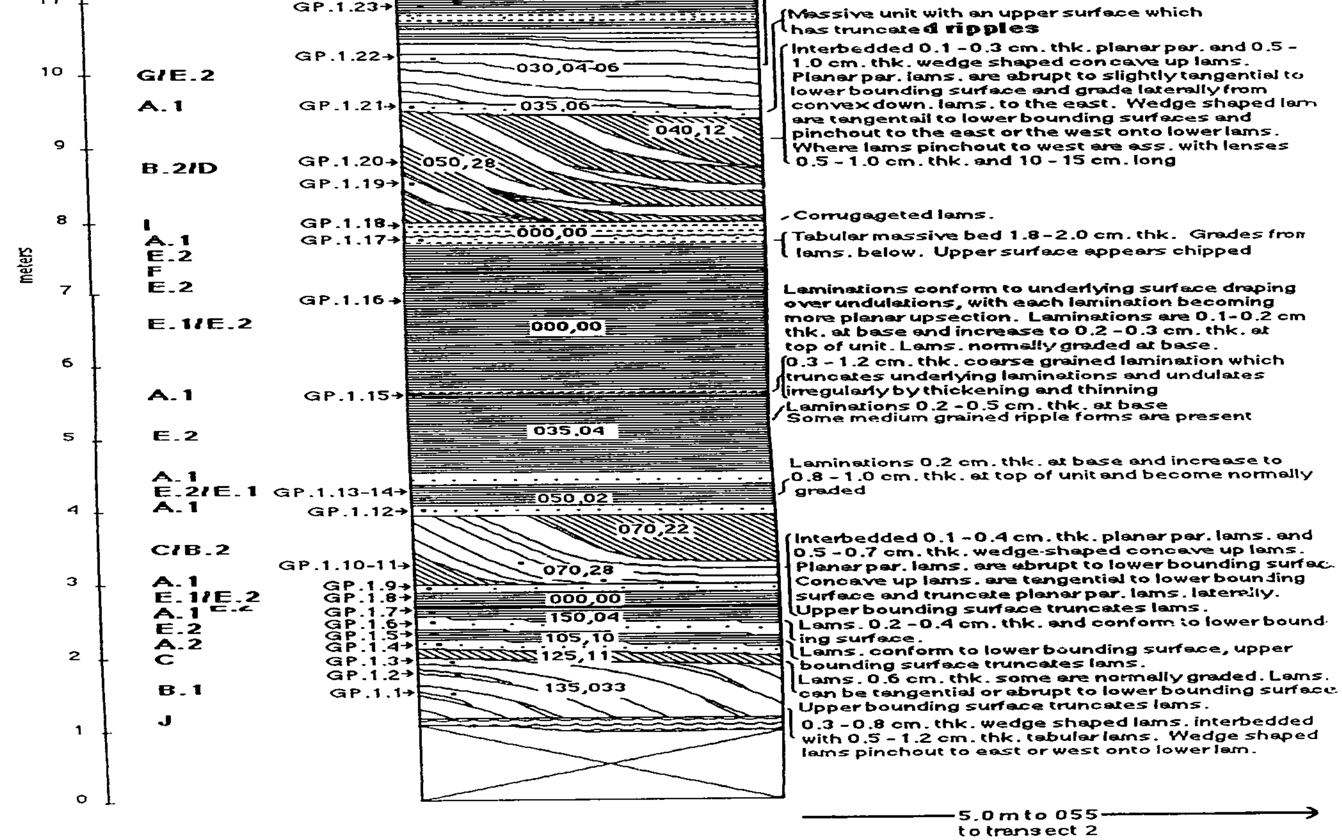

meters
G/E.2
A.1
B.2/D
I
A.1
E.2
F
E.2
E.1/E.2
A.1
E.2
A.1
E.2/E.1
A.1
C/B.2
A.1
E.1/E.2
A.1
E.2
A.2
C
B.1
J
GP.1.23
GP.1.22
GP.1.21
GP.1.20
GP.1.19
GP.1.18
GP.1.17
GP.1.16
GP.1.15
GP.1.13-14
GP.1.12
GP.1.10-11
GP.1.9
GP.1.8
GP.1.7
GP.1.6
GP.1.5
GP.1.4
GP.1.3
GP.1.2
GP.1.1
030,04-06
035,06
040,12
050,28
000,00
000,00
035,04
050,02
070,22
070,28
000,00
150,04
105,10
125,11
135,033
Massive unit with an upper surface which has truncated ripples
Interbedded 0.1 - 0.3 cm. thk. planar par. and 0.5 - 1.0 cm. thk. wedge shaped concave up lams. Planar par. lams. are abrupt to slightly tangential to lower bounding surface and grade laterally from convex down. lams. to the east. Wedge shaped lam are tangentail to lower bounding surfaces and pinchout to the east or the west onto lower lams. Where lams pinchout to west are ass. with lenses 0.5 - 1.0 cm. thk. and 10 - 15 cm. long
Corrugageted lams.
Tabular massive bed 1.8 - 2.0 cm. thk. Grades from lams. below. Upper surface appears chipped
Laminations conform to underlying surface draping over undulations, with each lamination becoming more planar upsection. Laminations are 0.1 - 0.2 cm thk. at base and increase to 0.2 - 0.3 cm. thk. at top of unit. Lams. normally graded at base.
0.3 - 1.2 cm. thk. coarse grained lamination which truncates underlying laminations and undulates irregularly by thickening and thinning
Laminations 0.2 - 0.5 cm. thk. at base
Some medium grained ripple forms are present
Laminations 0.2 cm. thk. at base and increase to 0.8 - 1.0 cm. thk. at top of unit and become normally graded
Interbedded 0.1 - 0.4 cm. thk. planar par. lams. and 0.5 - 0.7 cm. thk. wedge-shaped concave up lams. Planar par. lams. are abrupt to lower bounding surface. Concave up lams. are tangential to lower bounding surface and truncate planar par. lams. laterally.
Upper bounding surface truncates lams.
Lams. 0.2 - 0.4 cm. thk. and conform to lower bounding surface.
Lams. conform to lower bounding surface, upper bounding surface truncates lams.
Lams. 0.6 cm. thk. some are normally graded. Lams. can be tangential or abrupt to lower bounding surface.
Upper bounding surface truncates lams.
0.3 - 0.8 cm. thk. wedge shaped lams. interbedded with 0.5 - 1.2 cm. thk. tabular lams. Wedge shaped lams pinchout to east or west onto lower lam.
5.0 m to 055
to transect 2

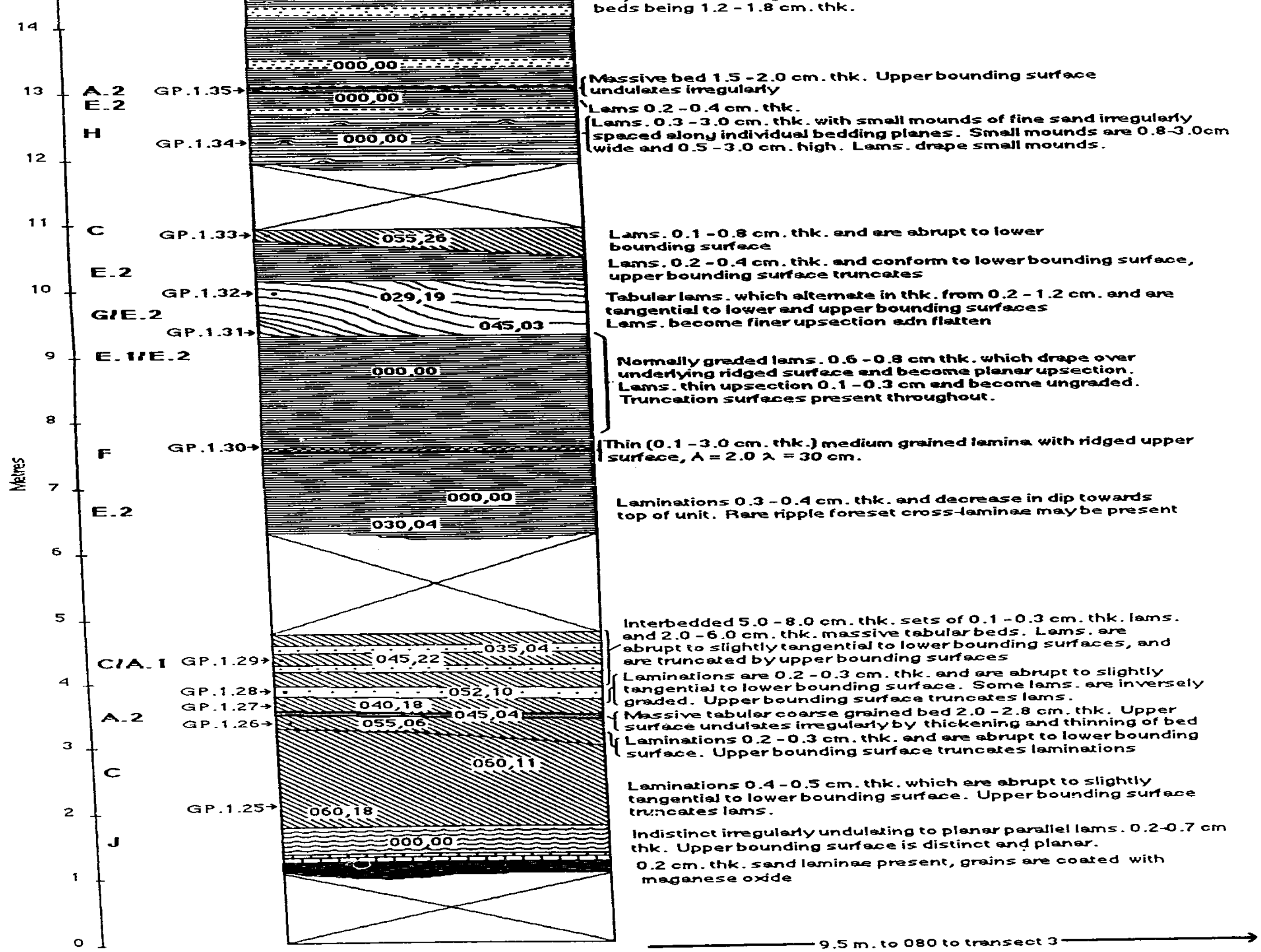

beds being 1.2 - 1.8 cm. thk.
Massive bed 1.5 - 2.0 cm. thk. Upper bounding surface undulates irregularly
Lams 0.2 - 0.4 cm. thk.
Lams. 0.3 - 3.0 cm. thk. with small mounds of fine sand irregularly spaced along individual bedding planes. Small mounds are 0.8-3.0cm wide and 0.5 - 3.0 cm. high. Lams. drape small mounds.
Lams. 0.1 - 0.8 cm. thk. and are abrupt to lower bounding surface
Lams. 0.2 - 0.4 cm. thk. and conform to lower bounding surface, upper bounding surface truncates
Tabular lams. which alternate in thk. from 0.2 - 1.2 cm. and are tangential to lower and upper bounding surfaces
Lams. become finer upsection adn flatten
Normally graded lams. 0.6 - 0.8 cm thk. which drape over underlying ridged surface and become planar upsection. Lams. thin upsection 0.1 - 0.3 cm and become ungraded. Truncation surfaces present throughout.
Thin (0.1 - 3.0 cm. thk.) medium grained lamina with ridged upper surface, A = 2.0 λ = 30 cm.
Laminations 0.3 - 0.4 cm. thk. and decrease in dip towards top of unit. Rare ripple foreset cross-laminae may be present
Interbedded 5.0 - 8.0 cm. thk. sets of 0.1 - 0.3 cm. thk. lams. and 2.0 - 6.0 cm. thk. massive tabular beds. Lams. are abrupt to slightly tangential to lower bounding surfaces, and are truncated by upper bounding surfaces
Laminations are 0.2 - 0.3 cm. thk. and are abrupt to slightly tangential to lower bounding surface. Some lams. are inversely graded. Upper bounding surface truncates lams.
Massive tabular coarse grained bed 2.0 - 2.8 cm. thk. Upper surface undulates irregularly by thickening and thinning of bed
Laminations 0.2 - 0.3 cm. thk. and are abrupt to lower bounding surface. Upper bounding surface truncates laminations
Laminations 0.4 - 0.5 cm. thk. which are abrupt to slightly tangential to lower bounding surface. Upper bounding surface truncates lams.
Indistinct irregularly undulating to planar parallel lams. 0.2-0.7 cm thk. Upper bounding surface is distinct and planar.
0.2 cm. thk. sand laminae present, grains are coated with maganese oxide
9.5 m. to 080 to transect 3
Metres
14
13
12
11
10
9
8
7
6
5
4
3
2
1
0
A.2
E.2
H
C
E.2
G/E.2
E.1/E.2
F
E.2
C/A.1
A.2
C
J
GP.1.35
GP.1.34
GP.1.33
GP.1.32
GP.1.31
GP.1.30
GP.1.29
GP.1.28
GP.1.27
GP.1.26
GP.1.25
000,00
000,00
000,00
055,26
029,19
045,03
000,00
000,00
030,04
035,04
045,22
052,10
040,18
045,04
055,06
060,11
060,18
000,00

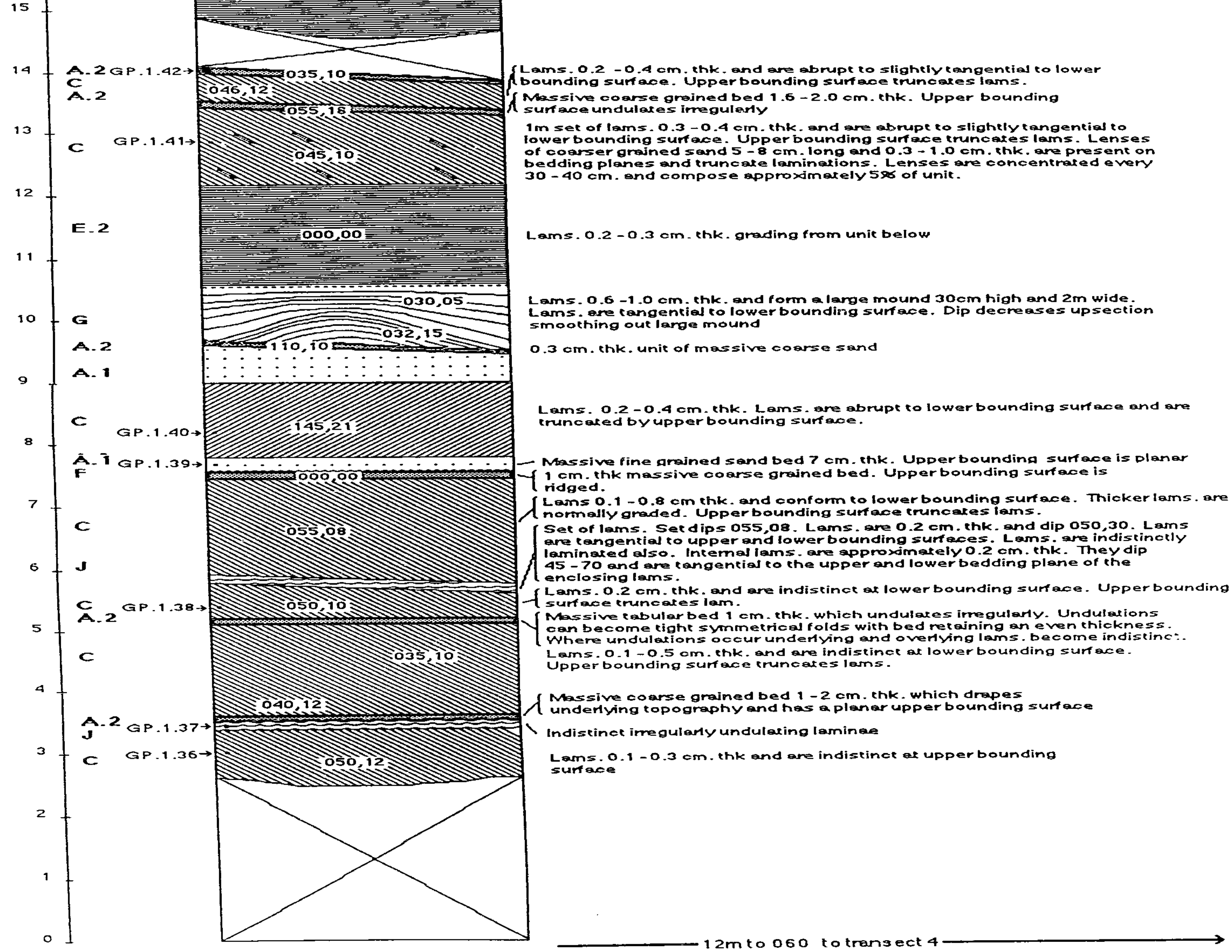
15
14 A.2 GP.1.42→ 035,10 046,12
C
Lams. 0.2 - 0.4 cm. thk. and are abrupt to slightly tangential to lower bounding surface. Upper bounding surface truncates lams.
A.2 055,18
Massive coarse grained bed 1.6 - 2.0 cm. thk. Upper bounding surface undulates irregulerly
13 C GP.1.41→ 045,10
1m set of lams. 0.3 - 0.4 cm. thk. and are abrupt to slightly tangential to lower bounding surface. Upper bounding surface truncates lams. Lenses of coarser grained sand 5 - 8 cm. long and 0.3 - 1.0 cm. thk. are present on bedding planes and truncate laminations. Lenses are concentrated every 30 - 40 cm. and compose approximately 5% of unit.
12 E.2 000,00
Lams. 0.2 - 0.3 cm. thk. grading from unit below
11
10 G 030,05 032,15
Lams. 0.6 - 1.0 cm. thk. and form a large mound 30cm high and 2m wide. Lams. are tangential to lower bounding surface. Dip decreases upsection smoothing out large mound
A.2 110,10
0.3 cm. thk. unit of massive coarse sand
9 A.1
C GP.1.40→ 145,21
Lams. 0.2 - 0.4 cm. thk. Lams. are abrupt to lower bounding surface and are truncated by upper bounding surface.
8 A.1 GP.1.39→
Massive fine grained sand bed 7 cm. thk. Upper bounding surface is planer
F 000,00
1 cm. thk massive coarse grained bed. Upper bounding surface is ridged.
7 C 055,08
Lams 0.1 - 0.8 cm thk. and conform to lower bounding surface. Thicker lams. are normally graded. Upper bounding surface truncates lams.
6 J
Set of lams. Set dips 055,08. Lams. are 0.2 cm. thk. and dip 050,30. Lams are tangential to upper and lower bounding surfaces. Lams. are indistinctly laminated also. Internal lams. are approximately 0.2 cm. thk. They dip 45 - 70 and are tangential to the upper and lower bedding plane of the enclosing lams.
C GP.1.38→ 050,10
Lams. 0.2 cm. thk. and are indistinct at lower bounding surface. Upper bounding surface truncates lam.
5 A.2
Massive tabular bed 1 cm. thk. which undulates irregularly. Undulations can become tight symmetrical folds with bed retaining an even thickness. Where undulations occur underlying and overlying lams. become indistinct.
C 035,10
Lams. 0.1 - 0.5 cm. thk. and are indistinct at lower bounding surface. Upper bounding surface truncates lams.
4 040,12
A.2 GP.1.37→
Massive coarse grained bed 1 - 2 cm. thk. which drapes underlying topography and has a planer upper bounding surface
J
Indistinct irregularly undulating laminae
3 C GP.1.36→ 050,12
Lams. 0.1 - 0.3 cm. thk and are indistinct at upper bounding surface
2
1
0
12m to 060 to transect 4

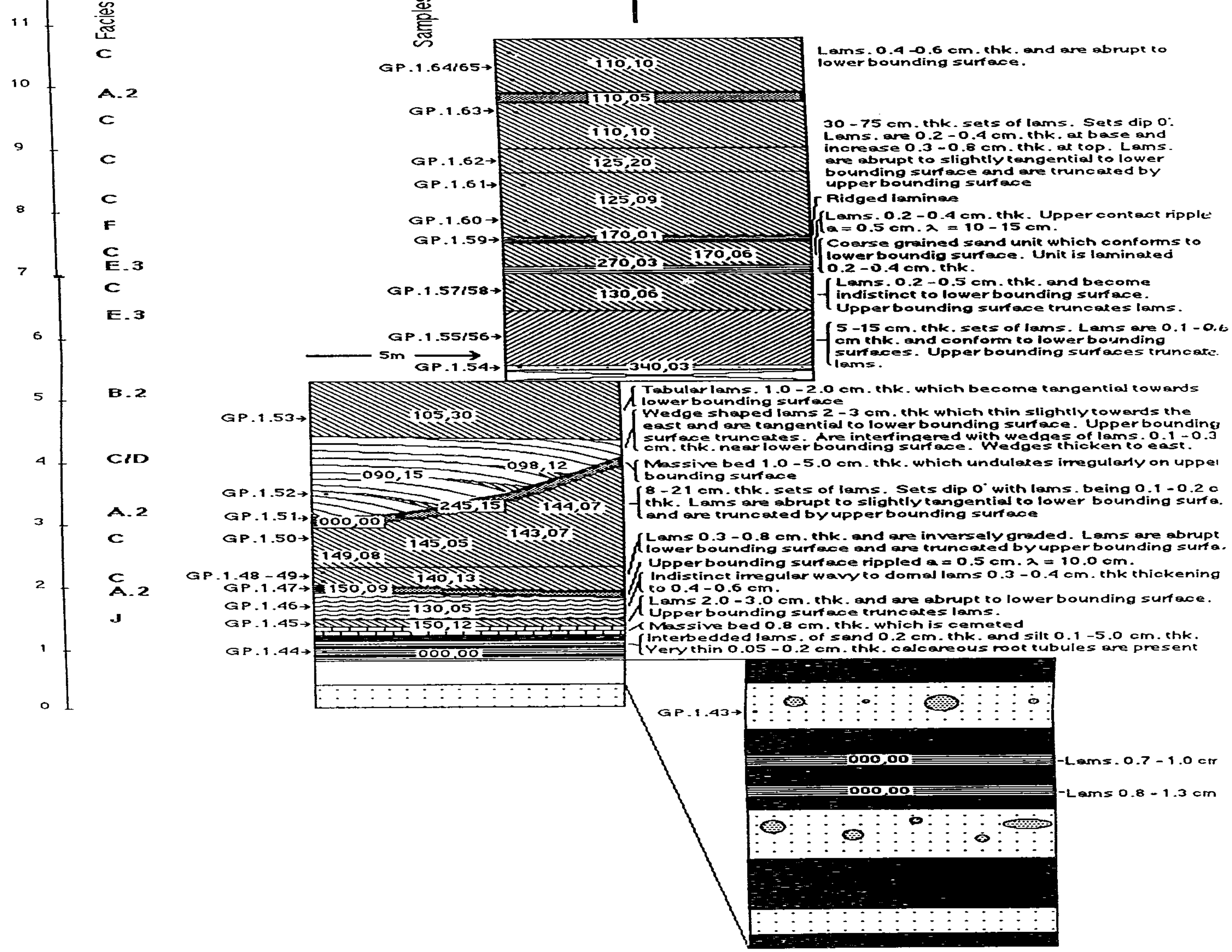

Facies
Samples
11
10
9
8
7
6
5
4
3
2
1
0
C
A.2
C
C
C
F
C
E.3
C
E.3
B.2
C/D
A.2
C
C
A.2
J
5m
GP.1.64/65
GP.1.63
GP.1.62
GP.1.61
GP.1.60
GP.1.59
GP.1.57/58
GP.1.55/56
GP.1.54
GP.1.53
GP.1.52
GP.1.51
GP.1.50
GP.1.48-49
GP.1.47
GP.1.46
GP.1.45
GP.1.44
GP.1.43
110,10
110,05
110,10
125,20
125,09
170,01
170,06
270,03
130,06
340,03
105,30
098,12
090,15
245,15
144,07
000,00
143,07
145,05
149,08
140,13
150,09
130,05
150,12
000,00
000,00
000,00
Lams. 0.4-0.6 cm. thk. and are abrupt to lower bounding surface.
30-75 cm. thk. sets of lams. Sets dip 0°. Lams. are 0.2-0.4 cm. thk. at base and increase 0.3-0.8 cm. thk. at top. Lams. are abrupt to slightly tangential to lower bounding surface and are truncated by upper bounding surface
Ridged laminae
Lams. 0.2-0.4 cm. thk. Upper contact ripple a = 0.5 cm. λ = 10-15 cm.
Coarse grained sand unit which conforms to lower boundig surface. Unit is laminated 0.2-0.4 cm. thk.
Lams. 0.2-0.5 cm. thk. and become indistinct to lower bounding surface. Upper bounding surface truncates lams.
5-15 cm. thk. sets of lams. Lams are 0.1-0.6 cm thk. and conform to lower bounding surfaces. Upper bounding surfaces truncate lams.
Tabular lams. 1.0-2.0 cm. thk. which become tangential towards lower bounding surface
Wedge shaped lams 2-3 cm. thk which thin slightly towards the east and are tangential to lower bounding surface. Upper bounding surface truncates. Are interfingered with wedges of lams. 0.1-0.3 cm. thk. near lower bounding surface. Wedges thicken to east.
Massive bed 1.0-5.0 cm. thk. which undulates irregularly on upper bounding surface
8-21 cm. thk. sets of lams. Sets dip 0° with lams. being 0.1-0.2 cm thk. Lams are abrupt to slightly tangential to lower bounding surface and are truncated by upper bounding surface
Lams 0.3-0.8 cm. thk. and are inversely graded. Lams are abrupt to lower bounding surface and are truncated by upper bounding surface.
Upper bounding surface rippled a = 0.5 cm. λ = 10.0 cm.
Indistinct irregular wavy to domal lams 0.3-0.4 cm. thk thickening to 0.4-0.6 cm.
Lams 2.0-3.0 cm. thk. and are abrupt to lower bounding surface.
Upper bounding surface truncates lams.
Massive bed 0.8 cm. thk. which is cemeted
Interbedded lams. of sand 0.2 cm. thk. and silt 0.1-5.0 cm. thk.
Very thin 0.05-0.2 cm. thk. calcareous root tubules are present
-Lams. 0.7-1.0 cm
-Lams 0.8-1.3 cm

SECTION : Grande Prairie 4 (GP.4) - transect 1 - Compound type 2 parabolic dune

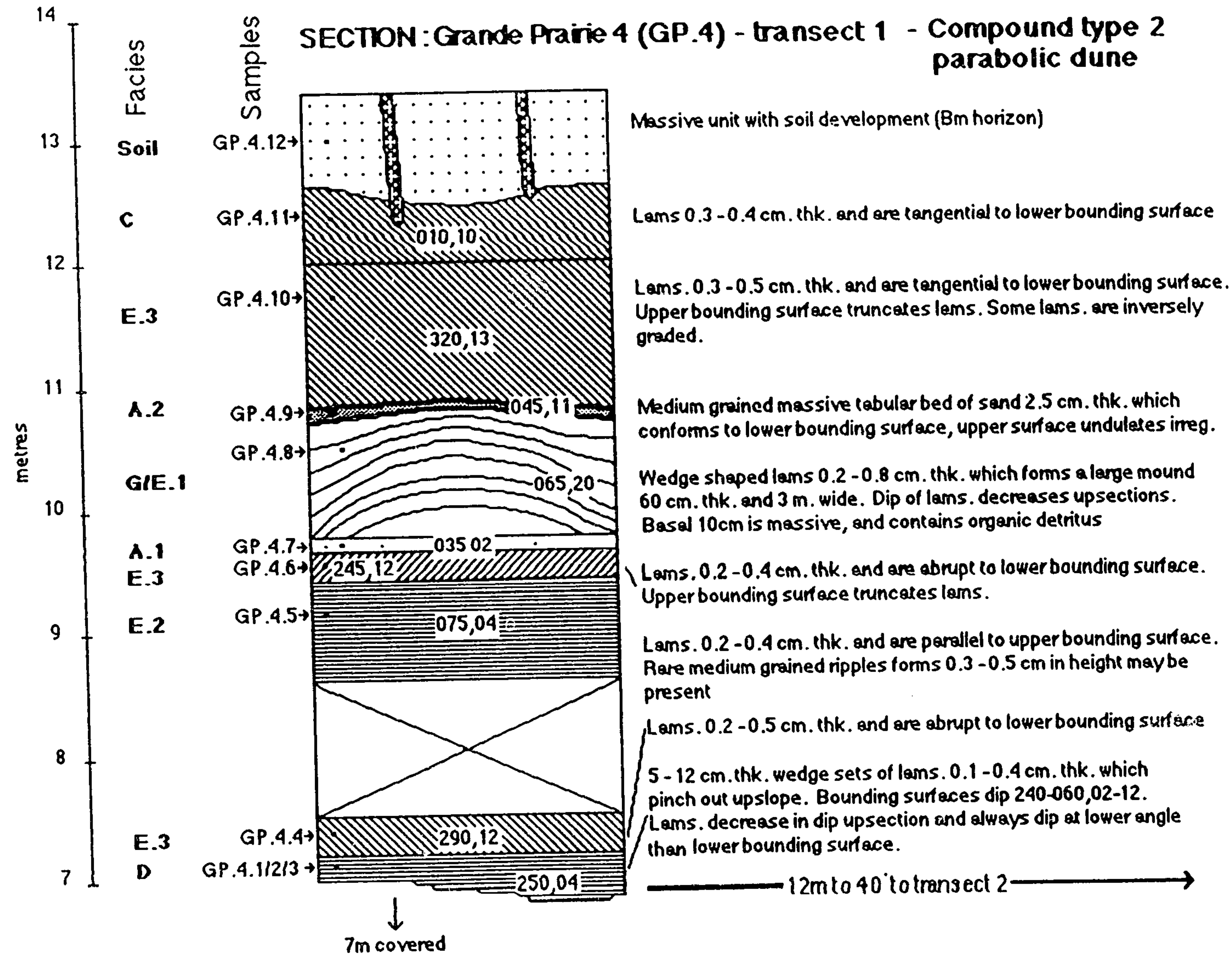

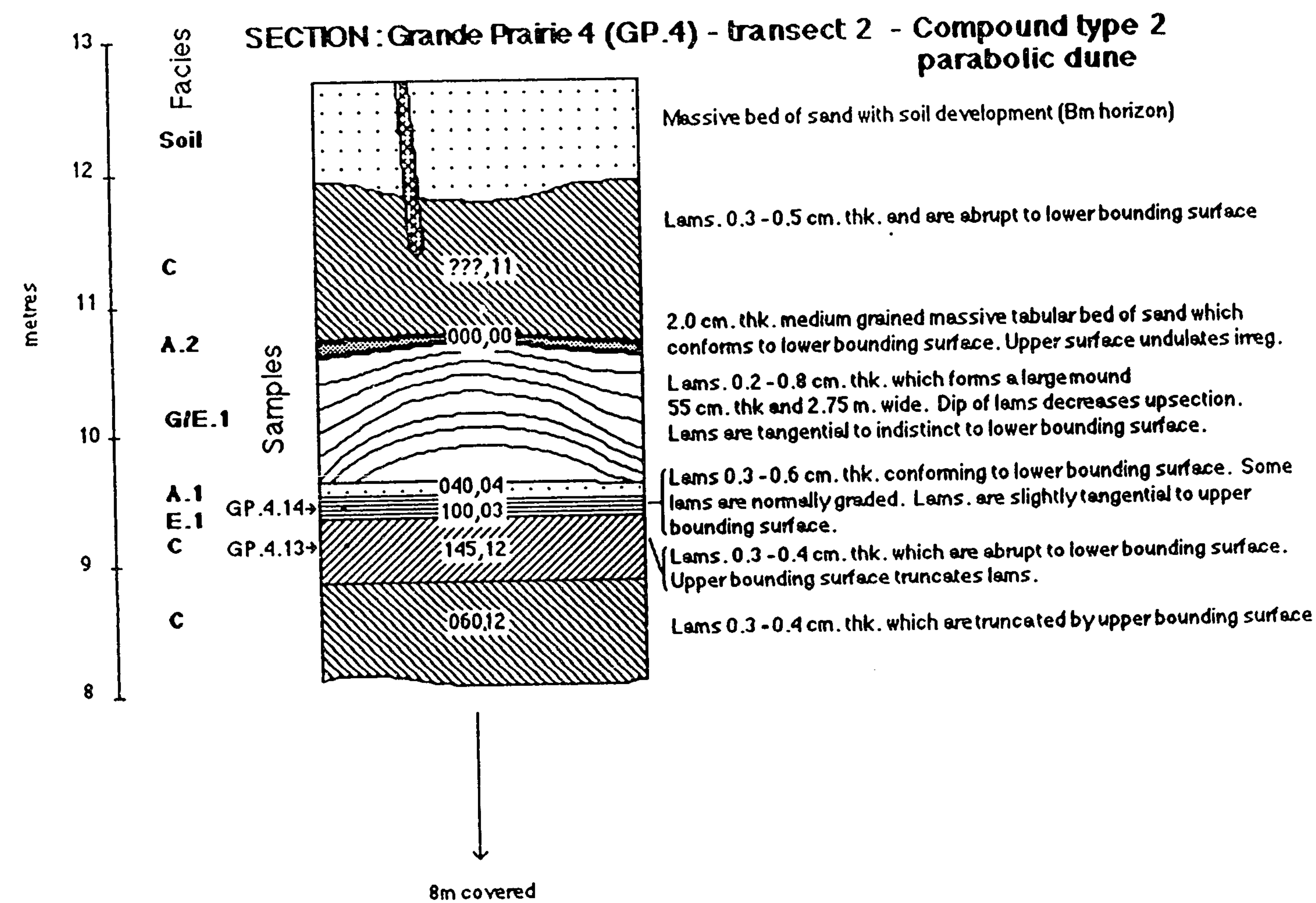
SECTION : Grande Prairie 4 (GP.4) - transect 2 - Compound type 2 parabolic dune
metres
13
12
11
10
9
8
Facies
Soil
C
A.2
G/E.1
A.1
E.1
C
C
Samples
GP.4.14→
GP.4.13→
???,11
000,00
040,04
100,03
145,12
060,12
Massive bed of sand with soil development (Bm horizon)
Lams. 0.3 - 0.5 cm. thk. and are abrupt to lower bounding surface
2.0 cm. thk. medium grained massive tabular bed of sand which conforms to lower bounding surface. Upper surface undulates irreg.
Lams. 0.2 - 0.8 cm. thk. which foms a large mound 55 cm. thk and 2.75 m. wide. Dip of lams decreases upsection. Lams are tangential to indistinct to lower bounding surface.
Lams 0.3 - 0.6 cm. thk. conforming to lower bounding surface. Some lams are normally graded. Lams. are slightly tangential to upper bounding surface.
Lams. 0.3 - 0.4 cm. thk. which are abrupt to lower bounding surface. Upper bounding surface truncates lams.
Lams 0.3 - 0.4 cm. thk. which are truncated by upper bounding surface
8m covered

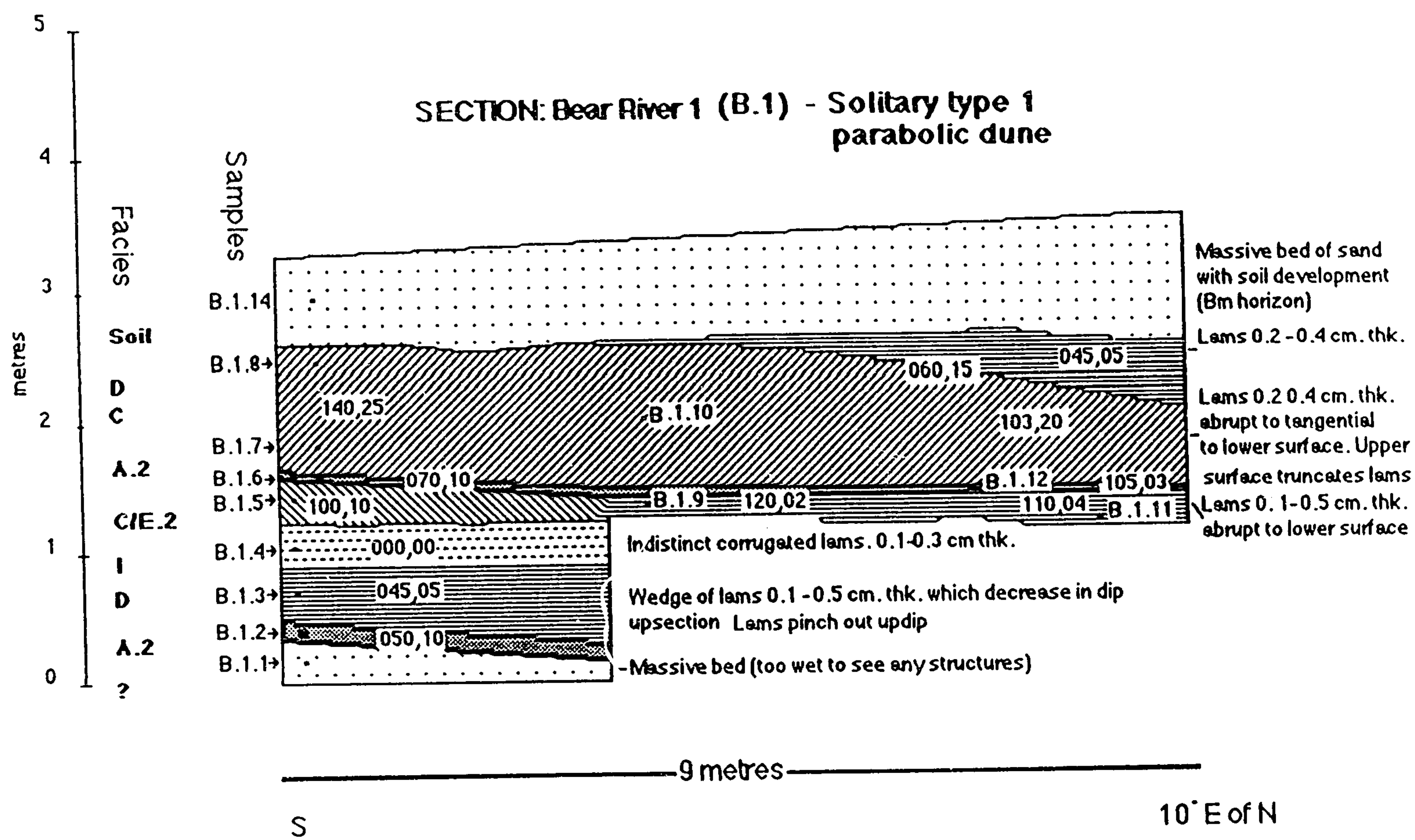
SECTION: Bear River 1 (B.1) - Solitary type 1 parabolic dune
metres
5
4
3
2
1
0
Facies
Soil
D
C
A.2
C/E.2
I
D
A.2
?
Samples
B.1.14
B.1.8
B.1.7
B.1.6
B.1.5
B.1.4
B.1.3
B.1.2
B.1.1
140,25
B.1.10
060,15
045,05
103,20
070,10
100,10
B.1.9
120,02
B.1.12
105,03
110,04
B.1.11
000,00
045,05
050,10
Massive bed of sand with soil development (Bm horizon)
Lams 0.2 - 0.4 cm. thk.
Lams 0.2 0.4 cm. thk. abrupt to tangential to lower surface. Upper surface truncates lams
Lams 0. 1-0.5 cm. thk. abrupt to lower surface
Indistinct corrugated lams. 0.1-0.3 cm thk.
Wedge of lams 0.1 - 0.5 cm. thk. which decrease in dip upsection Lams pinch out updip
-Massive bed (too wet to see any structures)
9 metres
S
10° E of N

SECTION : Goodwin 1 (G.1) - transect 1 - Dome dune

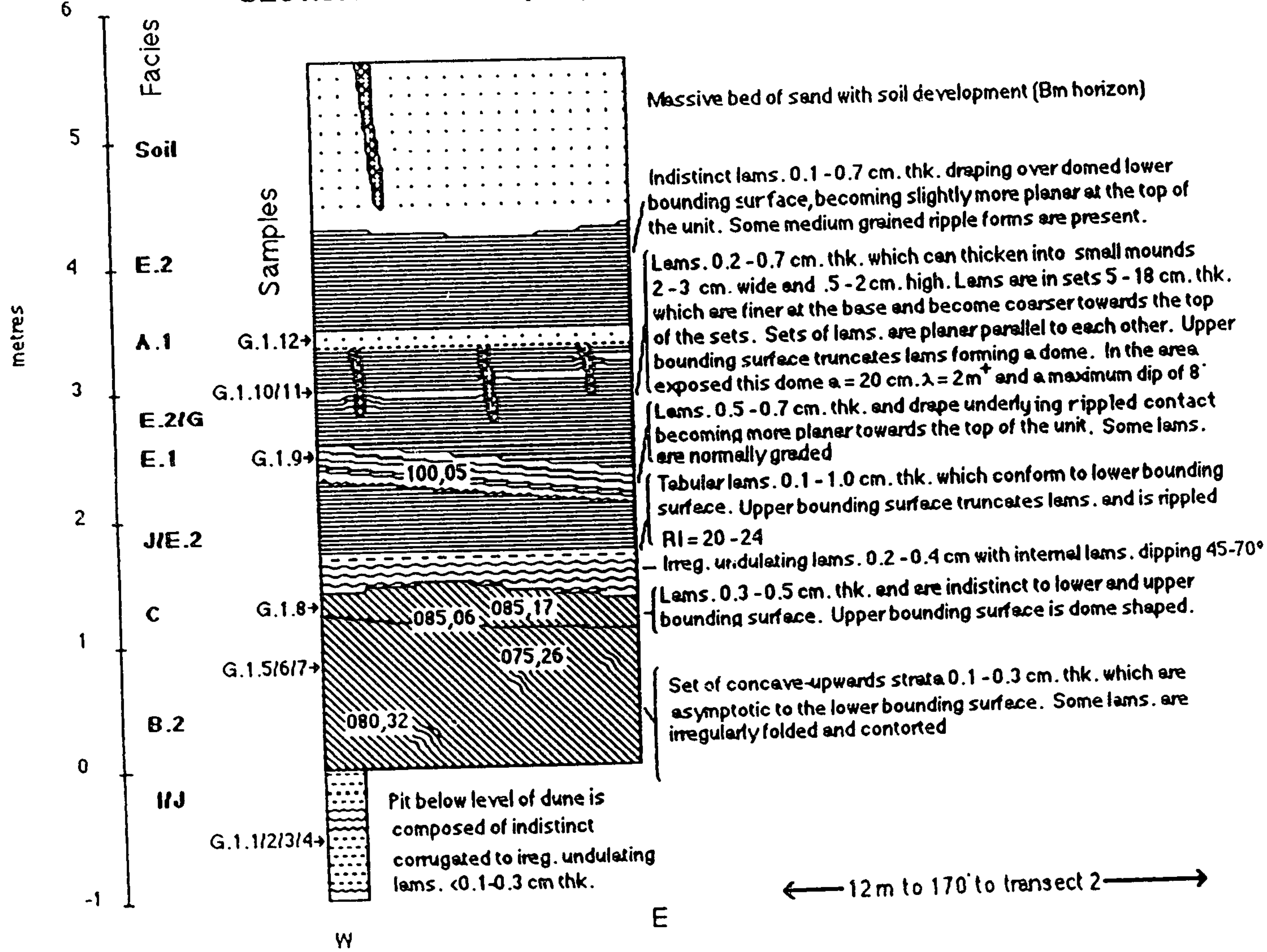

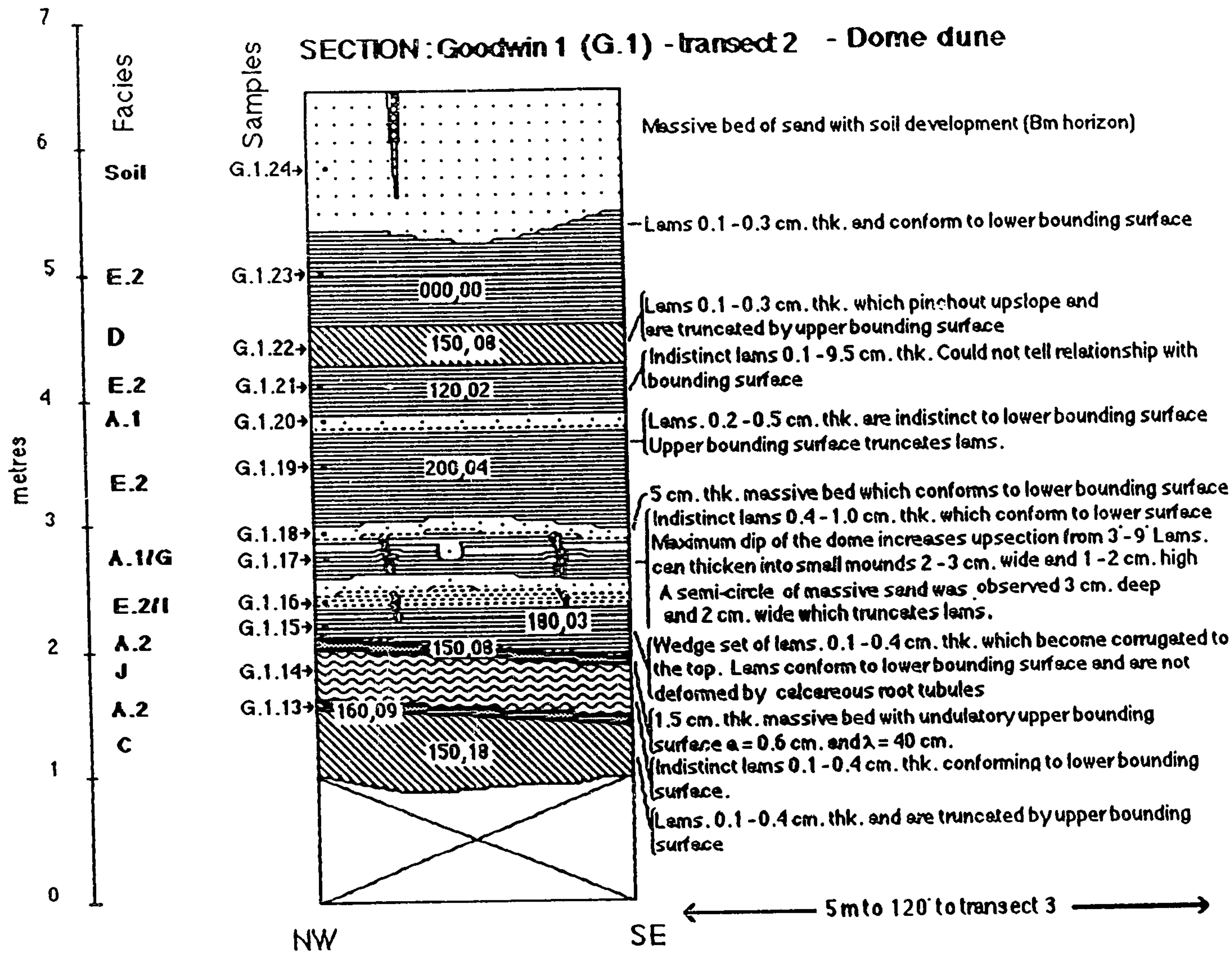

SECTION : Goodwin 1 (G.1) - transect 2 - Dome dune
metres
7
6
5
4
3
2
1
0
Facies
Soil
E.2
D
E.2
A.1
E.2
A.1/G
E.2/I
A.2
J
A.2
C
Samples
G.1.24
G.1.23
G.1.22
G.1.21
G.1.20
G.1.19
G.1.18
G.1.17
G.1.16
G.1.15
G.1.14
G.1.13
000,00
150,08
120,02
200,04
180,03
150,08
160,09
150,18
Massive bed of sand with soil development (Bm horizon)
Lams 0.1 - 0.3 cm. thk. and conform to lower bounding surface
Lams 0.1 - 0.3 cm. thk. which pinchout upslope and are truncated by upper bounding surface
Indistinct lams 0.1 - 9.5 cm. thk. Could not tell relationship with bounding surface
Lams. 0.2 - 0.5 cm. thk. are indistinct to lower bounding surface
Upper bounding surface truncates lams.
5 cm. thk. massive bed which conforms to lower bounding surface
Indistinct lams 0.4 - 1.0 cm. thk. which conform to lower surface
Maximum dip of the dome increases upsection from 3°-9° Lams. can thicken into small mounds 2 - 3 cm. wide and 1 - 2 cm. high
A semi-circle of massive sand was observed 3 cm. deep and 2 cm. wide which truncates lams.
Wedge set of lams. 0.1 - 0.4 cm. thk. which become corrugated to the top. Lams conform to lower bounding surface and are not deformed by calcareous root tubules
1.5 cm. thk. massive bed with undulatory upper bounding surface a = 0.6 cm. and λ = 40 cm.
Indistinct lams 0.1 - 0.4 cm. thk. conforming to lower bounding surface.
Lams. 0.1 - 0.4 cm. thk. and are truncated by upper bounding surface
NW
SE
5 m to 120° to transect 3

SECTION : Goodwin 1 (G.1) - transect 3 - Dome dune

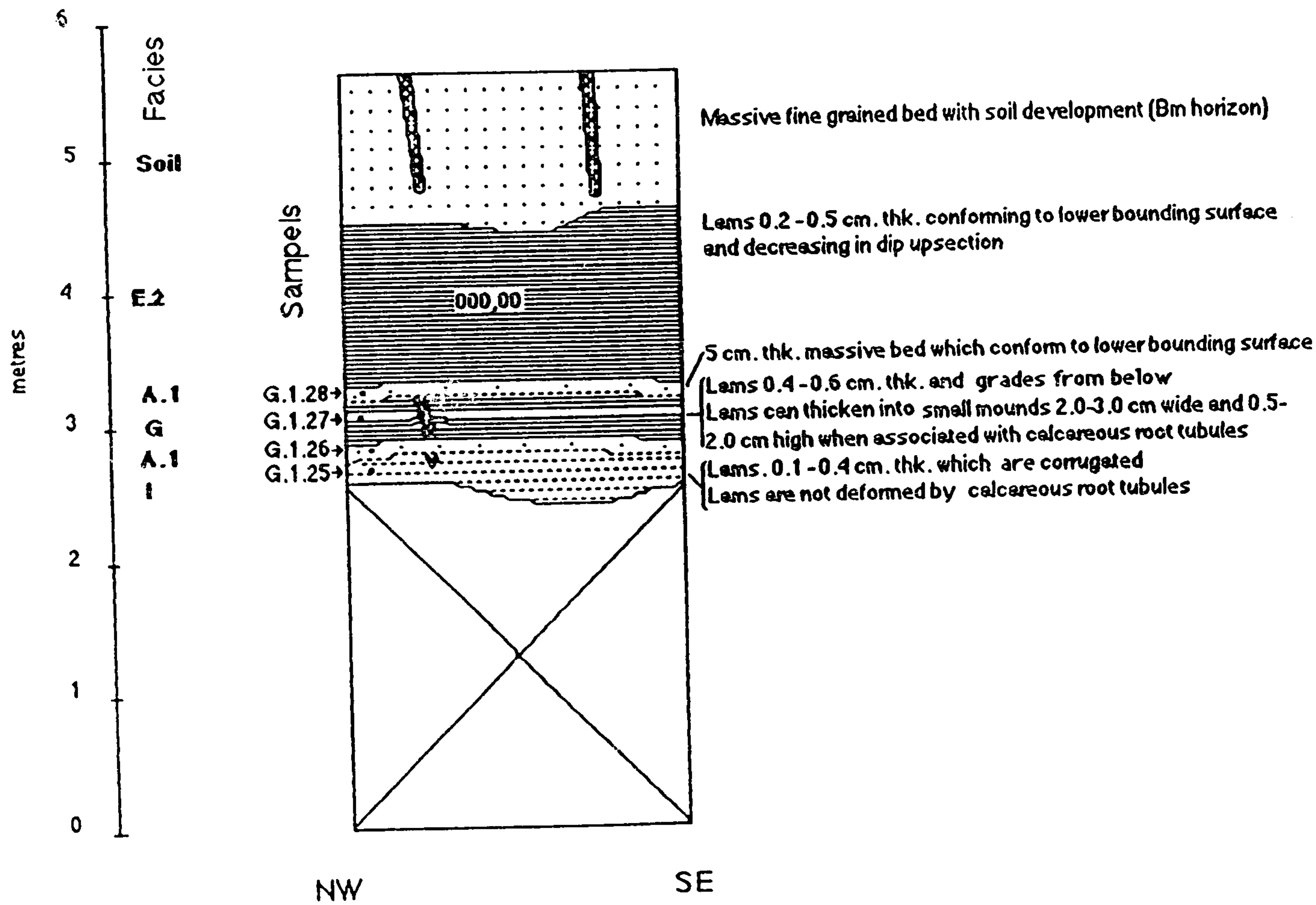

SECTION: Goodwin 2 (G.2) - transect 1 - Dome dune

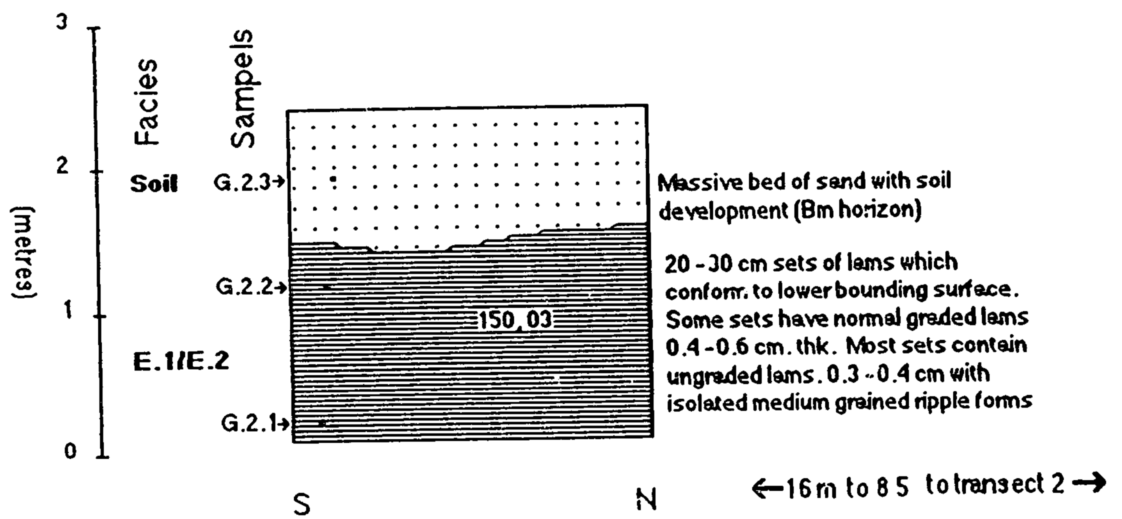

SECTION: Goodwin 2 (G.2) - transect 2 - Dome dune

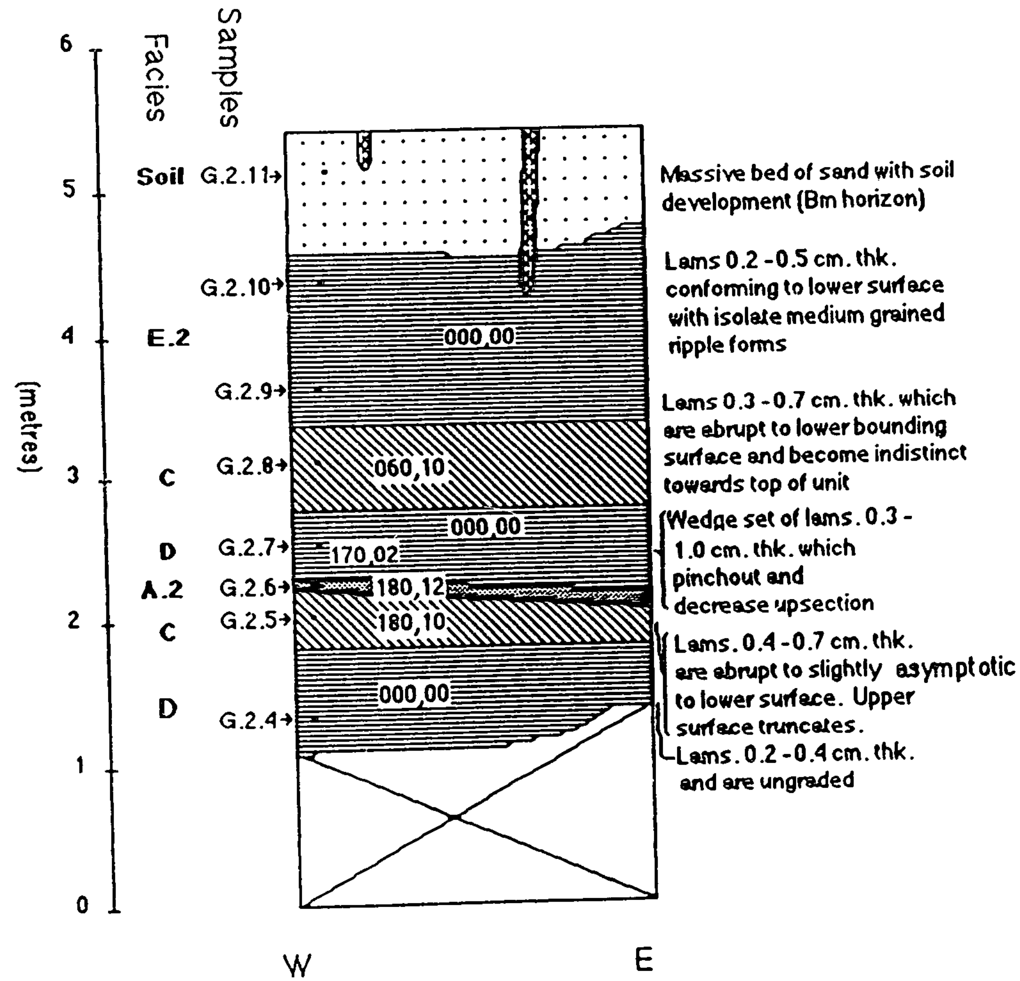

APPENDIX 2: QUANTIFICATION OF PARABOLIC DUNE MORPHOLOGY

No.	Nose Width (metres)	North Arm Length (metres)	South Arm Length (metres)	North - South Arm Length (metres)	Orientation
2	75	315	195	120	76
1	90	690	645	45	85.5
1	65	555	420	135	83.5
2	120	360	600	-240	94.5
2	105	360	225	135	84
2	75	390	480	-90	81.5
2	120	300	300	0	82
2	150	720	465	255	80
2	90	210	210	0	77
2	195	255	345	-90	76.5
2	165	240	315	-75	84
1	45	435	570	-135	90
2	195	450	224	226	80
2	90	180	420	-240	89.5
2	60	270	480	-210	84.5
1	60	630	420	210	84
2	90	270	270	0	85
2	90	240	285	-45	86

No.	Nose Width (metres)	North Arm Length (metres)	South Arm Length (metres)	North - South Arm Length (metres)	Orientation
2	150	210	180	30	69
2	75	210	240	-30	76
2	60	120	150	-30	64
2	165	480	480	0	76.5
2	60	300	300	0	76.5
2	90	210	300	-90	95.5
2	90	240	105	135	84
2	135	300	330	-30	81
2	90	360	390	-30	75
1	90	660	435	225	81.5
2	75	180	150	30	75
2	75	300	135	165	75.5
2	60	150	135	15	77.5
2	60	180	180	0	80
2	150	285	180	105	87
2	165	450	375	75	82.5
2	75	270	240	30	85
2	120	300	540	-240	82
1	50	525	585	-60	84
2	90	180	275	-90	86

No.	Nose Width (metres)	North Arm Length (metres)	South Arm Length (metres)	North - South Arm Length (metres)	Orientation
2	75	195	255	-60	81
2	75	300	390	-90	82.5
2	135	405	330	75	91
2	105	180	390	-210	97
2	90	225	330	-105	83
2	150	315	450	-135	9035
2	150	330	330	0	84.5
2	135	240	345	-105	76
2	120	420	240	180	94.5
2	135	255	300	-45	92.5
2	150	240	570	-330	96
2	135	270	360	-90	91
2	90	255	180	75	93
1	90	600	570	30	85
2	75	210	270	-60	89.5
2	210	345	360	-15	90.5
2	60	270	660	-390	91.5
2	60	255	165	90	76
1	60	285	570	-285	92
2	90	270	300	-30	91.5

No.	Nose Width (metres)	North Arm Length (metres)	South Arm Length (metres)	North - South Arm Length (metres)	Orientation
2	135	270	225	45	67.5
2	195	4535	480	-45	74.5
2	105	450	240	-90	78
2	105	180	270	-90	81.5
2	120	.300	180	120	81
2	90	300	330	-30	85.5
2	105	330	180	150	85
1	75	150	555	-405	88
2	105	420	510	-150	84.5
2	105	390	480	-90	79
2	135	435	420	15	82
2	465	570	630	-60	90.5
1	50	630	540	90	87
2	225	240	375	-135	90
2	120	270	270	0	87.5
2	90	150	180	-30	86
2	105	180	210	-30	92
2	150	285	285	0	82
2	210	330	375	-45	85
2	135	375	240	135	83

No.	Nose Width (metres)	North Arm Length (metres)	South Arm Length (metres)	North - South Arm Length (metres)	Orientation
2	120	210	240	-30	83
2	135	315	345	-30	82
2	135	315	435	-120	84.5
2	180	390	270	120	82.5
1	75	585	270	315	76
1	65	480	585	-105	88
2	105	360	690	-330	90
2	75	180	285	-105	81.5
2	300	300	315	-15	97
2	180	210	495	-285	107.5
2	135	360	210	150	85
2	90	165	180	-15	84.5
2	135	255	240	15	85.5
2	120	150	420	-270	100
2	105	180	210	-30	86.5
2	150	240	360	-120	91
2	210	300	360	-60	82.5
2	150	210	450	-240	96.5
1	85	645	345	330	78
2	90	255	195	60	80

No.	Nose Width (metres)	North Arm Length (metres)	South Arm Length (metres)	North - South Arm Length (metres)	Orientation
2	120	165	150	15	88.5
2	135	270	240	30	81.5
1	45	630	885	-255	94
2	180	240	570	-330	102.5
2	75	105	90	15	105.5
2	165	195	390	-195	89
2	105	360	360	0	76.5
2	75	165	210	-45	86
2	300	120	135	-15	90.5
2	180	180	330	-150	83.5
2	135	255	300	-45	79.5
2	90	225	315	-90	82
2	135	615	300	315	85
2	120	255	240	15	85
2	105	120	180	-60	94
2	150	225	285	-600	88
2	210	240	345	-150	88.5
1	50	600	240	360	79.5
2	210	210	195	195	81.5
2	90	510	480	480	104

No.	Nose Width (metres)	North Arm Length (metres)	South Arm Length (metres)	North - South Arm Length (metres)	Orientation
2	300	420	180	240	93
2	210	585	480	105	86.5
1	95	705	555	90	87.5
2	60	420	330	-30	76.5
2	195	270	300	-30	105
2	105	240	270	-135	78
2	75	300	435	-210	90
2	165	150	360	165	87
2	60	270	105	-165	80
2	165	150	315	-30	99.5
2	90	105	135	-45	87
2	165	210	255	-45	86.5
2	135	210	255	-30	85.5
2	180	270	300	-45	76
2	135	210	240	0	87.5
2	90	210	255	135	88
2	180	390	390	135	89
2	120	420	285	-15	88
2	150	585	450	-345	76.5
2	135	420	435	-15	78

No.	Nose Width (metres)	North Arm Length (metres)	South Arm Length (metres)	North - South Arm Length (metres)	Orientation
2	105	135	480	-345	99
2	105	210	225	-15	87.5
2	135	255	435	-180	90
2	150	330	330	0	77
2	135	180	180	0	86.5
2	270	360	390	-30	84.5
2	90	195	150	45	63
2	120	290	300	-10	76
2	150	315	360	-45	85
2	135	180	435	-255	91.5
2	315	540	300	240	78
2	270	300	510	-210	88.5
2	210	390	480	-90	77
2	165	300	300	0	81.5
2	165	210	270	-60	78.5
2	60	225	270	-45	75
2	45	285	165	120	89.5
2	240	120	330	-210	83
2	120	390	345	45	77.5
2	135	255	555	-300	88.5

No.	Nose Width (metres)	North Arm Length (metres)	South Arm Length (metres)	North - South Arm Length (metres)	Orientation
2	165	270	360	-90	93
2	180	315	330	-15	87
2	180	300	360	-60	92.5
2	180	270	240	30	90.5
2	120	225	450	-225	102
2	60	150	270	-120	91
1	65	240	600	-360	98
2	165	315	240	75	90
2	165	240	285	-45	94
2	120	330	210	120	76.5
2	75	240	390	-150	90
1	80	405	750	-345	93.5
2	120	300	180	120	89
2	105	510	285	225	82
2	120	360	420	-60	83.5
2	90	90	375	-285	102
2	120	330	450	-120	83
2	135	285	300	-15	93.5
2	75	210	180	30	87
2	150	285	185	100	72.5

No.	Nose Width (metres)	North Arm Length (metres)	South Arm Length (metres)	North - South Arm Length (metres)	Orientation
179	75	450	210	240	78
180	90	270	330	-60	90.5

APPENDIX 3: MEAN AND SORTING VALUES ARRANGED BY FACIES AND SAMPLE NUMBER

Facies	Sample	Mean (ø)	Sorting (ø)
A.1	GP.1.24	2.33	0.41
	GP.1.4	2.45	0.50
	GP.1.6	2.55	0.37
	GP.1.9	2.62	0.41
	GP.1.12	2.35	0.42
	GP.1.21	2.53	0.42
	GP.1.28	2.37	0.44
	GP.1.39	2.42	0.56
	GP.1.54	2.18	0.59
	GP.4.7	2.70	0.38
	GP.1.17	2.43	0.42
	G.1.12	2.85	0.47
	G.1.18	2.88	0.54
	G.1.20	2.80	0.61
	G.1.26	2.73	0.60
	G.1.28	2.62	0.54
A.2	GP.1.15	1.83	0.79
	GP.1.35	1.55	0.79

Facies	Sample	Mean (ø)	Sorting (ø)
A.2	GP.1.42	2.15	0.50
	GP.1.47	2.05	0.68
	GP.1.51	1.92	0.81
	GP.4.9	2.17	0.50
	B.1.2	1.87	0.50
	B.1.6	1.77	0.61
	B.1.12	1.87	0.55
	G.1.13	1.52	0.58
	G.2.6	1.72	0.67
B.1	P.1.3	2.72	0.41
	P.1.4	2.55	0.42
	P.2.2	2.45	0.49
	P.2.3	2.72	0.35
	GP.1.1	2.22	0.70
	GP.1.2	2.48	0.48
	GP.1.3	2.02	0.69
	GP.1.52	2.58	0.47
B.2	GP.1.11	2.45	0.40
	GP.1.12	2.05	0.56
	GP.1.19	2.48	0.33

Facies	Sample	Mean (ϕ)	Sorting (ϕ)
B.2	GP.1.53	2.53	0.52
	G.1.5	2.42	0.63
	G.1.6	2.70	0.66
	G.1.7	2.35	0.72
B.3	P.2.1	2.73	0.38
C	P.1.5	2.60	0.50
	P.2.4	2.73	0.36
	P.3.3	2.57	0.50
	GP.1.25	2.12	0.52
	GP.1.26	2.23	0.45
	GP.1.27	2.42	0.47
	GP.1.29	2.28	0.37
	GP.1.33	2.02	0.60
	GP.1.36	2.25	0.44
	GP.1.38	2.32	0.51
	GP.1.40	2.02	0.61
	GP.1.41	2.35	0.53
	GP.1.45	1.78	0.78
	GP.1.48	1.85	0.70
	GP.1.49	1.92	0.78

Facies	Sample	Mean (ø)	Sorting (ø)
C	GP.1.50	2.25	0.55
	GP.1.57	2.48	0.46
	GP.1.58	2.22	0.57
	GP.1.60	2.20	0.56
	GP.1.61	2.52	0.47
	GP.1.62	2.40	0.43
	GP.1.63	2.43	0.41
	GP.1.64	2.20	0.59
	GP.1.65	2.12	0.54
	GP.4.11	2.25	0.52
	GP.4.13	2.40	0.39
	B.1.5	2.50	0.62
	B.1.7	2.07	0.60
	B.1.8	2.02	0.58
	B.1.10	2.27	0.60
	G.1.8	2.70	0.67
	G.2.5	2.62	0.60
	G.2.8	2.37	0.64
D	P.2.5	2.35	0.48
	GP.1.20	2.33	0.44

Facies	Sample	Mean (ø)	Sorting (ø)
D	GP.4.1	2.27	0.47
	GP.4.2	2.65	0.36
	GP.4.3	2.33	0.49
	B.1.3	2.55	0.59
	B.1.13	2.10	0.58
	G.1.22	2.45	0.61
	G.2.4	2.65	0.59
	G.2.7	2.37	0.59
E.1	GP.1.14	2.22	0.55
	GP.4.14	2.47	0.36
	G.1.9	2.40	0.31
	G.2.1	2.52	0.66
E.2	P.1.2	1.98	0.53
	P.1.6	2.50	0.42
	P.3.2	2.63	0.49
	P.3.4	2.67	0.40
	HT.1.4	2.35	0.69
	GR.1.3	2.07	0.76
	GR.1.4	2.58	0.51
	GP.1.5	2.37	0.51

Facies	Sample	Mean (ø)	Sorting (ø)
E.2	GP.1.7	2.15	0.77
	GP.1.8	2.42	0.40
	GP.1.13	2.33	0.47
	GP.1.16	2.53	0.39
	GP.1.23	2.10	0.57
	GP.4.5	2.35	0.40
	B.1.9	2.25	0.52
	B.1.11	2.25	0.54
	G.1.11	2.45	0.58
	G.1.15	2.47	0.64
	G.1.19	2.65	0.53
	G.1.21	2.68	0.48
	G.1.23	2.38	0.58
	G.2.2	2.33	0.66
	G.2.9	2.03	0.59
	G.2.10	2.12	0.67
E.3	P.3.1	2.15	0.66
	GP.1.55	1.98	0.56
	GP.1.56	2.33	0.42
	GP.4.4	2.22	0.35

Facies	Sample	Mean (ø)	Sorting (ø)
E.3	GP.4.6	2.38	0.45
	GP.4.10	2.25	0.48
F	GP.1.30	2.00	0.92
	GP.1.59	1.83	0.62
G	GP.1.22	2.57	0.37
	GP.1.31	2.32	0.61
	GP.1.32	2.33	0.50
	GP.4.8	2.38	0.45
	G.1.10	2.50	0.60
	G.1.17	2.58	0.58
	G.1.27	2.50	0.58
H	GP.1.34	2.90	0.40
I	GP.1.18	2.45	0.40
	B.1.4	2.40	0.61
	G.1.4	2.33	0.72
	G.1.16	2.52	0.66
	G.1.25	2.38	0.66
J	P.1.1	2.62	0.57
	GP.1.37	2.43	0.36
	GP.1.46	2.23	0.59

Facies	Sample	Mean (ø)	Sorting (ø)
J	G.1.1	2.80	0.77
	G.1.2	2.58	0.80
	G.1.3	2.72	0.50
	G.1.14	2.52	0.69

APPENDIX 3.2: Summary of results of duplicate sample runs

Sample	Mean (ø) Run 1	Mean (ø) Run 2	Sorting (ø) Run 1	Sorting (ø) Run 2	Skewness (ø) Run 1	Skewness (ø) Run 2	Kurtosis (ø) Run 1	Kurtosis (ø) Run 2
HT.1.5	1.73	1.72	.73	.69	.15	.14	1.52	1.01
P.1.4	2.55	2.58	.42	.40	-.05	.17	1.19	1.04
P.2.10	2.72	2.75	.36	.34	.01	.01	.94	.98
P.3.5	2.58	2.63	.44	.39	-.13	.03	1.23	1.15
P.8.1(H)	3.90	3.95	—	—	—	—	—	—
GP.1.52	2.53	2.53	.52	.49	-.02	.00	1.19	.98
GP.1.63	2.22	2.18	.59	.58	-.11	-.10	.97	1.03
GP.3.1	2.37	2.38	.49	.51	.05	-.04	1.13	1.04
GP.3.6	2.52	2.55	.42	.40	.03	.10	1.28	1.28
GP.3.7	2.53	2.53	.41	.41	.10	-.03	1.15	1.18
GP.4.5	2.35	2.35	.40	.40	-.11	-.12	1.10	1.23
GP.4.14	2.47	2.48	.36	.39	.04	.17	1.33	1.18
B.1.5	2.50	2.48	.62	.62	.02	.02	1.15	.99
B.1.10	2.27	2.25	.60	.59	-.07	-.09	.96	1.03
G.1.5	2.42	2.37	.63	.60	.14	.07	1.07	.97
G.1.12	2.85	2.83	.47	.42	.18	-.36	1.27	.76
G.1.18	2.88	3.03	.54	.53	-.12	-.04	1.33	1.08
G.1.25	2.38	2.40	.66	.64	-.02	.02	.96	1.01
G.1.28	2.62	2.63	.54	.53	.04	.09	1.17	1.17
G.2.10	2.12	2.07	.67	.65	.24	.11	1.06	1.00